ORIGINAL ARTICLES

THE EFFECT OF CHLORIN E_6 DRUG ON PLATELET AGGREGATION ACTIVITY

Petrishchev N.N.[1, 2], **Galkin M.A.**[1], **Grishacheva T.G.**[1], **Dementjeva I.N.**[1], **Chefu S.G.**[1, 2]
[1]Pavlov First Saint Petersburg State Medical University, Saint Petersburg, Russia
[2]Almazov National Medical Research Centre, Saint Petersburg, Russia

Abstract

The goal of the study is to evaluate the effect of Radachlorin (OOO "RADA-PHARMA", Russia) (RC) on platelet aggregation in ex vivo and in vivo experiments. The experiments were conducted on male Wistar rats. Platelet aggregation activity was determined in platelet-rich plasma (PRP) using a turbidimetric method and the aggregation inducer was ADP at a final concentration of 1.25 μM. PRP samples containing RC were irradiated with ALOD-Granat laser device (OOO "Alkom Medika", Russia) at 662 nm wavelength with 0.05 W/cm^2 power density. After a 5-minute incubation of PRP with RC in the dark, dose-dependent inhibition of platelet aggregation was observed. Laser irradiation (12.5 J/cm^2 and, especially, 25 J/cm^2) increased the inhibitory effect of RC. 3 hours after intravenous administration of RC, the rate and intensity of platelets aggregation did not change, while disaggregation slowed down significantly. Irradiation at a dose of 5 J/cm^2 did not affect the platelets aggregation kinetics, and disaggregation slowed down even more at 10 J/cm^2, and at 20 J/cm^2 the rate and intensity of platelets aggregation decreased, and no disaggregation occurred.

In vitro, RC inhibited the ADP-induced platelet aggregation in rats in a dose-dependent manner; after laser irradiation, this effect was enhanced significantly. The effect of RC on circulating platelets leads to a change in their functional state, which manifests in slowing down the disaggregation after exposure to ADP. After laser irradiation (10 J/cm^2 and, especially, 20 J/cm^2), the severity of the functional changes increases. The role of decreasing the disaggregation activity of platelets in the mechanism of vascular thrombosis in the affected area of photodynamic therapy (PDT) is discussed.

Key words: chlorin e_6, photoactivation, ADP, platelet aggregation.
For citations: Petrishchev N.N., Galkin M.A., Grishacheva T.G., Dementjeva I.N., Chefu S.G. The effect of chlorin e_6 drug on platelet aggregation activity, *Biomedical Photonics*, 2019, vol. 8, no. 3, pp. 4–10. (in Russian). doi: 10.24931/2413–9432–2019–8–3–4–10.

Contacts: Grishacheva T.G., e-mail: laser82@mail.ru

ВЛИЯНИЕ ПРЕПАРАТА НА ОСНОВЕ ХЛОРИНА E_6 НА АГРЕГАЦИОННУЮ АКТИВНОСТЬ ТРОМБОЦИТОВ

Н.Н. Петрищев[1, 2], **М.А. Галкин**[1], **Т.Г. Гришачева**[1], **И.Н. Дементьева**[1], **С.Г. Чефу**[1, 2]
[1]Первый Санкт-Петербургский государственный медицинский университет им. акад. И.П. Павлова, Санкт-Петербург, Россия
[2]Национальный медицинский исследовательский центр им. В.А. Алмазова, Санкт-Петербург, Россия

Резюме

Цель исследования – изучение влияния радахлорина на агрегационную активность тромбоцитов в опытах *in vitro* и *ex vivo*. Опыты проведены на крысах-самцах линии Wistar. Агрегационную активность тромбоцитов определяли в плазме, обогащенной тромбоцитами (PRP), турбидиметрическим методом, индуктор агрегации – аденозиндифосфат (АДФ) в конечной концентрации 1,25 μM. Пробы PRP, содержащие радахлорин, облучали при плотности мощности 0,05 Вт/см^2. После темновой инкубации в течение 5 мин PRP с радахлорином наблюдали дозозависимое угнетение агрегации тромбоцитов. Лазерное облучение (плотность энергии 12,5 Дж/см^2 и 25 Дж/см^2) усиливало ингибирующее влияние радахлорина. Через 3 ч после внутривенного введения фотосенсибилизатора скорость и интенсивность агрегации тромбоцитов не изменялись, а дезагрегация значимо замедлялась. Облучение при плотности энергии 5 Дж/см^2 не повлияло на кинетику агрегации тромбоцитов, при 10 Дж/см^2 –дезагреция еще больше замедлялась, а при 20 Дж/см^2 – уменьшались скорость и интенсивность агрегации тромбоцитов, а дезагрегация не происходило.

В условиях *in vitro* радахлорин дозозависимо ингибирует АДФ-индуцированную агрегацию тромбоцитов крыс; после лазерного облучения этот эффект значимо усиливается. Воздействие радахлорина на циркулирующие тромбоцитов приводит к изменению их функционального состояния, что проявляется в замедлении дезагрегации после воздействия АДФ. После лазерного облучения (10–20 Дж/см^2) выраженность функциональных изменений увеличивается. Обсуждается вопрос о роли снижения дезагрегационной активности тромбоцитов в механизме тромбоза сосудов в зоне воздействия при фотодинамической терапии.

Ключевые слова: хлорин e_6, фотоактивация, АДФ, агрегация тромбоцитов.

Для цитирования: Петрищев Н.Н., Галкин М.А., Гришачева Т.Г., Дементьева И.Н., Чефу С.Г. Влияние препарата на основе хлорина e_6 на агрегационную активность тромбоцитов // Biomedical Photonics. – 2019. – Т. 8, № 3. – С. 4–10. doi: 10.24931/2413–9432–2019–8–3-4–10.

Контакты: Гришачева Т.Г., e-mail: laser82@mail.ru

Introduction

The data on the impact of photodynamic effects on platelet aggregation activity are scarce and highly controversial. *In vivo* experiments with the irradiation of blood vessels of the microcirculatory bloodstream after the administration of various photosensitizers (PS) reveal platelet adhesion and aggregation in the exposure area. It is assumed that their activation occurs due to the influence of biologically active substances (adenosine diphosphate (ADP), thromboxane A2, etc.) coming from damaged endothelium [1], but some authors do not exclude photodynamic activation of platelets circulating in the blood [2]. *In vitro* experiments showed that the combined action of various PS and irradiation leads to the development of structural and functional changes in platelets, including a decrease in their aggregation activity [3–9]. In both experimental and clinical photodynamic therapy of neoplasms, PS is usually administered intravenously 2–3 hours before irradiation, and, therefore, circulating blood cells, including platelets, are exposed to the PS for a long time, which makes it possible to assume that this affects their photosensitivity.

The goal of this work was to study the effect of radachlorin on platelet aggregation activity *in vitro* and *ex vivo* before and after photoactivation.

Materials and methods

The experiments were performed on male Wistar rats weighing 240–280 g (Federal State Unitary Enterprise "Rappolovo Laboratory Animals Farm") in accordance with the "Guidelines for the Use of Laboratory Animals for Scientific and Educational Purposes at the First Pavlov State Medical University of St. Petersburg" [10], compiled on the basis of Directive 2010/63/EC of the European Parliament and of the Council of the European Union of 22 September 2010 on the protection of animals used for scientific purposes.

The animals were fed an unlimited diet of standard K-120 food (Manufacturer: Inform-Korm, Russia) and given unlimited quantity of water, and had a specific light regime of 12 hours to 12 hours (light: darkness ratio). The temperature was maintained within the range of 22–25°C, and the relative humidity was 50 to 70%. The quarantine lasted for 14 days.

Blood sampling for platelet aggregation was performed from the jugular vein in anesthetized rats (20% urethane solution, 5 ml/kg intraperitoneally). Sodium citrate (3.2%) in a 9:1 ratio was used as a blood stabilizer. To obtain platelet-rich plasma (PRP), blood was centrifuged for 10 min (200 g) at room temperature. Part of the PRP was collected in a plastic tube, and platelet-poor plasma (PPP) was obtained from the remaining blood by centrifugation for 30 min (1700 g), which was used to calibrate the optical density scale of the aggregometer and dilute PRP to a platelet concentration of $200–300 \cdot 10^9$/l. A platelet aggregation study was performed within 2 hours after PRP was produced.

Platelet aggregation activity was determined by a turbidimetric method with an AT-01 aggregometer (Manufacturer: NPF Medtech, Russia); ADP (Manufacturer: CHRONO-LOG Corporation, USA) at a final concentration of 1.25 μM was used as an aggregation inducer.

During the study, the following aggregogram indicators were recorded:

– the maximum amplitude of aggregation (MA) refers to the maximum increase in the optical transmission coefficient from the moment of ADP introduction, as a % to the optical transmission of platelet-free plasma;

– t_1 is time needed to reach MA, s;

– V_{agr} is the aggregation rate, which is MA/t_1, $\%\times s^{-1}$;

– t_2 is the time needed to halve MA, s;

– V_{disagr} is the disaggregation rate, $½\ MA/t_2$, $\%\times s^{-1}$.

PRP samples were irradiated in a polypropylene cuvette (d = 7 mm, h = 45 mm) with ALOD-Granat semiconductor laser apparatus (manufacturer: OOO Alkom Medica, Russia), wavelength: 662 nm. A fiber with a lens for external irradiation was used (OOO Polironik, Russia), fixed in a clamp stand. The fiber end face was positioned at a distance of 40 mm from the sample surface.

The photosensitizer used was a 0.35% solution of radachlorin (OOO RADAPHARMA, Russia, registration certificate No. ЛС-001868 dated December 16, 2011). After intravenous administration, the concentration of radachlorin in rat plasma was determined by spectrophotometry. At the time of administration, the calculated concentration of radachlorin, taking the hematocrit into account, was 160 μg per 1 ml of plasma. PPP was diluted to half the concentration with PBS (phosphate-buffered saline, pH 7.4) and the optical density was determined at 662 nm wth an SF-2000 spectrophotometer (AO LOMO, Russia). 800 μl of the drug was introduced into a quartz cuvette (l = 0.5 cm), the measurement was carried out in comparison with the plasma of control rats diluted to a half of the concentration with PBS. The concentration of radachlorin in the plasma was determined on the basis of a calibration graph plotted for radachlorin diluted in the

control plasma in PBS, to the concentration in range from 2.5 to 30 μg/ml.

In the first group of experiments, the effect of radachlorin on platelet aggregation *in vitro* was investigated. Radachlorin at a final concentration of 10, 20 and 40 μg/ml was added to the standard platelet content plasma, and after a 5-minute incubation in the dark, platelet aggregation activity was determined.

In the group of experiments that followed, the effect of photoactivated radachlorin on platelet aggregation *in vitro* was investigated. Radachlorin (14 μg/ml) was introduced into the plasma with the standard platelet count, and, after a 5-minute incubation in the dark, the sample was irradiated and platelet aggregation activity was determined. In the comparison group, the effect on platelet aggregation of irradiation with the same dose was investigated. Radiation exposure modes: the power density on the sample surface was 0.05 W/cm^2, and the energy density was 12.5 and 25 J/cm^2.

In the third group of experiments, an intravenous bolus injection of radachlorin (5 mg/kg) was administered into the tail vein of the animals. Before blood sampling, the animals were kept in the dark. After 3 hours, a blood sample was taken from the jugular vein, platelet-standard plasma was produced and then irradiated, and platelet aggregation activity was determined. Radiation exposure modes: the power density on the sample surface was 0.05 W/cm^2, and the energy density was 5, 10, and 20 J/cm^2.

The statistical analysis of the results was performed with IBM SPSS Statistics Version 20.0 software package. The significance of differences between the measured parameters was evaluated with Mann-Whitney U test. The differences were considered statistically significant at p values under 0.05. The results are presented as median (lower/upper quartile). A correlation analysis was performed with the use of the Spearman test.

Results and discussion

In our experiments, adenosine diphosphate (ADP) at a concentration of 1.25 μM was used to induce platelet aggregation in rat blood; the aggregation was reversible. The data on the effect of radachlorin on platelet aggregation *in vitro* are given in Table 1. After a 5-minute incubation of PRP with radachlorin, the kinetics of the process changed: the aggregation intensity decreased, aggregation and disaggregation slowed down. The severity of these effects directly depended on the concentration of radachlorin. As can be seen from Table 1, the decrease in platelet aggregation activity during incubation with radachlorin was dose-dependent (Spearman's rank correlation coefficient r = –0.915; p <0.001).

In the next group of experiments, after a 5-minute dark incubation of PRP with radachlorin, the samples were irradiated (12.5 and 25 J/cm^2). As an additional control, platelet aggregation immediately after laser irradiation in the same doses was studied in samples which contained no PS. As can be seen from the data in Table 2, laser irradiation of PRP (especially at a dose of 25 J/cm^2) led to a significant increase in the intensity of platelet aggregation; however, the kinetics of the process did not change significantly. After irradiation of PRP previously incubated with radachlorine, a decrease in the intensity of aggregation and a slowdown in disaggregation were observed, especially at a dose of 25 J/cm^2. Thus, photoactivation of radachlorin enhanced its inhibitory effect on ADP-induced rat platelet aggregation, whereas no stimulating effect of irradiation on aggregation was observed.

Таблица 1
Влияние радахлорина на АДФ-индуцированную агрегацию тромбоцитов *in vitro*
Table 1
The effect of radachlorin on ADP-induced platelet aggregation *in vitro*

Группа Group	Число крыс (N) Number of rats (N)	Максимальная амплитуда агрегации (MA), % Maximal aggregation amplitude (MA), %	Скорость агрегации ($V_{агр}$), %×с$^{-1}$ Aggregation rate (V_{aggr}), % × s^{-1}	Скорость дезагрегации ($V_{дезагр}$), %×с$^{-1}$ Disaggregation rate ($V_{disaggr}$), % × s^{-1}
Контроль Control	10	55,5 (51–61,7)	0,42 (0,39–0,45)	0,31 (0,26–0,34)
Радахлорин, 10 мкг/мл Radachlorin, 10 μg/ml	5	46 (44–49)*	0,35 (0,29–0,37)*	0,15 (0,15–0,19)*
Радахлорин, 20 мкг/мл Radachlorin, 20 μg/ml	5	36 (30–41)*	0,23 (0,23–0,29)*	0,12 (0,11–0,12)*
Радахлорин, 40 мкг/мл Radachlorin, 40 μg/ml	5	21 (21–28)*	0,2 (0,17–0,22)*	0,08 (0,08–0,09)*

* – p<0,01 по сравнению с контролем (без радахлорина)
* – p<0.01 compared to control (without Radachlorin)

Таблица 2
Влияние фотоактивированного (12,5 и 25 Дж/см²) радахлорина (14 мкг/мл) на АДФ-индуцированную агрегацию тромбоцитов
Table 2
The effect of photoactivated (12.5 and 25 J/cm²) radachlorin (14 μg/ml) on ADP-induced platelet aggregation

Показатель Criterion	Контроль (n=10) Control (n=10)	Лазерное облучение, Дж/см² Laser irradiation, J/cm²		Радахлорин (n=5) Radachlorin (n=5)	Радахлорин + лазерное облучение, Дж/см² Radachlorin + laser irradiation, J/cm²	
		12,5 (n=5)	25 (n=5)		12,5 (n=5)	25 (n=5)
Максимальная амплитуда агрегации (МА), % Maximal aggregation amplitude (MA), %	55,5 (51–61,7)	76 (76–77)*	81 (81–82)*	37 (36–39)*	29 (26–30)*#	18 (8–18)*#
Скорость агрегации ($V_{агр}$), %×с$^{-1}$ Aggregation rate (V_{aggr}), % ×s^{-1}	0,42 (0,39–0,45)	0,59 (0,57–0,64)	0,8 (0,74–0,82)	0,28 (0,26–0,29)	0,09 (0,0,08–0,15)#	0,07 (0,02–0,09)#
Скорость дезагрегации ($V_{дезагр}$), %×с$^{-1}$ Disaggregation rate ($V_{disaggr}$), % ×s^{-1}	0,31 (0,26–0,34)	0,34 (0,32–034)	0,3 (0,29–0,33)	0,13 (0,13–0,14)*	Нет дезагрегации No disaggregation	

* – p<0,01 по сравнению с контролем; # – p<0,01 по сравнению с радахлорином без лазерного облучения.
* – p<0.01 compared to control; # – p<0.01 compared to Radachlorin without laser irradiation.

Таблица 3
Влияние фотоактивированного (5, 10, 20 Дж/см²) радахлорина (через 3 ч после внутривенного введения в дозе 5 мг/кг) на АДФ-индуцированную агрегацию тромбоцитов
Table 3
The effect of photoactivated (5, 10, 20 J/cm²) Radachlorin (3 hours after intravenous administration at a dose of 5 mg/kg) on ADP-induced platelet aggregation

Группа Group	Число крыс (N) Number of rats (N)	Максимальная амплитуда агрегации (МА), % Maximal aggregation amplitude (MA), %	Скорость агрегации ($V_{агр}$), %×с$^{-1}$ Aggregation rate (V_{aggr}), % × s^{-1}	Скорость дезагрегации ($V_{дезагр}$), %×с$^{-1}$ Disaggregation rate ($V_{disaggr}$), % × s^{-1}
Контроль Control	**10**	**55,5 (51–61,7)**	**0,42 (0,39–0,45)**	**0,31 (0,26–0,34)**
в/в-введение радахлорина за 3 ч до забора крови IV-administration of Radachlorin 3 hours before blood sampling	5	68 (67–74)*	0,44 (0,41–0,46)	0,22 (0,18–0,23)*
Облучение 5 Дж/см² Irradiation 5 J/cm²	5	65 (64–68)	0,41 (0,36–0,49)	0,21 (0,15–0,22)*
Облучение 10 Дж/см² Irradiation 10 J/cm²	5	56 (56–57)	0,45 (0,43–0,46)	0,12 (0,1–0,13)#
Облучение 20 Дж/см² Irradiation 20 J/cm²	5	36 (32–37)#	0,08 (0,06–0,18)#	Нет N/A

* – p<0,05 по сравнению с контролем; # – p<0,01 по сравнению с контролем.
* – p<0.05 compared to control; # – p<0.01 compared to control

In the third group of experiments, 3 hours after intravenous administration of radachlorin to rats, blood was collected, PRP was produced, and samples were subjected to laser irradiation in different doses, and platelet aggregation activity was determined.

Based on the blood volume in rats (63 ml/kg), the maximum plasma concentration of radachlorin immediately after its administration was 160 μg/ml. 3 hours after intravenous administration, the residual concentration of PS in rat PRP blood was (38.0±1.3) μg/ml, or 24% of the initial concentration, which is consistent with the published data (10–30%) [11–14]. In this case, platelet aggregation activity did not change, and the rate of disaggregation significantly decreased. *In vitro* experiments with comparable concentrations of radachlorin (20, 40 μg/ml) showed a significantly more pronounced effect ($p < 0.01$) (Table 3.).

As can be seen from the data in Table 3, after the irradiation of PRP at a dose of 5 J/cm^2, no changes in the kinetics of platelet aggregation activity were observed, and at a dose of 10 J/cm^2, the rate of disaggregation significantly slowed down, and after irradiation at a dose of 20 J/cm^2, the intensity and spead of platelet aggregation significantly decreased, while disaggregation was not observed.

The above studies showed that radachlorin (which has chlorin e_6 as its main active substance) has a direct effect on platelet aggregation in rat blood, the effect being more pronounced in *in vitro* than in *ex vivo* experiments.

In vitro, the addition of radachlorin dose-dependently reduced the intensity of ADP-induced aggregation, which is consistent with the literature [15], and also led to a slowdown in the rate of disaggregation. This effect has not been described before. According to J.Y. Park et al. [15], chlorin e_6 affects almost all processes that are activated after the interaction of ADP with purine receptors, i. e., it acts similar to P_2Y_{12}-receptor blockers. However, this mechanism is not the only one, since we previously described the inhibitory effect of radachlorin on collagen-induced platelet aggregation in rats, which is not associated with purine receptors activation [16].

Platelet disaggregation is currently believed to be an active process. The mechanisms initiating it constantly occur in platelets, preventing their activation and aggregation in the blood flow [17]. As can be seen from the data in Table 2, radachlorin dose-dependently inhibited the rate of both aggregation and, to an even greater extent, disaggregation. A model of ADP-induced reversible platelet aggregation in rats showed that the P_2Y_{12} receptor inhibitor (CS-747) decreased the intensity of aggregation and did not affect the rate of disaggregation [18]. This confirms our assumption that the point of application of radachlorin is not only purine receptors, but also other platelet receptors.

At a high concentration of radachlorin, hardly any aggregation of rat platelets activated by ADP and collagen occurred. The aggregatogram in this case had the same pattern as in the case of Glanzmann's disease (genetic deficiency of GPIIb/IIIa receptors). Perhaps the main mechanism of the effect of radachlorin on platelet aggregation and disaggregation is associated with its effect on membrane receptors, including GPIIb/IIIa. The severity of the expression of GP receptors and the strength of their bounding with fibrinogen determine the intensity of aggregation and the possibility of disag-

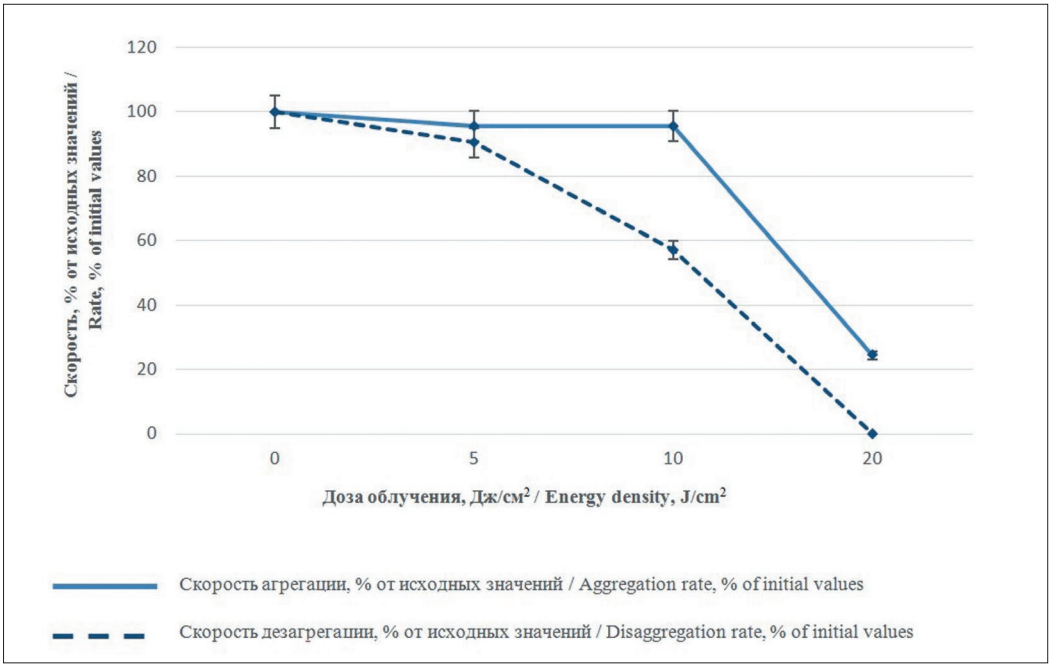

Рис. 1. Изменение скорости агрегации и дезагрегации тромбоцитов в зависимости от дозы облучения
Fig. 1. Change in the rate of aggregation and disaggregation of platelets depending on the dose of radiation

gregation. It is possible that with a high concentration of radachlorin, fibrinogen becomes irreversibly bound to GP receptors. One of the mechanisms of sharp inhibition of platelet aggregation *in vitro* at high concentrations of radachlorin, especially after light activation, may be the loss (shedding) of GP receptors. A similar effect on the platelet GP receptors is produced by a temperature increase [19].

Upon photoactivation of radachlorin, its effect on platelet aggregation and disaggregation was significantly stronger, with the process of disaggregation being more sensitive.

During PDT, the PS circulating in the blood penetrate into blood cells, including platelets; after irradiation, PS photoactivation occurs, probably resulting in photodynamic damage to platelets. It remains unclear to what extent this may affect the formation of blood clots and impaired microcirculation in the area of PDT. Very tentatively, the answer to this question can be obtained in *ex vivo* experiments by studying the aggregation activity of platelets after their prolonged contact with PS in the bloodstream.

According to our data, 3 hours after the intravenous administration of radachlorin, the rate of aggregation did not change, and the rate of disaggregation significantly decreased. Subsequent *in vitro* laser irradiation had an inhibitory effect on both processes, with a more significant impact on the disaggregation rate (Fig. 1). Based on these data, it can be assumed that irradiation of photosensitized platelets in the area of PDT can lead to a change in their functional activity, but the severity of these changes is unlikely to be significant for microcirculation disturbance. A decrease in disaggregation activity can be considered as a factor contributing to thrombosis during platelet activation by thrombogenic factors (ADP, thromboxane A2, etc.), which are released from damaged endothelial cells in the PDT zone.

Conclusion

In vitro, radachlorin dose-dependently inhibits ADP-induced rat platelet aggregation; after laser irradiation, this effect significantly increases. The effect of radachlorin on circulating platelets leads to a change in their functional state, which is manifested in a slowdown in disaggregation. After laser irradiation, the functional changes become more severe. Decreased platelet disaggregation activity may be significant in the mechanism of vascular thrombosis in the area of PDT exposure.

REFERENCES

1. Senge M.O., Radomski M.W. Platelets, photosensitizers, and PDT, *Photodiagnosis and Photodynamic Therapy*, 2013, no. 10, pp. 1–16.
2. Zhou Chuannong. Mechanisms of tumor necrosis induced by photodynamic therapy, *Journal of Photochemistry and Photobiology, B: Biology*, 1989, no. 3, pp. 299–318.
3. Zieve P.D., Solomon H.M., Krevans J.R. The effect of hematoporphyrin and light on human platelets. I. Morphologic, functional, and biochemical changes, *J. Cell. Physiol.*, 1966, no. 67, pp. 271–279. Doi: 10.1002/jcp.1040670207.
4. Solomon H.M., Zieve P.D., Krevans J.R. The effect of hematoporphyrin and light on human platelets. II. Uptake of hematoporphyrin, *J Cell Physiol*, 1966, Apr, vol. 67, no. 2, pp. 281–284.
5. Zieve P.D., Solomon H.M. The effect of hematoporphyrin and light on human platelets. III. Release of potassium and acid phosphatase, *J. Cell. Physiol.* 1966, № 68, pp. 109–111. Doi: 10.1002/jcp.1040680204.
6. Samal A.B., Zorina T.E., Cherenkevich S.N. Chlorin e6 sensitized photoinhibition of platelet aggregation: participation of reactive oxygen species, *Gematologiya i transfuziologiya*, 1991, vol. 36, no. 4, pp. 19–21. (In Russ.).
7. Samal A.B., Zorina T.E., Veselko N.I., Hmara N.F., Cherenkevich S.N. Chlorin e6 photosensitized inhibition of human platelet aggregation, *Farmakologiya i toksikologiya*, 1991, vol. 54, no. 1, pp. 32–34. (In Russ.).
8. Hendersen B.W., Wieman T.J., Haydon P.S. The effects of thrombocytopenia on vessel stasis and macromolecular leakage therapy using photofrin, *Photochem Photobiol.*, 1997, no. 66, pp. 513–517.
9. Zorina T.N., Dalidovich A.A., Marchenko L.N., Krivonosov V.V., Kravchenko I.E., Zorin V.P. Mechanisms of photodynamic therapy of neovascular ocular fundus diseases, *Materialy nauchno-prakticheskoj konferencii*, by eds. S.M. Smotrin et al., Grodno, GrSMU, 2011, pp. 27–30. (In Russ.).

ЛИТЕРАТУРА

1. Senge M.O., Radomski M.W. Platelets, photosensitizers, and PDT // Photodiagnosis and Photodynamic Therapy. – 2013. – Vol. 10. – P. 1–16.
2. Chuannong Z. Mechanisms of tumor necrosis induced by photodynamic therapy // Journal of Photochemistry and Photobiology. B: Biology. – 1989. – No. 3. – P. 299–318.
3. Zieve P.D., Solomon H.M., Krevans J.R. The effect of hematoporphyrin and light on human platelets. I: Morphologic, functional, and biochemical changes // J. Cell. Physiol. – 1966. – Vol. 67. – P. 271–279. Doi:10.1002/jcp.1040670207.
4. Solomon H.M., Zieve P.D., Krevans J.R. The effect of hematoporphyrin and light on human platelets. II: Uptake of hematoporphyrin // J. Cell. Physiol. – 1966. – Vol. 67, No. 2. – P. 281–284.
5. Zieve P.D., Solomon H.M. The effect of hematoporphyrin and light on human platelets. III: Release of potassium and acid phosphatase // J. Cell. Physiol. – 1966. – Vol. 68. – P. 109–111. Doi: 10.1002/jcp.1040680204.
6. Самаль А.Б., Зорина Т.Е., Черенкевич С.Н. Сенсибилизированное хлорином e_6 фотоингибирование агрегации тромбоцитов: участие активных форм кислорода // Гематол. и трансфузиол. – 1991. – Т. 36, № 4. – С. 19–21.
7. Самаль А.Б., Зорина Т.Е., Веселко Н.И. Фотосенсибилизированное хлорином e_6 ингибирование агрегации тромбоцитов человека // Фармакол. и токсикол. – 1991. – Т. 54, № 1. – С. 32–34.
8. Hendersen B.W. Wieman T.J., Haydon P.S. The effects of thrombocytopenia on vessel stasis and macromolecular leakage therapy using photofrin // Photochem Photobiol. – 1997. – Vol. 66. – P. 513–517.
9. Зорина Т.Н., Далидович А.А., Марченко Л.Н. Механизмы фотодинамической терапии неоваскулярных заболеваний глазного дна // Материалы науч.-практ. конф. / под ред. С. М. Смотрина [и др.]. – Гродно: ГрГМУ, 2011. – С. 27–30.

10. Belozerceva I.V., Dravolina O.A., Tur M.A. *Rukovodstvo po ispol'zovaniyu laboratornyh zhivotnyh dlya nauchnyh i uchebnyh celej v PSPbGMU im. akad. I.P. Pavlova* [Guidelines for the use of laboratory animals for scientific and educational purposes at Pavlov FSPbSMU], by. E.E. Zvartau as eds. Sankt-Peterburg, SPbSMU, 2014, 80 p.
11. Privalov V.A., Lappa A.V., Seliverstov O.V., Faizrakhmanov A.B. et al. Clinical Trials of a New Chlorin Photosensitizer for Photodynamic Therapy of Malignant Tumors. Proc, *SPIE The International Society for Optical Engineering*, 2002, p. 4612. Doi: 10.1117/12.469355.
12. Shi H., Liu Q., Qin X., Wang P., Wang X. Pharmacokinetic study of a novel sonosensitizer chlorin-e6 and its sonodynamic anti-cancer activity in hepatoma-22 tumor-bearing mice, *Biopharm Drug Dispos*, 2011, Sep; vol. 32, no. 6, pp. 319–32. Doi: 10.1002/bdd.761.
13. Shton I.O., Sarnatskaya V.V., Prokopenko I.V., Gamaleia N.F., Gamaleia N.F. Chlorin e6 combined with albumin nanoparticles as a potential composite photosensitizer for photodynamic therapy of tumors, *Exp. Oncol*, 2015, Dec, vol. 37, no. 4, pp. 250–254. PMID: 26710836.
14. Volovetsky A.B., Sukhov V.S., Balalaeva I.V., Dudenkova V.V. et al. Pharmacokinetics of Chlorin e6-Cobalt Bis(Dicarbollide) Conjugate in Balb/c Mice with Engrafted Carcinoma, *Int. J. Mol. Sci*, 2017, vol. 18, no. 12, pp. 2556. Doi: 10.3390/ijms18122556.
15. Park J.Y., Ji H.D., Jeon B.R., Im E.J., Son Y.M., Lee J.Y., Lee D.H., Lee Y.C., Hyun E., Jia Q. et al. Chlorin e6 prevents ADP-induced platelet aggregation by decreasing PI3K-Akt phosphorylation and promoting cAMP production, *Evid Based Complement Alternat Med*, 2013. Doi: 10.1155/2013/569160.
16. Grishacheva T.G., Dement'eva I.N., Chefu S.G., Petrishchev N.N. Effect of Radachlorin photosensitizer and photodynamic treatment on collagen-induced platelet aggregation, *Lazernaya medicina*, 2017, no. 4, pp. 42–46. (In Russ.).
17. Maayani S., Tagliente T.M., Schwarz T., Craddock-Royal B., Alcala C., Marrero G., Martinez R. Deaggregation is an integral component of the response of platelets to ADP in vitro: kinetic studies of literature and original data, *Platelets*. 2001, vol. 12, no. 5, pp. 279–291. Doi: 10.1080/09537100120071004.
18. Sugidachi A., Asai F., Ogawa T., Inoue T. and Koike H. The in vivo pharmacological profile of CS–747, a novel antiplatelet agent with platelet ADP receptor antagonist properties, *British Journal of Pharmacology*, 2000, № 129, pp. 1439–1446. Doi: 10.1038/sj.bjp.0703237.
19. Wang Z., Cai F., Chen X. et al. The Role of Mitochondria-Derived Reactive Oxygen Species in Hyperthermia-Induced Platelet Apoptosis. *PLoS ONE*, 2013, vol. 8, no. 9, pp. e75044. Doi: 10.1371/journal.pone.0075044.

10. Белозерцева И.В., Драволина О.А., Тур М.М. Руководство по использованию лабораторных животных для научных и учебных целей в ПСПбГМУ им. акад. И. П. Павлова / под ред. Э.Э. Звартау. – СПб.: СПбГМУ, 2014. – 80 с.
11. Privalov V.A., Lappa A.V., Seliverstov O.V. Clinical Trials of a New Chlorin Photosensitizer for Photodynamic Therapy of Malignant Tumors // Proc. SPIE The International Society for Optical Engineering. – 2002. – P. 4612. Doi: 10.1117/12.469355.
12. Shi H., Liu Q., Qin X. et al. Pharmacokinetic study of a novel sonosensitizer chlorin-e6 and its sonodynamic anti-cancer activity in hepatoma-22 tumor-bearing mice // Biopharm. Drug. Dispos. – 2011. – Vol. 32, № 6. – P. 319–332. Doi: 10.1002/bdd.761.
13. Shton I.O., Sarnatskaya V.V., Prokopenko I.V. Chlorin e6 combined with albumin nanoparticles as a potential composite photosensitizer for photodynamic therapy of tumors // Exp. Oncol. – 2015. – Vol. 37, № 4. – P. 250–254. PMID: 26710836.
14. Volovetsky A.B., Sukhov V.S., Balalaeva I.V. et al. Pharmacokinetics of Chlorin e6-Cobalt Bis(Dicarbollide) Conjugate in Balb/c Mice with Engrafted Carcinoma // Int. J. Mol. Sci. – 2017. – Vol. 18, № 12. – P. 2556. Doi: 10.3390/ijms18122556.
15. Park J.Y., Ji H.D., Jeon B.R. et al. Chlorin e6 prevents ADP-induced platelet aggregation by decreasing PI3K-Akt phosphorylation and promoting cAMP production // Evid Based Complement Alternat Med. – 2013. Doi: 10.1155/2013/569160.
16. Влияние фотосенсибилизатора радахлорина и фотодинамического воздействия на индуцированную коллагеном агрегацию тромбоцитов / Т. Г. Гришачева, И. Н. Дементьева, С. Г. Чефу, Н. Н. Петрищев // Лазер. мед. – 2017. – № 4. – С. 42–46.
17. Maayani S., Tagliente T. M., Schwarz T. et al. Deaggregation is an integral component of the response of platelets to ADP in vitro: kinetic studies of literature and original data // Platelets. – 2001. – № 12 (5). – P. 279–291. Doi: 10.1080/09537100120071004.
18. Sugidachi A., Asai F., Ogawa T. et al. The in vivo pharmacological profile of CS–747, a novel antiplatelet agent with platelet ADP receptor antagonist properties // British Journ. of Pharmacology. – 2000. – № 129. – P. 1439–1446. Doi: 10.1038/sj.bjp.0703237.
19. Wang Z., Cai F., Chen X. et al. The Role of Mitochondria-Derived Reactive Oxygen Species in Hyperthermia-Induced Platelet Apoptosis // PLoS ONE. – 2013. – Vol. 8, № 9. – P. e75044. Doi: 10.1371/journal.pone.0075044.

EXPERIMENTAL STUDIES OF OPTOACOUSTIC EFFECT ON THE MODEL OF ERYTHROCYTES IN THE PRESENCE OF CARBON NANOPARTICLES

Kravchuk D.A.[1], **Orda-Zhigulina D.V.**[2, 3]
[1]Southern Federal University, Taganrog, Russia
[2]OOO "Parametrika", Taganrog, Russia
[3]The Southern Scientific Centre of the Russian Academy of Sciences, Rostov-on-Don, Russia

Abstract

Experimental model has been developed to study optoacoustic signal from model blood cells presented by polystyrene microspheres with nanoparticles. It was found out that nanoparticles due to their strong absorption of light significantly affect the coefficient of cellular optical absorption, while the thermophysical parameters, namely the coefficient of thermal expansion, compressibility and isobaric specific heat of cells remain unchanged, since nanoparticles occupy a small intracellular volume compared to the cell volume. Optoacoustic signals were obtained using model solutions at various concentrations of cells and nanoparticles using 1064 nm laser. The results of experimental measurements using LIMO 100–532/1064-U system based on Nd:YAG showed that the amplitude of the optoacoustic signal increased without increasing the temperature in the laser area.

Keywords: optoacoustic signal, hematocrit, aggregation, erythrocytes, spectral power density, laser.

For citations: Kravchuk D.A., Orda-Zhigulina D.V. Experimental studies of optoacoustic effect on the model of erythrocytes in the presence of carbon nanoparticles, *Biomedical Photonics*, 2019, vol. 8, no. 3, pp. 11–18. (in Russian) doi: 10.24931/2413–9432–2019–8–3-11–18.

Contacts: Kravchuk D.A., e-mail: kravchukda@sfedu.ru

ЭКСПЕРИМЕНТАЛЬНЫЕ ИССЛЕДОВАНИЯ ОПТОАКУСТИЧЕСКОГО ВОЗДЕЙСТВИЯ НА МОДЕЛЬ ЭРИТРОЦИТОВ В ПРИСУТСТВИИ УГЛЕРОДНЫХ НАНОЧАСТИЦ

Д.А. Кравчук[1], **Д.В. Орда-Жигулина**[2, 3]
[1]Южный федеральный университет, Таганрог, Россия
[2]ООО «Параметрика», Таганрог, Россия
[3]Южный научный центр РАН, Ростов-на-Дону, Россия

Резюме

Разработана экспериментальная модель для изучения оптико-акустического сигнала от моделей клеток крови, представляющих собой полистирольные микросферы с наночастицами. Установлено, что наночастицы из-за их сильного поглощения света существенно влияют на коэффициент клеточного оптического поглощения, при этом теплофизические параметры, а именно коэффициент теплового расширения, сжимаемость и изобарическая удельная теплоемкость клеток остаются неизменными, так как наночастицы занимают незначительный внутриклеточный объем по сравнению с объемом самой клетки. Оптоакустические сигналы были получены с использованием модельных растворов при различных концентрациях клеток и наночастиц для воздействия лазером с длиной волны 1064 нм. Экспериментальные данные, полученные с помощью лазерной установки LIMO100–532/1064-U на основе Nd:YAG, показали, что амплитуда оптоакустического сигнала возрастала без увеличения температуры в зоне воздействия лазера.

Ключевые слова: оптоакустический сигнал, гематокрит, агрегация, эритроциты, спектральная плотность мощности, лазер.

Для цитирования: Кравчук Д.А., Орда-Жигулина Д.В. Экспериментальные исследования оптоакустического воздействия на модель эритроцитов в присутствии углеродных наночастиц // Biomedical Photonics. – 2019 – Т. 8, № 3 – С. 11–18. doi: 10.24931/2413–9432–2019–8–3-11–18.

Контакты: Кравчук Д.А., e-mail: Kravchukda@sfedu.ru

Introduction

Optoacoustic (OA) imaging represents combined technology used for imaging in biological tissues, which is provided by recording broadband ultrasonic (US) signals generated in biological tissues illuminated by laser. Unlike ionizing imaging techniques such as X-ray, computed tomography, positron emission tomography, only low-energy photons and US waves are used in optoacoustic transformation. For example, photon energy of visible infrared light for optoacoustic imaging is only about 2 eV, while the energy of typical X-rays for radiography is about 10–100 keV. Thus, optoacoustic imaging is safe method of non-invasive studies, especially promising for frequent application. Pure optical imaging techniques such as optical coherence tomography, fluorescence imaging and various types of optical microscopy are widely used in biomedicine and are applied to study cells and biological structures. Mainly spectroscopic features of the interaction of light and tissue, internal optical contrasts (scattering, absorption, refractive index, polarization, etc.) are used in these methods. For depths about millimeter pure optical imaging techniques use short wave of coherent light and provide high-resolution imaging for biomedical research, both at the cellular scale and for individual organs and tissues. However, beyond millimeter depth photons are strongly scattered in biological tissues, which limits the spatial resolution of purely optical imaging techniques for most biomedical applications where imaging of deeper tissue layers is required while maintaining relatively high resolution [1]. The relative low spatial resolution of this method prevents further clinical application and reduces the potential of this technique in diagnostic medicine, although during the early development of malignancy and hemorrhage there is significant contrast of optical scattering/absorption along with key physiological changes (hemoglobin, oxygenation, etc.).

In contrast to the strong scattering of the optical beam, the scattering of US waves in biological tissues is two or three orders weaker [2, 3], as a result US wave provides improved signal-to-noise ratio and higher spatial resolution compared to the diffuse photon wave for deeply located objects in biological tissues. Independent image contrast, which is absent in other imaging methods such as ultrasonography, radiography and magnetic resonance imaging (MRI), is used as one of the key optical biomarkers for tumor detection by optical absorption provided by OA imaging [4–7].

Various metallic and non-metallic nanoparticles are widely used as contrast agents in OA imaging techniques to improve its sensitivity. Biomedical imaging uses various nanoscale structures such as nanospheres, nanorods, silver, gold nanosystems, and carbon nanotubes (CNTs) as contrast enhancers.

Analysis of a lot of works published mainly in the last three years, concerning the problem of toxicity of nanotubes in living organisms and environment showed: in [8] it is noted that nanotubes are widely used in biomedicine and in conjunction with proteins play important role in the potential cytotoxicity of nanomaterials. The effect of fibrinogen shells on the biodegradation and cytotoxicity of single-wall CNTs was studied. Investigations have shown that fibrinogen binding reduces the toxicity of CNTs without affecting their biodegradation in activated cells, which opens up new opportunities in the development of safe nanotubes for biomedical applications; [9] provides critical review of available data on the effects of CNTs on human health to assess the risks associated with the use of CNTs. The CNTs parameters most likely to control toxicity, namely length, metal content, tendency to aggregation/agglomeration and chemical composition of the surface, were determined. It is noted that since CNTs have a great useful potential, it is necessary to carefully select their parameters to avoid harmful effects. In [10] it is noted that CNTs have shown promising potential in various biomedical applications. Two groups of mice were studied, which were injected with different CNTs. As a result, no significant toxicity was detected for the administered doses in any of the groups. The paper [11] discusses aspects of the use of CNTs in the treatment of melanoma, such as reducing toxicity and increasing biocompatibility. The authors propose methods to solve the problem and talk about the prospects of CNTs as a means of drug's delivery to the tumor.

Carbon nanoparticles are most suitable for diagnosis and therapy due to their simple and rapid preparation, tunable light scattering and absorption properties, ability to bind to target cells, and lack of toxicity.

Summarizing the data of the studies conducted by numerous authors, the following can be noted. The toxicity of nanotubes is not fully understood, but there is evidence that functionalized (associated with any material) nanotubes exhibit low toxicity. Toxicity also depends on the parameters of the nanotubes, such as the length and number of walls. In general, CNTs represent effective tool in therapy and diagnosis, which is noted by all authors.

The presented experimental work is based on previous studies by both the authors and other scientists [9–14]. The aim of the work is experimental verification of the theoretical model of the optoacoustic effect in the moving medium in the presence of nanoscale particles [15]. In comparison with the studies of other authors [16, 17], acoustic signal from nano objects in the moving liquid which is placed in the tube and connected to pump was registered in experiment.

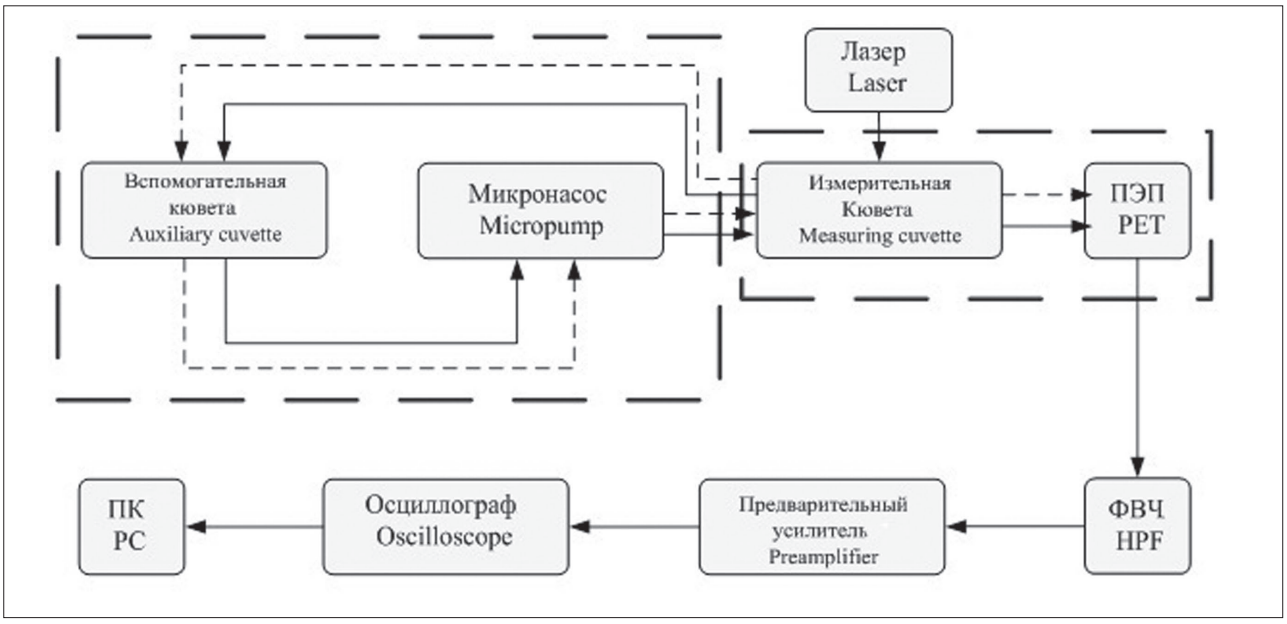

Рис. 1. Структурная схема экспериментальной установки для исследования формирования акустического сигнала в суспензиях при оптоакустическом преобразовании
Fig. 1. Block diagram of the experimental setup for the study of the formation of an acoustic signal in suspensions during optoacoustic conversion

Materials and methods

The block diagram of measurement of amplitude time realization and acoustic waves spectrum as a result of OA transformation in model liquid is shown in Fig. 1. The model fluid contains erythrocyte models and nanoscale objects (carbon nanotubes), the fluid velocity was constant, the temperature was 37±1 °C.

The pump makes it possible to form volumetric fluid velocity identical to the volumetric blood flow velocity in the human body (4 liter/min) [18–23]. When converted into linear velocity for a tube with a diameter 7 mm, we obtain 2.89 cm/s, this corresponds to the size of the arteriole in the human body and the speed of blood flow in it.

The laser beam was directed to the surface of a moving model liquid located in a measuring thermostatic cell [24]. As a result of the optoacoustic transformation, acoustic waves are formed in the model liquid, which interact with the models of erythrocytes and the conglomerate of nanoscale particles and liquid flow, amplitude and profile of the acoustic signal were changed. The acoustic signal was detected by piezoceramic transducer (probe), fed to the high-pass filter to isolate the useful signal and suppress the low-frequency noise of the laser.

Digital oscilloscope based on LabView platform (National Instruments, USA) records experimental data values. The oscilloscope is connected to personal computer (PC), where data was processing in Matlab software (MathWorks, USA), that allows to compare theoretical calculations and experimental data.

Pulses with duration 84 ns and repetition period 10 kHz was formed by LIMO 100–532/1064-U [12, 24] by single-mode Nd: YAG laser with variable power level 0.1–100 W, the installation parameters are given in table. 1.

The laser pulse repetition rate, which determines the fundamental harmonic frequency of the generated optoacoustic signal, was set programmatically in Labview as 10 kHz [12–14].

When exposed to laser beam (with the laser parameters given in table 1) acoustic waves were formed on the model liquid in cuvette as a result of OA transformation. Experiments were carried out for different types of model solutions with models of erythrocytes and carbon nanotubes.

In the experiment a number of model fluids with fillers were used to model blood and red blood cells. Next, consider the types of liquids and their characteristics.

Таблица 1
Параметры измерительной установки LIMO 100–532/1064–4
Table 1
LIMO 100–532/1064–4 measurement system parameters

Длительность импульса, нс Pulse duration, ns	84
Однородность пучка лазерного излучения, % Laser beam homogeneity, %	98,5
Энергия в импульсе (E), мДж Pulse energy (E), mJ	11
Диаметр лазерного луча (d), мм Laser beam diameter (d), mm	3,5

Sodium phosphate solution (sodium chloride solution, sodium hydrophosphate Na_2HPO_4, potassium chloride KCl and potassium dihydrophosphate KH_2PO_4) was prepared as a homogeneous absorbing medium for the experiment. Osmotic concentration and pH (7.32) of the solution are identical to blood plasma.

Polystyrene microspheres (PST) with diameter 5, 8, 15 and 20 microns (Fig. 2), produced in "Diapharm" LCC (Russia) were used for simulation. The size of polystyrene spheres was chosen to match the size of red blood cells, which are normally biconvex discs with a diameter of about 5–6 microns and average thickness of 2.0 microns. The optical absorption coefficient of the spheres is in good agreement with the data for erythrocytes in equivalent concentrations. Erythrocytes were experimentally modeled with spherical polystyrene spheres to test the theoretical model, where scattering objects were modeled as spheres in the first order approximation. Currently, the authors have moved to the next stage: theoretical modeling of real forms of red blood cells and calculation of optoacoustic response. To confirm the theoretical results, the production of polystyrene "erythrocytes", i.e. biconvex discs, will be provided.

To count the number of microspheres, the technique of counting red blood cells in the Goryaev chamber was used: it is necessary to count microspheres in five large squares located in different places of the solution sample, for example, diagonally. Thus, knowing the sum of the microspheres in five large squares (80 small), we found the arithmetic mean number of microspheres in one small square. Multiplying the found number by 4000 (the volume of the chamber space over one small square is 1/4000) we obtained the number of microspheres in 1 mm^3 of diluted blood. As a result, we got the number in terms of 1 liter of blood, i.e. the number of millions of microspheres.

The suspension was further diluted with deionized water to obtain lower concentrations (100 % = $5 \cdot 10^6$ particles/μliter).

Nanoparticles are known to be used in medicine as contrast enhancers in various optical imaging techniques such as optical coherence tomography, fluorescence imaging, and optical reflection microscopy. CNTs are cylindrical molecules that consist of rolled sheets of single-layer carbon atoms (graphene). CNTs with average length 5 μm and diameter 20 nm, which were manufactured in the Scientific Educational Center "Nanotechnology" of Southern Federal University, were used in experiment. Nanotubes are structured particles that do not dissolve in water or organic liquids. Mixing in ultrasonic bath was applied for their suspension. The output result was closer to carbon nanofibers with an average length 70–100 μm and diameter 30–50 nm.

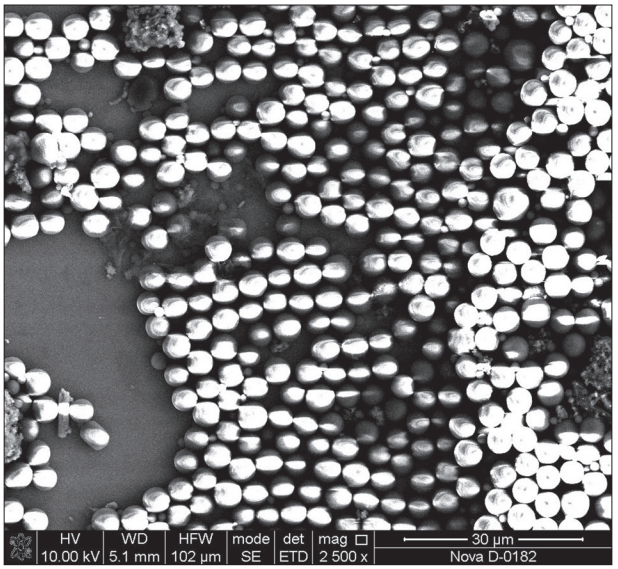

Рис. 2. Полистирольные микросферы в модельном растворе (70% микросфер) (Nova Nanolab 600)
Fig. 2. Polystyrene microspheres in a model solution (70% microspheres) (Nova Nanolab 600)

Results

During the experiments on investigation of acoustic signal generation in model suspensions, control images of the solutions were taken (Fig. 2) using the scanning electron microscope Nova Nanolab 600 (FEI Company, the Netherlands) and microscope Olympus X-71 (NTEGRA Vita, Russia).

As seen in Fig. 2, carbon nanotubes assemble into conglomerates, while "capturing" microspheres. This process can be viewed using images obtained with the scanning microscope Nova Nanolab 600 (Fig. 3).

The ability of nanoparticles and their conglomerates to encapsulate substances is demonstrated in Fig. 4.

The time of laser exposure was about 80 ns (time of signal peak growth). The signal amplitude increased by 28% with the increase of laser power by 15%. At the same time, we note that the relaxation time after the peak of heating changed, so at the power 0.085 W, the relaxation time was 9.2 μs, and at 0.1 W – 18.5 μs. This is further illustrated in Fig. 5.

On Fig. 6 the profiles of acoustic signal generated in sodium-phosphate solution and sodium-phosphate solution with 52% of microspheres are given, which corresponds to hematocrit parameters [8–10].

From Fig. 6 it is seen that the relaxation time in the solution without microspheres is 0.52 ms. In the presence of microspheres, the relaxation time of the acoustic signal decreases (up to 0.45 ms) due to absorption and scattering of the optical signal by the spheres, while an increase in the signal amplitude and shift in the signal spectrum towards lower frequency is observed (Fig. 7), which also indicates on the greater absorption capac-

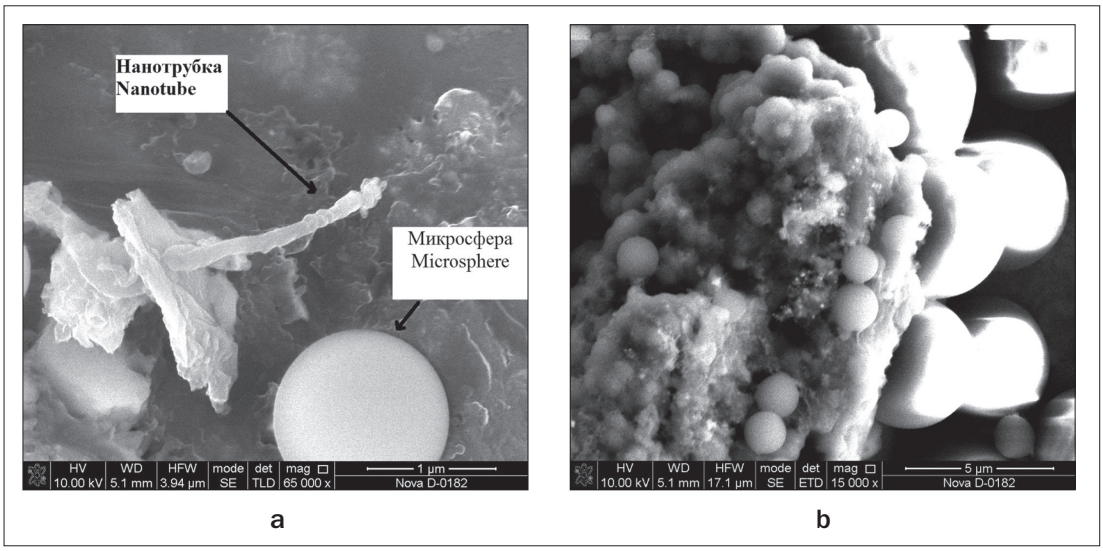

Рис. 3. Раствор полистирольных микросфер:
a – полистирольная микросфера с нанотрубкой;
b – конгломерат наночастиц с микросферами в модельном растворе (Nova Nanolab 600)
Fig. 3. Polystyrene microspheres solution:
a – polystyrene microsphere with nanotube;
b – conglomerate of nanoparticles with microspheres in a model solution (Nova Nanolab 600)

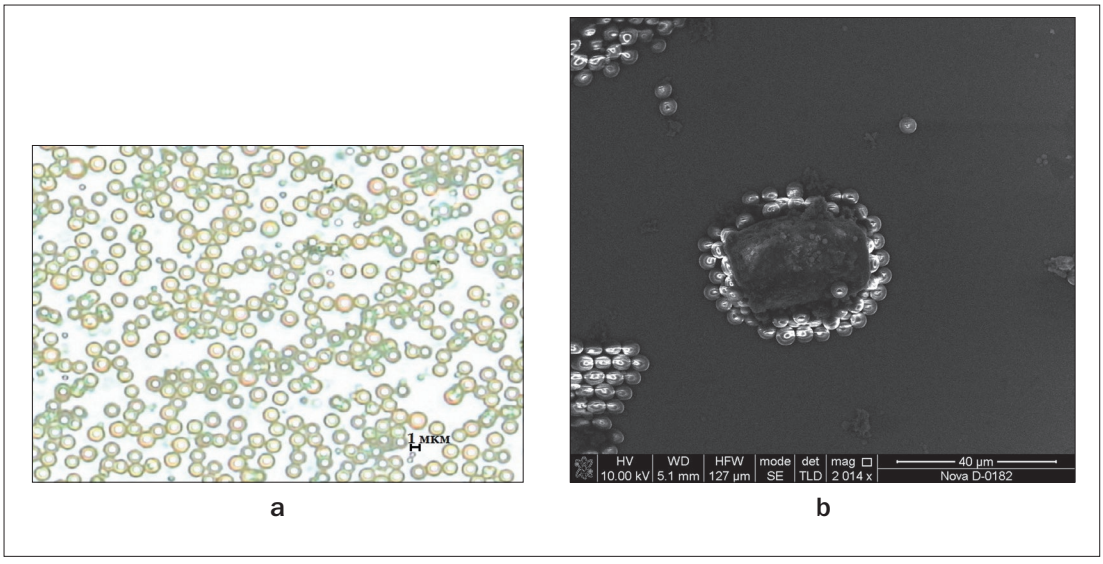

Рис. 4. Натрий-фосфатный раствор с микросферами и углеродными наночастицами:
a – изображение, полученное на оптическом микроскопе Olympus X-71
b – изображение, полученное на растровом микроскопе Nova Nanolab 600
Fig. 4. Sodium phosphate solution with microspheres and carbon nanoparticles:
a – image from Olympus X-71 optical microscope;
b – image from scanning electron microscope Nova Nanolab 600

ity of solution. Fluctuations of the relaxation part of the signal due to multiple reflections from microspheres are also observed in the profile of the acoustic signal with microspheres.

Conclusion

The authors of this work theoretically [13, 14, 24] and experimentally [12, 15] investigated the OA signal in a moving liquid in the presence of CNTs. Since it is supposed to diagnose erythrocytes by blood flow, experimental installation was designed and tested that allows to simulate the movement of blood in a vessel. It is shown that at low velocities (in medium vessels) the influence of the flow can be neglected.

Experimental studies of the effect of contrast agents based on nanoparticles on the formation of the opto-

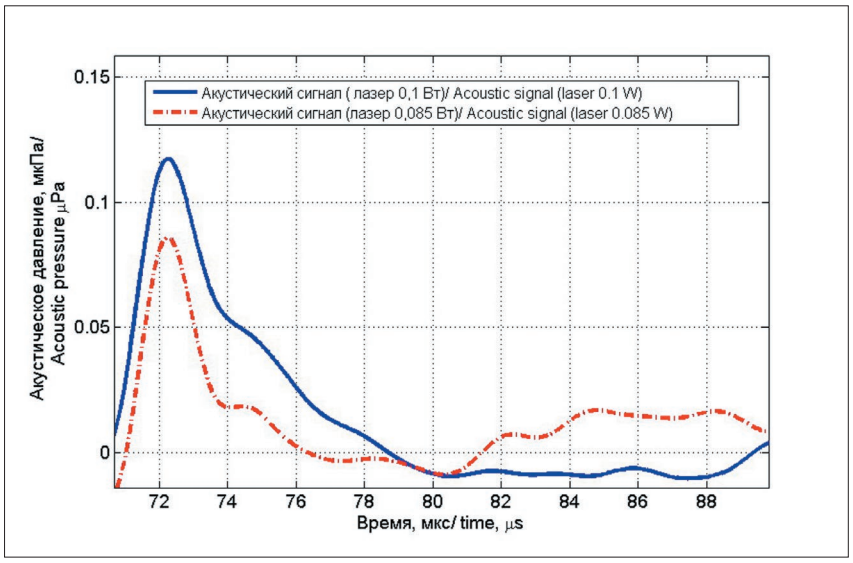

Рис. 5. Акустический сигнал, зарегистрированный в водном растворе при различных используемых мощностях
Fig. 5. Acoustic signal registered in aqueous solution at various used laser power

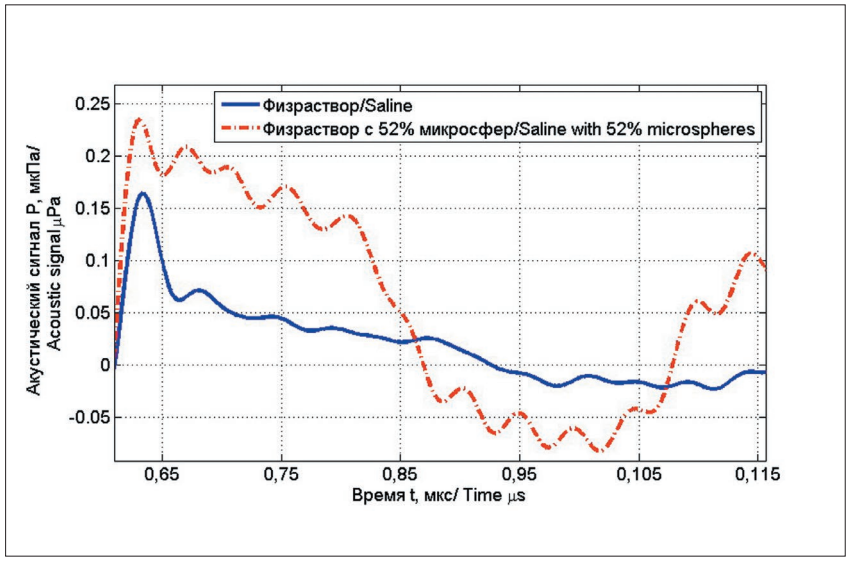

Рис. 6. Регистрируемые опытные значения оптоакустического сигнала в чистом физрастворе и физрастворе, содержащем микросферы
Fig. 6. Recorded experimental optoacoustic signal in pure saline and saline containing microspheres

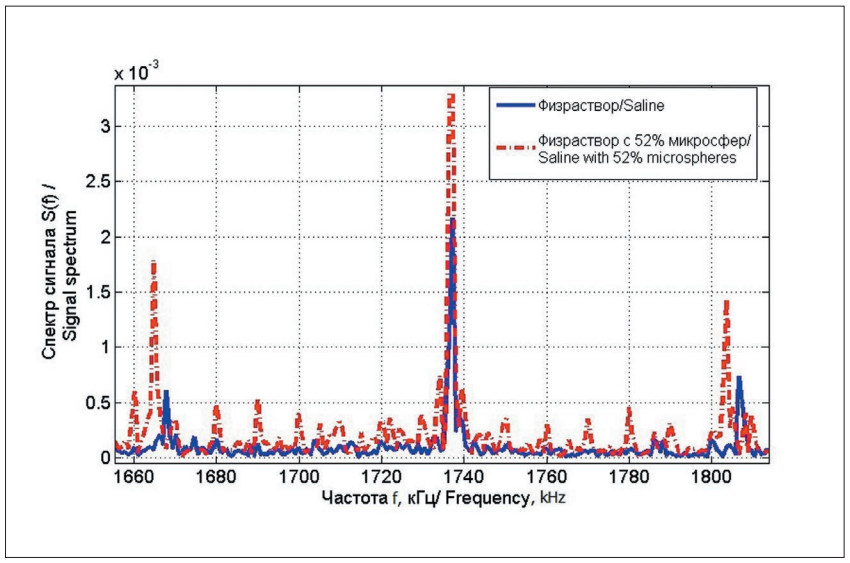

Рис. 7. Спектр оптоакустического сигнала в чистом физрастворе и физрастворе, содержащем микросферы
Fig. 7. Optoacustic signal spectrum in pure saline and saline containing microspheres

acoustic signal showed an increase in the amplitude of the OA signal due to increased absorption by CNTs. The OA signal form at high concentration of nanoparticles confirms the theoretical calculations of the forms of the optoacoustic signal obtained in previously published works [13, 14, 24].

These results can be used in the design of systems for rapid diagnosis of blood for the presence of bacterial, cancer cells, the degree of aggregation of red blood cells.

This publication was sponsored by South Federal University.

REFERENCES

1. Yuan Z., Zhang Q., Jiang H. 3D diffuse optical tomography imaging of osteoarthritis: Initial results in finger joints, *J. Biomed Opt*., 2007, vol. 12, 034001.
2. Duck F.A. *Physical properties of tissue: a comprehensive reference book*. Academic Press, London, UK, 1990.
3. Xu M., Wang L.V. Photoacoustic imaging in biomedicine, *Rev Sci Instrum,* 2006, vol. 77, pp. 041101–041122.
4. Brecht H., Su R., Fronheiser M., Ermilov S.A., Conjusteau A., Oraevsky A.A. Wholebody three-dimensional optoacoustic tomography system for small animals, *J. Biomed Opt*., 2009, vol. 14(6), 064007.
5. Sun Y., Sobe E.S., Jiang H. First assessment of three-dimensional quantitative photoacoustic tomography for in vivo detection of osteoarthritis in the finger joints, *Med Phys*, 2011, vol. 38(7), p. 4009.
6. Wang X., Pang Y., Ku G., Xie X., Stoica G., Wang L.V. Noninvasive laser-induced photoacoustic tomography for structural and functional in vivo imaging of the brain, *Nat Biotechnol,* 2003, vol. 21, pp. 803–806.
7. Laufer J., Zhang E., Raivich G., Beard P. Three-dimensional noninvasive imaging of the vasculature in the mouse brain using a high resolution photoacoustic scanner, *Appl Opt*, 2009, vol. 48, pp. 299–306.
8. Lu N., Sui Y., Ding Y., Tian R., Peng, Y. Fibrinogen binding-dependent cytotoxicity and degradation of single-walled carbon nanotubes, *Journal of Materials Science: Materials in Medicine*, 2018, vol. 29(8), pp. 1–8.
9. Johnston H.J., Hutchison G.R., Christensen F.M., Peters S., Hankin S., Aschberger K., Stone V. A critical review of the biological mechanisms underlying the in vivo and in vitro toxicity of carbon nanotubes: The contribution of physico-chemical characteristics, *Nanotoxicology*, 2010, vol. 4(2), pp. 207–46. doi: 10.3109/17435390903569639
10. Ahmadi H., Ramezani M., Yazdian-Robati R., Behnam B., Azarkhiavi R.K, Nia H.A., Mokhtarzadeh A., Riahi M.M., Razavi B., Abnous, K. Acute toxicity of functionalized single wall carbon nanotubes: A biochemical, histopathologic and proteomics approach, *Chemico-Biological Interactions*, 2017, vol. 275, pp. 196–209.
11. Carvalho L.E., Piqueira J., Maria D. Advances in Carbon Nanotubes for Malignant Melanoma: A Chance for Treatment, *Molecular Diagnosis & Therapy*, 2018, vol. 22(6), pp. 703–715.
12. Starchenko, I.B., Kravchuk D.A., Kirichenko I.A. An optoacoustic laser cytometer prototype, *Biomedical Engineering*, 2018, vol. 51, no. 5, pp. 308–312.
13. Kravchuk D.A. Mathematical model of detection of intra-erythrocyte pathologies using optoacoustic method, *Biomedical Photonics*, 2018, vol. 7, no. 3, pp. 36–42. (in Russian)
14. Kravchuk D.A., Starchenko I.B. A theoretical model for diagnosing the effect of oxygenation of erythrocytes using optoacoustic signals, *Prikladnaya fizika*, 2018, no. 4, pp. 89–94. (in Russian)
15. Orda-Zhigulina D.V., Orda-Zhigulina M.V., Starchenko I.B., Kravchuk D.A. Experimental setup for the study of optoacoustic flow cytometry, *Modelirovanie, optimizaciya i informatsionnye tekhnologii*, 2018, vol. 6,. no. 3, pp. 19–29. (In Russian)

ЛИТЕРАТУРА

1. Yuan Z., Zhang Q., Jiang H. 3D diffuse optical tomography imaging of osteoarthritis: Initial results in finger joints // J Biomed Opt. – 2007. – Vol. 12. – 034001.
2. Duck F.A. Physical properties of tissue: a comprehensive reference book. – Academic Press, London, UK, 1990.
3. Xu M., Wang L.V. Photoacoustic imaging in biomedicine // Rev Sci Instrum. – 2006. – vol. 77. – P. 041101–041122.
4. Brecht H., Su R., Fronheiser M., et al. Wholebody three-dimensional optoacoustic tomography system for small animals // J Biomed Opt. – 2009. – Vol. 14(6). – 064007.
5. Sun Y., Sobe E.S., Jiang H. First assessment of three-dimensional quantitative photoacoustic tomography for in vivo detection of osteoarthritis in the finger joints // Med Phys. – 2011. – Vol. 38(7). – P. 4009.
6. Wang X., Pang Y., Ku G., et al. Noninvasive laser-induced photoacoustic tomography for structural and functional in vivo imaging of the brain // Nat Biotechnol. – 2003. – Vol. 21. – P. 803–806.
7. Laufer J., Zhang E., Raivich G., Beard P. Three-dimensional noninvasive imaging of the vasculature in the mouse brain using a high resolution photoacoustic scanner // Appl Opt. – 2009. – Vol. 48. – P. 299–306.
8. Lu N., Sui Y., Ding Y., et al. Fibrinogen binding-dependent cytotoxicity and degradation of single-walled carbon nanotubes // Journal of Materials Science: Materials in Medicine. – 2018. – Vol. 29(8). – P. 1–8.
9. Johnston H.J., Hutchison G.R., Christensen F.M., et al. A critical review of the biological mechanisms underlying the in vivo and in vitro toxicity of carbon nanotubes: The contribution of physico-chemical characteristics // Nanotoxicology. – 2010. – Vol. 4(2). – P. 207–46. doi: 10.3109/17435390903569639
10. Ahmadi H., Ramezani M., Yazdian-Robati R., et al. Acute toxicity of functionalized single wall carbon nanotubes: A biochemical, histopathologic and proteomics approach // Chemico-Biological Interactions. – 2017. – Vol. 275. – P. 196–209.
11. Carvalho L.E., Piqueira J., Maria D. Advances in Carbon Nanotubes for Malignant Melanoma: A Chance for Treatment // Molecular Diagnosis & Therapy. – 2018. – Vol. 22(6), – P. 703–715.
12. Starchenko I.B., Kravchuk D.A., Kirichenko I.A. An optoacoustic laser cytometer prototype // Biomedical Engineering. – 2018. – Vol. 51, No. 5. – P. 308–312.
13. Кравчук Д.А. Математическая модель обнаружения внутриэритроцитарных инфекций с помощью оптоакустического метода // Biomedical Photonics. – 2018. – Т. 7. – № 3. – С. 36–42.
14. Кравчук Д.А., Старченко И.Б. Теоретическая модель для диагностики эффекта кислородонасыщения эритроцитов с помощью оптоакустических сигналов // Прикладная физика. – 2018. – № 4. – С. 89–94.
15. Орда-Жигулина Д.В., Орда-Жигулина М.В., Старченко И.Б., Кравчук Д.А. Экспериментальная установка для исследования оптоакустической проточной цитометрии // Моделирование, оптимизация и информационные технологии. – 2018. – Т. 6, № 3. – С. 19–29.
16. Menyaev Y.A., Carey K.A., Nedosekin D.A., et al. Preclinical photoacoustic models: application for ultrasensitive single cell malaria diagnosis in large vein and artery // Biomedical optics express. – 2016. – Vol. 7, No. 9, pp. 3643–3658.

16. Menyaev Y.A., Carey K.A., Nedosekin D.A., Sarimollaoglu M., Galanzha E.I., Stumhofer J.S., Zharov V.P. Preclinical photoacoustic models: application for ultrasensitive single cell malaria diagnosis in large vein and artery, *Biomedical optics express*, 2016, vol. 7, no. 9, pp. 3643–3658.
17. Menyaev Y.A., Nedosekin D.A., Sarimollaoglu M., Juratli M.A., Galanzha E.I., Tuchin V.V., Zharov V.P. Optical clearing in photoacoustic flow cytometry, Biomedical optics express, 2013, vol. 4, no. 12, p. 3040. DOI:10.1364/BOE.4.003030
18. Belova T.V., Zavalishina S.Yu., Medvedev I.N. *Fiziologiya krovi i krovoobrashcheniya. Uchebnoe posobie* [Physiology of blood and blood circulation. Study guide]. Moscow, Lan Publ., 2015. 176 p.
19. Abakumova T.V., Gening, T.P., Mikhailov N.L., Dolgova D.R., Poludnyakova L.V. *Fiziologiya krovi. Uchebnoe posobie* [Blood physiology. Study guide]. Ulyanovsk: Ulyanovsk State University Publ., 2017. 60 p.
20. Alipov N.N. *Osnovy medicinskoj fiziologii* [Fundamentals of medical physiology]. Moscow, Praktika Publ., 2008. 496 p.
21. Lipunova E.A., Skorkina M.Yu. *Fiziologiya krovi* [Blood physiology]. Belgorod, BelGU, 2007. 324 p.
22. Kamkin A.G., Kamensky A.A. *Fundamental'naya i klinicheskaya fiziologiya* [Fundamental and clinical physiology]. Moscow, Academy Publ., 2004. 405 p.
23. Atkov O.Yu., Balakhonova T.V., Gorokhova S.G., Saidova M.A., Smolyaninova N.G., Aleksandrova-Tebenkova E.G., Arakelyants A.A., Popova E.Yu. *Ul'trazvukovoe issledovanie serdca i sosudov* [Ultrasound examination of the heart and blood vessels], ed. Atkova O. Yu. Moscow, Eksmo, 2015. 456 p.
24. Starchenko I.B., Malyukov S.P., Orda-Zhigulina D.V., Saenko A.V. Measuring complex for laser diagnostics of bioobjects using nanoparticles based on LIMO 100, *Prikaspiiskii zhurnal upravlenie i vysokie tekhnologii,* 2013, vol. 22, no. 2, pp. 166–173. (In Russian)
17. Menyaev Y.A., Nedosekin D.A., Sarimollaoglu M., et al. Optical clearing in photoacoustic flow cytometry // Biomedical optics express. – 2013. – Vol. 4, No. 12. – p. 3040. DOI:10.1364/BOE.4.003030
18. Белова Т.В., Завалишина С.Ю., Медведев И.Н. Физиология крови и кровообращения. Учебное пособие. – Москва: Лань, 2015. – 176 с.
19. Абакумова Т.В., Генинг Т.П., Михайлова Н.Л. и др. Физиология крови. Учебное пособие. – Ульяновск: Ульяновский государственный университет, 2017. – 60 с.
20. Алипов Н.Н. Основы медицинской физиологии. – М.: Практика, 2008. – 496 с.
21. Липунова Е.А., Скоркина М.Ю. Физиология крови. – Белгород: БелГУ, 2007. – 324 с.
22. Камкин А.Г., Каменский А.А. Фундаментальная и клиническая физиология. – М.: Академия, 2004. – 405 с.
23. Атьков О.Ю., Балахонова Т.В., Горохова С.Г. и др. Ультразвуковое исследование сердца и сосудов / под ред. Атькова О.Ю. – Москва: Эксмо, 2015. – 456 с.
24. Старченко И.Б., Малюков С.П., Орда-Жигулина Д.В., Саенко А.В. Измерительный комплекс для лазерной диагностики биообъектов с использованием наночастиц на базе LIMO 100 // Прикаспийский журнал управление и высокие технологии. – 2013. – Т. 22, № 2. – С. 166–173.

ANALYSIS OF EFFICIENCY OF PHOTODYNAMIC TEETH BLEACHING WITH THE USE OF PHOTOSENSITIZER CHLORINE E_6

Korshunova A.V.[1], Makarov V.I.[2], Ryabova A.V.[2], Romanishkin I.D.[2], Zorina O.A.[1, 3], Krechina E.K.[1], Ponomarev G.V.[4]

[1]Federal State Institution Central Research Institute of Dental and Maxillofacial Surgery, Moscow, Russia
[2]Prokhorov General Physics Institute of the Russian Academy of Sciences, Moscow, Russia
[3]The First Sechenov Moscow State Medical University, Moscow, Russia
[4]Institute of Biomedical Chemistry of the Russian Academy of Sciences, Moscow, Russia

Abstract

Teeth whitening is one of the most sought-after procedures in aesthetic dentistry. Discolorites that are difficult to whiten, caused by dentin changes or enamel defects, can be eliminated by oxidizing the chromogens with chemical agents that penetrate to the enamel and dentin. In recent years, the method of photodynamic bleaching (PDB) is considered to be minimally invasive. It does not use hydrogen peroxide that leads to increased sensitivity of teeth, and is relatively effective over time. A convenient solution for PDB would be to use chlorin e_6 as a photosensitizer, which has a high quantum yield of singlet oxygen generation, low phototoxicity, rapid elimination, on the one hand, and photobleaching capability, on the other. This paper presents quantitative data on the study of the effectiveness of PDB with chlorine e_6: color change for 100 teeth after the procedure, chlorine e_6 penetration into the tooth tissues, evaluation of the interstitial efficiency of the generation of singlet oxygen and photobleaching of chlorine e_6 during laser exposure. It has been statistically established that for one PDB procedure, the tooth color saturation (*C*) varies on average by 0.5 tones on the VITA scale, and the lightness of color (*L*) in some cases increases by more than 10 units.

Keywords: photodynamic teeth bleaching, photosensitizer, chlorin e_6, singlet oxygen generation.

For citations: Korshunova A.V., Makarov V.I., Ryabova A.V., Romanishkin I.D., Zorina O.A., Krechina E.K., Ponomarev G.V. Analysis of photodynamic teeth bleaching efficiency with the use of photosensitizer chlorine e_6, *Biomedical photonics*, 2019, vol. 8, no. 3, pp. 19–28. (in Russian) doi: 10.24931/2413–9432–2019–8–19–28.

Contacts: Korshunova A.V., e-mail: korshunovaanna.cniis@gmail.com

АНАЛИЗ ЭФФЕКТИВНОСТИ ФОТОДИНАМИЧЕСКОГО ОТБЕЛИВАНИЯ ЗУБОВ С ИСПОЛЬЗОВАНИЕМ ФОТОСЕНСИБИЛИЗАТОРА ХЛОРИН E_6

А.В. Коршунова[1], В.И. Макаров[2], А.В. Рябова[2], И.Д. Романишкин[2], О.А. Зорина[1, 3], Е.К. Кречина[1], Г.В. Пономарев[4]

[1]Центральный научно-исследовательский институт стоматологии и челюстно-лицевой хирургии, Москва, Россия
[2]Институт общей физики им. А.М. Прохорова РАН, Москва, Россия
[3]Первый МГМУ им. И.М. Сеченова (Сеченовский Университет), Москва, Россия
[4]Научно-исследовательский институт биомедицинской химии имени В.Н. Ореховича, Москва, Россия

Резюме

Отбеливание зубов является одной из самых востребованных процедур в эстетической стоматологии. Трудно поддающиеся отбеливанию дисколориты, вызванные изменениями дентина или дефектами эмали, могут быть устранены путем окисления хромогенов с помощью химических агентов, проникающих в эмаль и дентин. В последние годы фотодинамическое отбеливание зубов (ФДОЗ) рассматривается как минимально инвазивный и относительно эффективный по времени метод, при котором не используется перекись водорода, применение которой приводит к повышенной чувствительности зубов. Для ФДОЗ может использоваться фотосенсибилизатор (ФС) хлорин e_6, обладающий высоким квантовым выходом генерации синглетного кислорода, низкой фототоксичностью, быстрым выведением, с одной стороны, и способностью к фотообесцвечиванию, с другой. В настоящей работе

представлены количественные данные исследования эффективности ФДОЗ с хлорином e_6: изменение цвета для 100 зубов после процедуры, оценка проникновения ФС в ткани зуба, оценка внутритканевой эффективности генерации синглетного кислорода и интенсивности фотообесцвечивания ФС при лазерном воздействии. Статистически установлено, что за одну процедуру ФДОЗ насыщенность цвета зубов (*C*) изменяется в среднем на 0,5 тона по шкале VITA, а светлота цвета (*L*) в отдельных случаях повышается более чем на 10 единиц.

Ключевые слова: фотодинамическое отбеливание зубов, фотосенсибилизатор, хлорин e_6, генерация синглетного кислорода

Для цитирования: Коршунова А.В., Макаров В.И., Рябова А.В., Романишкин И.Д., Зорина О.А., Кречина Е.К., Пономарев Г.В. Анализ эффективности фотодинамического отбеливания зубов с использованием фотосенсибилизатора хлорин e_6 // Biomedical photonics. – 2019. – Т. 8, № 3. – С. 19–28. doi: 10.24931/2413–9432–2019–8–3–19–28.

Контакты: Коршунова А.В., e-mail: korshunovaanna.cniis@gmail.com

Introduction

Every year, cosmetic dentistry is becoming more and more popular among the population. One of the main procedures to correct the aesthetic imperfections of teeth is their whitening [1]. Many types of discolorites affect the appearance of teeth. The causes of discoloration vary, as does the rate at which they are removed [2]. The discoloration of the teeth may be external or internal.

External stains usually occur as a result of the accumulation of chromatogenic substances on the external surface of the tooth. These stains are localized mainly in the acquired dental film and are generated either by the Millard reaction between sugars and amino acids (including chemical rearrangements and reactions between sugars and amino acids) or are acquired as a result of the retention of exogenous chromophores [3]. Chemical analysis of the stains caused by chromatogenic food demonstrates the presence of furfurals and their derivatives. The majority of external tooth stains can be removed using standard preventative procedures, of which there are a large number today. One such method is the use of pastes with a whitening effect and other abrasive methods [4]. However, over time, such spots darken and become more resistant, but, as a rule, they can still be bleached [5].

Internal stains are usually caused by deeper stains or defects in enamel. They are a consequence of aging, as well as the consumption of chromatogenic foods and drinks, smoking, taking tetracycline antibiotics, excessive fluoride taking, severe jaundice in infancy, porphyria, microcracks in enamel, physiological and pathological abrasion of teeth, tooth decay and restorations. As a result of aging and thinning of the tooth enamel, the underlying dentin layers tend to darken due to the formation of secondary dentin, which is darker and more opaque than the original, primary dentin. The combination of these processes leads to the darkening of the teeth.

Excess fluoride in drinking water above 1–2 ppm can cause metabolic changes in ameloblasts, which leads to defects in the matrix and improper calcification of the teeth [6].

Color changes when taking medication can occur both before and after the complete formation of the tooth. Tetracycline is incorporated into dentin during tooth calcification, probably by chelating with calcium to form tetracycline orthophosphate, which causes a discoloration. Also, internal stains are associated with hereditary conditions (for example, imperfect amelogenesis and imperfect dentinogenesis) [7]. Blood entering the dentinal tubules and metals released from dental restoration materials also cause discoloration of teeth.

Internal tooth pigmentation cannot be removed using regular preventative procedures. Nevertheless, it can be eliminated by bleaching with the help of chemical agents penetrating enamel and dentin to oxidize chromogenes [8]. Stains caused by aging, genetics, smoking or coffee respond better to whitening [9], blue-gray stains due to tetracycline — worse [10], and spots of brown fluorosis are moderately sensitive [11].

Techniques for chemical whitening, in which the color of enamel and dentin changes from dark to light due to the ability of active chemical components to pass through enamel and dentin and penetrate all parts of the tooth, causing oxidative breakdown of colored pigments are actively being developed [12]. However, this effect also has a negative effect on tooth enamel, pulp and periodontal tissue [13, 14].

To reduce bleaching time in the clinic, various methods are used to accelerate the decomposition of hydrogen peroxide, including chemical (alkaline pH), physicochemical (photooxidation), and physical (heating) methods [15, 16]. Hydrogen peroxide is optically transparent in the visible spectral range; however, it can absorb ultraviolet, medium infrared and far-infrared light, which leads to its decomposition. When bleaching with intense light sources, the addition of various dyes to the whitening gels leads to an improvement in the absorption of

light in the gel and, as a result, to a decrease in the heating of the tooth pulp. In addition to heating the gel (photothermic effect) [17], dyes can also cause photochemical reactions [18].

The sources of coherent and incoherent radiation used to catalyze the hydrogen peroxide bleaching process include quartz tungsten halogen lamps, plasma arc lamps, mercury lamps, light-emitting diodes (LEDs) and lasers with various wavelengths [19–21].

In general, pigments that give the color of a tooth are cyclic molecules with π-π conjugated electronic bonds. During bleaching, π-π bonds are destroyed due to oxidation (that is, loss of electrons) or other chemical reactions, and the molecules take the form of a broken ring, which leads to a loss of their light-absorbing properties. Although hydrogen peroxide is most widely used for teeth whitening, there are a large number of other oxidizing agents (O_2, $HO_2^{\cdot}$, NaClO, O_3, $HO^{\cdot}$). When choosing agents for whitening teeth, their oxidizing ability should be taken into account, that is, they must generate reactive oxygen species that can diffuse the easiest into dentin, and be non-aggressive and non-toxic [22]. Singlet oxygen ($^1O_2$) is a very strong oxidizing agent capable of decomposing organic molecules, however, due to its high reactivity, it cannot be stored, and its use is possible only when generated *in situ* as necessary [23].

The method of photodynamic therapy (PDT), based on the generation of singlet oxygen by photosensitizers (PS) when they are irradiated with specific wavelengths, was initially presented in dentistry as an antimicrobial option — it was used to disinfect antibiotic-resistant microorganisms without causing resistance [24]. Now PDT is actively used in the treatment of dental caries and its complications, and is also widely used in periodontics, implantology, pathologies of the oral mucosa and maxillofacial surgery [25, 26]. The most commonly used photosensitizers in dentistry are phenothiazine-based dyes, such as toluidine blue, methylene blue and malachite green, they are photostable, and a slight change in tooth color can serve as a side effect of their use [27].

In recent years, the method of photodynamic bleaching (PDB) has been considered as minimally invasive and relatively effective in time, its use for bleaching one of the most difficult groups of tooth discolorites caused by taking tetracycline antibiotics is especially important. The most effective for PDB is the use of a potassium titanyl phosphate crystal laser ($KTiOPO_4$, KTP laser) in combination with a sulforhodamine B photosensitizer and a high concentration of hydrogen peroxide (Smartbleach® gel, Smartbleach International, Belgium) [28]. Moreover, PDB allows achieving a greater effect in a single procedure than can be expected from several months of application of bleaching mouth guards [29].

A convenient solution for PDB without the use of hydrogen peroxide, which leads to increased tooth sensitivity, can be the use of chlorin e_6 photosensitizer, which has a high quantum yield of singlet oxygen generation, low phototoxicity, rapid elimination, on the one hand, and the ability to photobleach, on the other [30]. In our earlier study, we studied the dynamics of chlorin e_6 accumulation in a 1% Geleofor gel compound in tooth tissues depending on the time of application [31]. To evaluate and select the optimal effectiveness of tooth PDB in this work, in addition to clinical observation of discoloration using a VITA spectrophotometer, quantitative characteristics of the PS penetration into the tissues of the extracted teeth were determined, interstitial efficiency of singlet oxygen generation and photobleaching of chlorin e_6 in the PDF were evaluated.

Materials and methods

Photosensitizer

Chlorin e_6, a natural derivative of chlorophyll, was used as a PS in the study as part of a 1% Geleofor gel (OOO "Lazer-Medcentr", Russia).

Tooth samples for the study

For laboratory studies, teeth of the frontal group, removed according to periodontal and surgical indications, were used. Before the research, the enamel surface was thoroughly cleaned with a brush and Detatrine-Z paste (Septodont, France). The teeth were stored in distilled water until the study. No more than two hours passed from the moment of tooth extraction to the start of the study. To assess the accumulation of chlorin e_6, both the extracted teeth and the cuts of the extracted teeth of the frontal group were obtained. In total, 100 extracted frontal teeth were used in the study. The distribution of the examined teeth shades on the Vita scale was as follows: 78 teeth - A shades (reddish-brown) and 22 teeth - B shades (yellowish-red).

To determine the optimal time for PS application, during which it penetrates the tooth tissue to the entire dentin depth necessary for effective PDB, a gel containing PS was applied to the entire vestibular surface of the extracted tooth using a dental brush for 1, 5, 10, 20 minutes. Next, the PS was washed off with running water and a tooth was cut along the vertical axis into thin cuts using a disk-shaped diamond dental bur.

Study of the PS distribution in the thickness of the tooth using laser scanning confocal microscopy

The interstitial distribution of chlorin e_6 after the gel application on the enamel was studied through laser scanning confocal microscopy using LSM-710 microscope (Carl Zeiss, Germany). To obtain the images, we used a Plan-Apochromat lens with a magnification of 10x (0.3 aperture). Thin sections of teeth were placed on 0.17 mm thick coverslips and observed in the plane of cut. To excite autofluorescence of tooth tissues and fluorescence of chlorin e_6, an argon laser (Lasos Laser GmbH, Germany) with a wavelength of 488 nm was used; autofluorescence

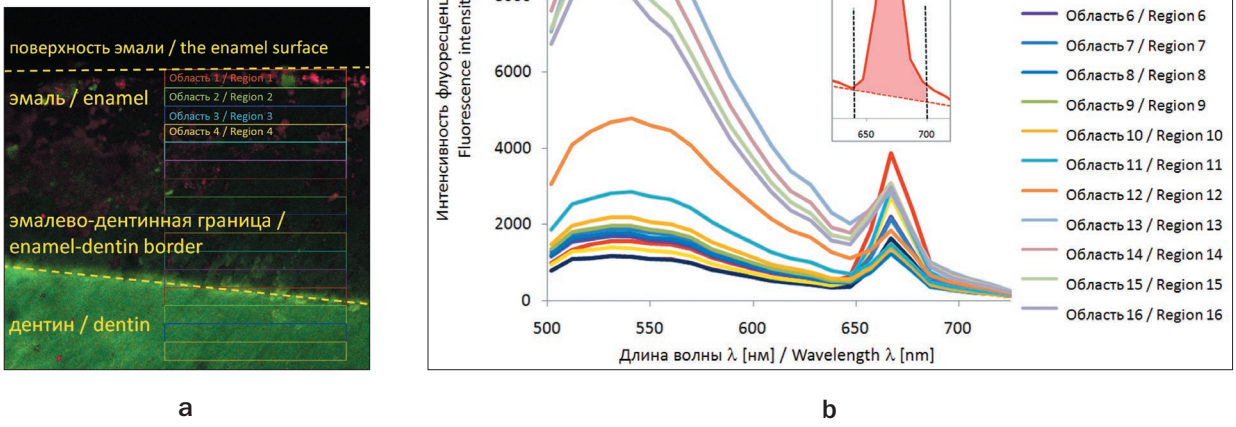

Рис. 1. Спектрально-разрешенное флуоресцентное изображение шлифа зуба, на эмаль которого был апплицирован ФС в течение 1 мин. Изображение получено при возбуждении 488 нм:
a – схема выделения прямоугольных областей на микроскопическом флуоресцентном изображении шлифа зуба для количественной оценки диффузии ФС;
b – спектры флуоресценции с выделенных прямоугольных областей шлифа зуба с шагом 40 мкм вглубь эмали от поверхности. На вкладке закрашена область под пиком флуоресценции хлорина e_6, которую использовали для построения зависимости интенсивности флуоресценции хлорина e_6 в тканях зуба на глубине от поверхности эмали

Fig. 1. Spectral-resolved fluorescent image of tooth section after 1 minute of photosensitizer application on the enamel. Image taken at 488 nm excitation:
a – a scheme for the selection of rectangular areas on a microscopic fluorescent image on the tooth section for the quantitative assessment of the photosensitizer's diffusion;
b – fluorescence spectra from selected rectangular areas of tooth section with 40 microns step into the depth of the enamel from the surface. On the inset an area under the chlorin e_6 fluorescence peak, which was used to plot the chlorin e_6 fluorescence intensity in the tooth tissue on the depth from the enamel surface, is highlighted

and fluorescence of PS were detected with 10 nm spectral resolution in the range of 500–750 nm. The result was a spectrally resolved fluorescence image of a tooth cut. Statistical and spectral analysis was carried out using ZEN software (Carl Zeiss, Germany). To quantify the PS diffusion deep into the tooth, the image of the tooth section was separated into rectangular regions at different depths from the enamel surface with a height of 40 μm and a width of 500 μm (Fig. 1*a*). Then we used the integrated fluorescence intensity of PS, averaged over the area of these rectangular regions (Fig. 1*b*). The integrated fluorescence intensity of PS was calculated from the total fluorescence spectrum by subtracting the "shoulder" of autofluorescence in the region of 640–700 nm and integrating the obtained signal over wavelengths (tab in Fig. 1*b*).

Study of the generation of singlet oxygen in the depth of the tooth

To detect the generation of singlet oxygen ($^1O_2$), we used Singlet Oxygen Sensor Green reagent (SOSG, Molecular Probes®, USA), highly selective towards $^1O_2$ and not reacting to other reactive oxygen species, such as hydroxyl radical and superoxide anion [32]. SOSG has weak blue fluorescence with excitation maxima at 372 nm and 393 nm and emission maxima at 395 nm and 416 nm. In the presence of $^1O_2$, SOSG begins to fluoresce in the green range with excitation and emission maxima of 504 nm and 525 nm, respectively, which are easy to detect. Sections of teeth, on whose enamel PS was applied for a certain time, in saline with the addition of SOSG reagent were subjected to laser irradiation with a wavelength of 633 nm directly by a scanning laser (that is, PDB was carried out in the cut plane).

The power density produced by the scanning laser beam emerging from the objective lens in the object plane was calculated as follows. The spatial resolution of the confocal microscope is determined by the size of the illuminated spot limited by diffraction. The size of the focusing spot, assuming uniform illumination, is a function of the excitation

wavelength (λ_{EX}) and the numerical aperture (NA) of the objective:

$$S_{spotsize} = (1{,}22\lambda_{EX})/NA$$

Therefore, for a wavelength of 633 nm and a 10x lens with an aperture of 0.3, the spot size was 2.6 μm. Accordingly, the area of a circle with such a diameter is $5.2*10^{-8}$ cm^2, and the power density for 5 mW of laser output power is 96 kW/cm^2. To obtain one image, the laser scanned twice at a speed of 1.27 μs/pixel. Thus, during the acquisition of a single image, the radiation dose was 0.244 J/cm^2, and the time-averaged dose for a 1064 × 1064 pixels image was 170 mW/cm^2, which is comparable with the radiation power density of 100 mW/cm^2 in clinical conditions.

During a series of scans, fluorescent signals from PS and SOSG were recorded. By isolating the rectangular areas in the image of the tooth thin section at different depths from the enamel surface with a rectangle height of 40 μm, we obtained the time dependences of the photosensitizer bleaching and SOSG fluorescence rise.

The study of the PS concentration on the fluorescence spectra depending on the time of PS application and the dose of laser irradiation during PDB

The concentration of PS in tooth tissues was determined by measuring fluorescence intensity using LESA-01-Biospec fiber-optic spectrometer (OOO BIOSPEC, Russia). Collecting diffuse scattered light from tooth tissues when excited by laser radiation of 633 nm by a fiber optic catheter, fluorescence of PS was recorded in contact with the enamel and dentin surfaces on the tooth cut.

A study of the effect of the light dose on photobleaching of the PS was carried out using the Harmony LED device (OOO Laser-Medcentr, Russia) with a wavelength of λ = 400±10 nm. The laser power density was 100 mW/cm^2.

The total light dose was 180 J/cm^2, which corresponds to 30 minutes of exposure. After 10, 20, and 30 min from the onset of light exposure, the fluorescence spectra of PS were measured to evaluate the PS remaining in the tooth tissues, which was being bleached during the PDB.

Clinical evaluation of tooth color after PDB

The assessment of the color change of the frontal group of teeth before and after the PDB was determined using VITA Easyshade® V spectrophotometer (VITA Zahnfabrik, Germany). To determine the tooth color, the surface of the studied crown part of the tooth was cleaned and measurements were taken in the averaging mode before and after the PDB. The measuring tip was tightly applied at right angles to the surface of the tooth enamel covering the dentin. The tooth color characteristics such as lightness of color (L) and color saturation (intensity or purity) (C) were recorded. The lightness of color in comparison with the number of gray tones is determined in the range from black (L = 0) to white (L = 100). Color saturation (C) is the difference between the color and the gray tone of the same lightness, measured as the distance from the neutral axis. Based on the results, 2D histograms of saturation (C) and lightness (L) of the color of the teeth before and after the PDF were plotted. The results were processed in Python 3 by the method of kernel density estimation using matplotlib and seaborn graphic packages [33, 34].

Results and discussion

According to the fluorescence microscopy, the dependences of the PS fluorescence on the depth from the

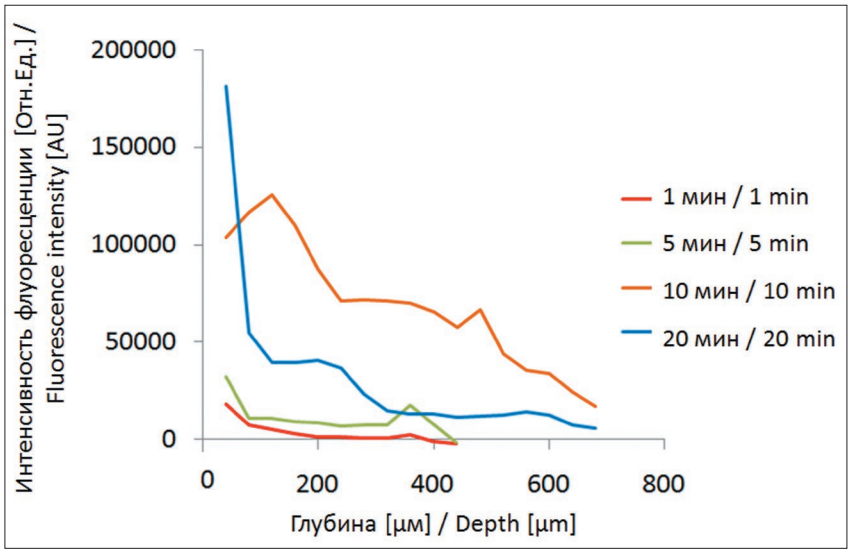

Рис. 2. Интенсивность флуоресценции ФС на глубине от поверхности эмали при различной продолжительности аппликации ФС
Fig. 2. The photosensitizer fluorescence intensity at the depth from the enamel surface for various application times

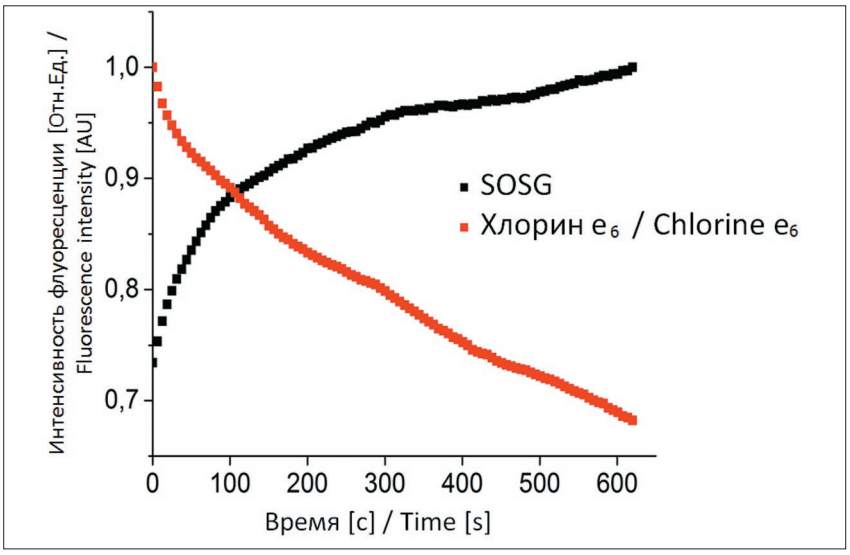

Рис. 3. Зависимость обесцвечивания ФС (красный) и разгорания флуоресценции SOSG (черный) во время ФДОЗ шлифа зуба, усредненное по всей толщине эмали
Fig. 3. The dependence of the bleaching of the photosensitiser (red) and the rise of SOSG fluorescence (black) during PDB of tooth section, averaged over the entire thickness of the enamel

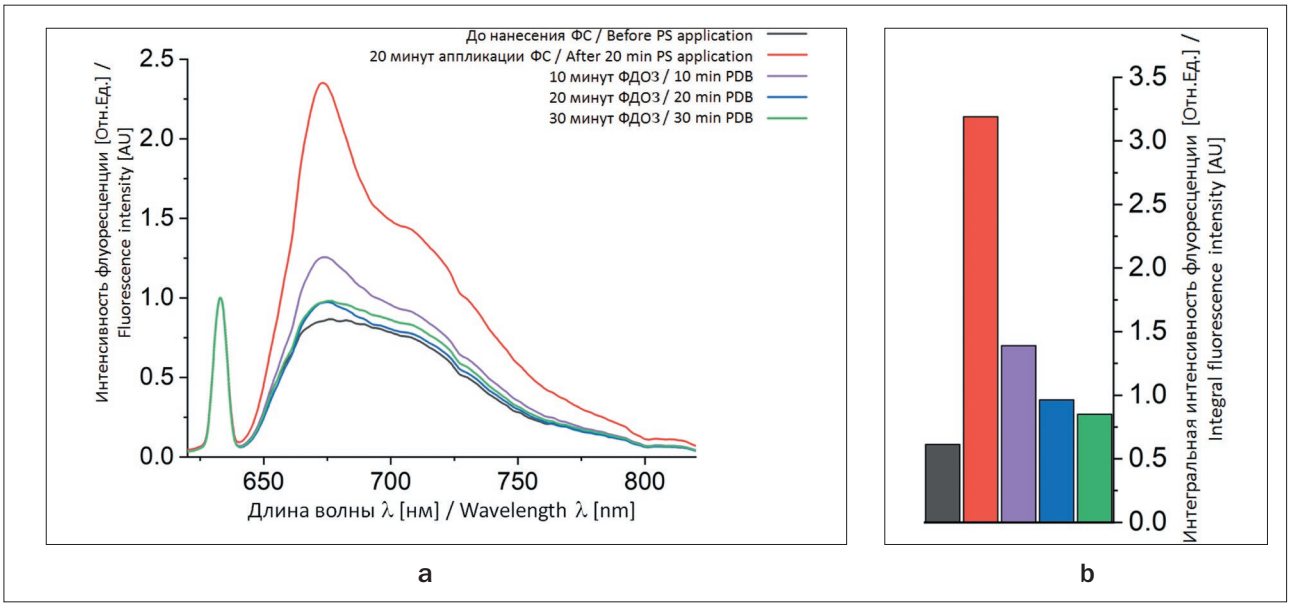

Рис. 4. Спектры флуоресценции зуба до аппликации ФС, сразу после, и спустя каждые 10 мин облучения (*a*). Интегральная интенсивность флуоресценции от зуба, нормированная на пик лазерного рассеяния (*b*)
Fig. 4. Fluorescence spectra of the tooth before the photosensitiser application, immediately after, and after every 10 minutes of irradiation (*a*). Integral fluorescence intensity from the tooth, normalized on the peak of the scattered laser (*b*)

enamel surface were plotted for different times of the PS application on the enamel surface (Fig. 2).

The highest concentration of PS is observed at the enamel surface. It then gradually decreases, which corresponds to the physical diffusion of substances. However, at the border of enamel and dentin, there is a small relative increase in the PS concentration (in different teeth, the border of dentin and enamel was at different depths). The tendency for the total PS presence increase with time of the PS application is also clearly observed.

The dependences of PS bleaching and SOSG singlet oxygen sensor flare-up are obtained depending on the depth of the enamel surface on the tooth cut during the PDB. The averaged values of the PS bleaching

Рис. 5. Визуальная оценка цвета удаленных зубов до и после процедуры фотодинамического отбеливания в соответствии с классической шкалой Вита
Fig. 5. Visual color matching of the extracted teeth before and after the procedure of PDB using classical Vita scale

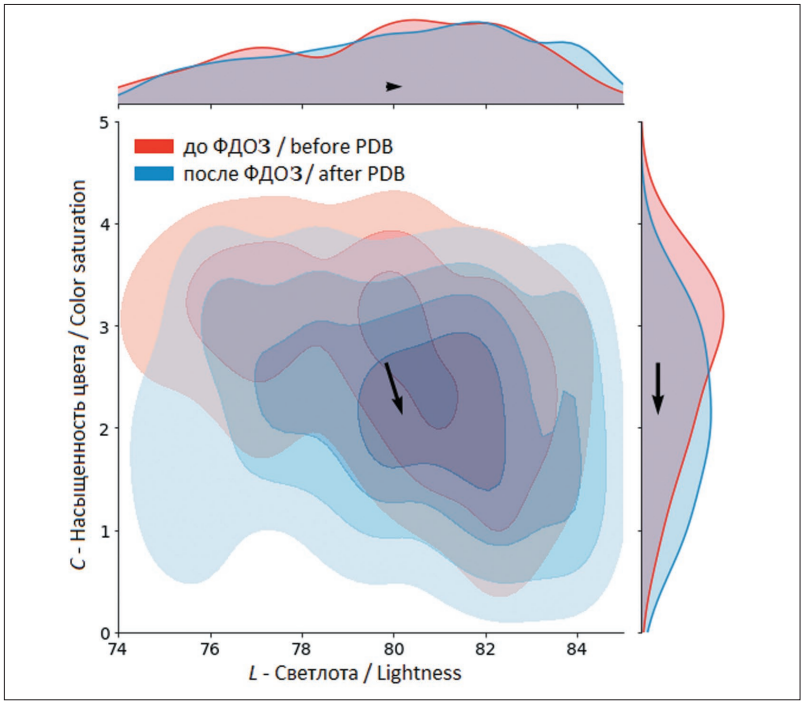

Рис. 6. Статистическое распределение цвета 100 зубов до (розовый) и после (голубой) процедуры фотодинамического отбеливания. Оценка цвета зубов выполнена с использованием спектрофотометра VITA Easyshade® V Вита, приведены данные в координатах насыщенности цвета (C) и светлоты цвета (L). По осям отложены распределения значений C и L до и после процедуры фотодинамического отбеливания. Черной стрелкой представлено усредненное изменение цвета зубов в эксперименте
Fig. 6. The statistical distribution of 100 teeth color before (red) and after (blue) the PDB procedure. Evaluation of the teeth color was performed using a VITA Easyshade® V Vita spectrophotometer; data in the coordinates of color saturation (C) and color lightness (L) are presented. Along the axes, the distributions of C and L values are plotted before and after the photodynamic bleaching procedure. The black arrow represents the average discoloration of the teeth in the overall experiment

over the entire thickness of the enamel and the singlet oxygen sensor flaring are presented in Fig. 3. Based on these data, 10 min after the start of irradiation, the PS is bleached by a third of the initial concentration, and the fluorescence of the SOSG singlet oxygen sensor reaches a plateau.

The nature of the PS bleaching in the tooth tissue during PDB is confirmed by fluorescence spectroscopy. Thus, tooth fluorescence before application of the PS gel, immediately after, and after every 10 min of irradiation, repeats the dependence of the PS fluorescence intensity obtained on the tooth cut under a confocal microscope (Fig. 4).

The teeth appearance before and after the PDB compared with the classic Vita scale is presented in Fig. 5. Also, it was found that PDB can be more effective if the enamel is periodically moistened during the procedure. Similar results of *in vitro* studies on enhancing the photobleaching effect of resin-based restorative materials in water were obtained in [35].

In addition to the classic Vita score, tooth color data were obtained before and after the PDB using VITA Easyshade® spectrophotometer. It was statistically established that in one FDB procedure, the average change in lightness of color (L) was 0.36 units, with a maximum bleaching reaching 11.4 units, and a minimum of 4.7. At the same time, the average change in tooth color saturation (C) was -0.5 units, the maximum bleaching occurred by –2 tones, the minimum – 0.

The results are comparable with the review comparing conventional tooth bleaching and photobleaching [36].

Conclusion

The PS (chlorin e_6) used in the study penetrates deep into the tooth tissues over time (enamel and dentin), which makes it possible to conduct PDB throughout the entire tissue depth. After 20 min PS application to the tooth surface, the fluorescence of chlorin e_6 was detected both in the depth of the enamel and in dentin. Although the average interstitial concentration of PS decreases with depth, it still reaches values sufficient to conduct effective PDB.

To achieve a significant effect from PDB, the singlet oxygen generation over the entire thickness of enamel and dentin is necessary, which was experimentally proved using the SOSG singlet oxygen sensor and photobleaching of the PS.

To determine the effectiveness of PDB, objective data on tooth color were obtained before and after PDB using the Vita scale and VITA Easyshade® spectrophotometer. It was shown that the average change in lightness of color (L) was 0.36 units, and the maximum bleaching reached 11.4 units. Also, the average change in tooth color saturation (C) was 0.5 units, for individual teeth achieving a 2-tone change. Thus, the use of the PDB allows effective aesthetic correction of tooth color.

This work was carried out within the state assignment of the Federal Agency for Scientific Organizations of Russia ("Physical methods in medicine and biology", No. 0024–2019–0003).

REFERENCES

1. Goldstein R.E, Chu S., Lee E., Stappert C.F.J. *Goldstein's Esthetics in Dentistry*, 3rd Edition. Wiley-Blackwell, 2018. 1576 p.
2. Jordan R.E., Boksman L. Conservative vital bleaching treatment of discolored dentition, *Compend. Contin. Educ. Dent.*, 1984, vol. 5(10), pp. 803–5, 807.
3. Viscio D., Gaffar A., Fakhry-Smith S., Xu T. Present and future technologies of tooth whitening, *Compend. Contin. Educ. Dent.*, 2000, suppl. 28, pp. 36–43.
4. Subramanian S., Appukuttan D., Tadepalli A., Gnana P.P., Victor D.J. The Role of Abrasives in Dentifrices, *J. Pharm. Sci. & Res.*, 2017, vol. 9(2), pp. 221–224.
5. Goldstein R.E., Garber D.A. *Complete Dental Bleaching*, 1st ed. Chicago, Quintessence Publishing Inc, 1995. p. 165.
6. Dodson D., Bowles W. Production of minocyclines pigment by tissue extracts, *J. Dent. Res.*, 1991, vol. 70, pp. 424.
7. Nathoo S.A. The chemistry and mechanisms of extrinsic and intrinsic discoloration, *J. Am. Dent. Assoc.*, 1997, vol. 128, pp. 6–10.
8. *Bleaching Techniques in Restorative Dentistry. An Illustrated Guide*, Edited By Linda Greenwall. 1st edition. London, CRC Press, 2001. 428 p. doi.org/10.3109/9780203417430.
9. Haywood V.B. Overview and status of mouthguard bleaching, *J. Esthet. Dent.*, 1991, vol. 3, pp. 157–161.
10. Leonard R.H., Van Haywood Jr.B., Caplan D.J., Tart N.D. Nightguard vital bleaching of tetracycline-stained teeth: 90

ЛИТЕРАТУРА

1. Goldstein R.E, Chu S., Lee E., Stappert C.F.J. Goldstein's Esthetics in Dentistry / 3rd Edition. – Wiley-Blackwell, 2018. – 1576 p.
2. Jordan R.E., Boksman L. Conservative vital bleaching treatment of discolored dentition // Compend. Contin. Educ. Dent. – 1984. – Vol. 5(10). –P. 803–5, 807.
3. Viscio D., Gaffar A., Fakhry-Smith S., Xu T. Present and future technologies of tooth whitening // Compend. Contin. Educ. Dent. – 2000. —Suppl. 28. – S. 36–43.
4. Subramanian S., Appukuttan D., Tadepalli A., et al. The Role of Abrasives in Dentifrices // J. Pharm. Sci. & Res. – 2017. —Vol. 9(2). – P. 221–224.
5. Goldstein R.E., Garber D.A. Complete Dental Bleaching / first ed. – Quintessence Publishing Inc. Chicago, 1995. – P. 165.
6. Dodson D., Bowles W. Production of minocyclines pigment by tissue extracts // J. Dent. Res. –1991. – Vol. 70(Spec Iss). – P.424.
7. Nathoo S.A. The chemistry and mechanisms of extrinsic and intrinsic discoloration // J. Am. Dent. Assoc. –1997. – Vol.128(Suppl). – P. 6–10.
8. Bleaching Techniques in Restorative Dentistry. An Illustrated Guide / Edited By Linda Greenwall. 1st Edition. – London: CRC Press, 2001. – 428 p. doi.org/10.3109/9780203417430
9. Haywood V.B. Overview and status of mouthguard bleaching // J. Esthet. Dent. –1991. – Vol.3. – P. 157–161.

months post treatment, *J. Esthet. Restor. Dent.*, 2003, vol. 15, pp. 142–152.
11. Haywood V.B., Leonard R.H., Nelson C.F., Brunson W.D. Effectiveness, side effects and long-term status of nightguard vital bleaching, *J. Am. Dent. Assoc.*, 1994, vol. 125, pp. 1219–1226.
12. Fasanaro T.S. Bleaching Teeth: History, Chemicals, and Methods Used for Common Tooth Discolorations, *J. Esthetic and Restorative Dentistry*, 1992, vol. 4(3), pp. 71–78. doi:10.1111/j.1708–8240.1992.tb00666.x
13. Alqahtani M.Q. Tooth-bleaching procedures and their controversial effects: A literature review, *Saudi Dent J*, 2014, vol. 26(2), pp. 33–46. doi:10.1016/j.sdentj.2014.02.002
14. Trentino A.C., Soares A.F., Duarte M.A., Ishikiriama S.K., Mondelli R.F. Evaluation of pH Levels and Surface Roughness After Bleaching and Abrasion Tests of Eight Commercial Products, *Photomed Laser Surg*, 2015, vol. 33(7), pp. 372–7. doi: 10.1089/pho.2014.3869.
15. SuliemanM., AddyM., ReesJ. S. Development and evaluation of a method in vitro to study the effectiveness of tooth bleaching, *J. Dentistry*, 2003, vol. 31(6), pp. 415–422.
16. JoinerA. The bleaching of teeth: a review of the literature, *J. Dentistry*, 2006, vol. 34(7), pp. 412–419.
17. Verheyen P., Walsh L.J., Wernish J., Schoop U., Moritz A. *Laser-assisted bleaching in Oral Laser Application*. Chapter 10. by MoritzA. as ed. Berlin, Germany: Quintessenz-Verlags-Gmbh., 2006. pp. 407–448.
18. Baik J.W., Rueggeberg F.A., Liewehr F.R. Effect of light-enhanced bleaching on in vitro surface and intrapulpal temperature rise, *J. of Esthetic and Restorative Dentistry*, 2001, vol. 13(6), pp. 370–378.
19. Sydney G.B., Barletta F.B., Sydney R.B. In vitro analysis of effect of heat used in dental bleaching on human dental enamel, *Brazilian Dental Journal*, 2002, vol. 13(3), pp. 166–169.
20. Wetter N.U., Walverde D.A., Kato I.T., Eduardo C.D.P. Bleaching efficacy of whitening agents activated by xenon lamp and 960-nm diode radiation, *Photomedicine and Laser Surgery*, 2004, vol. 22(6), pp. 489–493.
21. Zhang C., Wang X., Kinoshita J.-I., Zhao B., Toko T., Kimura Y., Matsumoto K. Effects of KTP laser irradiation, diode laser, and LED on tooth bleaching: a comparative study, *Photomedicine and Laser Surgery*, 2007,vol. 25(2), pp. 91–95.
22. Frysh H. Chemistry of bleaching in *Complete Dental Bleaching*, by Goldstein R.E. and Garber D.A. as eds. Chicago, Ill, USA, Quintessence, 1995. pp. 25–33.
23. Kashima-Tanaka M., Tsujimoto Y., Kawamoto K., Senda N., Ito K.,Yamazaki M. Generation of free radicals and/or active oxygen by light or laser irradiation of hydrogen peroxide or sodium hypochlorite, *Journal of Endodontics*, 2003, vol. 29(2), pp. 141–143.
24. Takasaki A.A., Aoki A., Mizutani K., Schwarz F., Sculean A., Wang C.Y., Koshy G., Romanos G., Ishikawa I., Izumi Y. Application of antimicrobial photodynamic therapy in periodontal and periimplant diseases, *Periodontol*, 2009, vol. 51, pp. 109–140.
25. Gursoy H., Ozcakir-Tomruk C., Tanalp J., Yilmaz S. Photodynamic therapy in dentistry: a literature review, *Clin Oral Investig*, 2013, vol. 17(4), pp. 1113–25. doi: 10.1007/s00784–012–0845–7
26. Makarov V.I., Akhlyustina E.V., Farrakhova D.S., Pominova D.V., Ryabova A.V., Loschenov V.B. Photonic methods for quality evaluation of skin engraftment (review), *Biomedical Photonics*, 2016, vol. 5, no. 3, pp.30–40. (in Russian)
27. Costa L.M., Matos F. de S., Correia A.M., Carvalho N.C., Faria-E-Silva A.L., Paranhos L.R., Ribeiro M.A. Tooth color change caused by photosensitizers after photodynamic therapy: An in vitro study, *J Photochem Photobiol B*, 2016, vol. 160, pp. 225–228. doi: 10.1016/j.jphotobiol.2016.04.019
28. Bennett Z.Y., Walsh L.J. Efficacy of LED versus KTP laser activation of photodynamic bleaching of tetracycline-stained dentine, *Lasers in Medical Science*, 2014, vol. 30(7), pp. 1823–8. doi: 10.1007/s10103–014–1675–4.

10. Leonard R.H., Van Haywood Jr.B., Caplan D.J., Tart N.D. Nightguard vital bleaching of tetracycline-stained teeth: 90 months post treatment // J. Esthet. Restor. Dent. – 2003. – Vol.15. – P. 142–152.
11. Haywood V.B., Leonard R.H., Nelson C.F., Brunson W.D. Effectiveness, side effects and long-term status of nightguard vital bleaching // J. Am. Dent. Assoc. –1994. – Vol.125. – P. 1219–1226.
12. Fasanaro T.S. Bleaching Teeth: History, Chemicals, and Methods Used for Common Tooth Discolorations // J. Esthetic and Restorative Dentistry. –1992. – Vol.4(3).– P. 71–78. doi:10.1111/j.1708–8240.1992.tb00666.x
13. Alqahtani M.Q. Tooth-bleaching procedures and their controversial effects: A literature review // Saudi Dent J. – 2014. – Vol. 26(2). – P. 33–46. doi:10.1016/j.sdentj.2014.02.002
14. Trentino A.C., Soares A.F., Duarte M.A., et al. Evaluation of pH Levels and Surface Roughness After Bleaching and Abrasion Tests of Eight Commercial Products // Photomed Laser Surg.– 2015. – Vol.33(7). – P. 372–7. doi: 10.1089/pho.2014.3869.
15. SuliemanM., AddyM., ReesJ.S. Development and evaluation of a method in vitro to study the effectiveness of tooth bleaching // J. Dentistry. – 2003. – Vol. 31(6). – P. 415–422.
16. Joiner A. The bleaching of teeth: a review of the literature // J. Dentistry. – 2006. –Vol. 34(7). – P. 412–419.
17. Verheyen P., Walsh L.J., Wernish J., et al. Laser-assisted bleaching. in Oral Laser Application. Chapter 10. / by MoritzA.as ed. –Berlin, Germany: Quintessenz-Verlags-Gmbh., 2006. – P. 407–448.
18. Baik J.W., Rueggeberg F.A., Liewehr F.R. Effect of light-enhanced bleaching on in vitro surface and intrapulpal temperature rise // J. of Esthetic and Restorative Dentistry. – 2001. – Vol. 13(6). – P. 370–378.
19. Sydney G.B.,Barletta F.B., Sydney R.B. Invitro analysis of effect of heat used in dental bleaching on human dental enamel // Brazilian Dental Journal. – 2002. – Vol.13(3). – P. 166–169.
20. Wetter N.U., Walverde D.A., Kato I.T., Eduardo C.D.P. Bleaching efficacy of whitening agents activated by xenon lamp and 960-nm diode radiation // Photomedicine and Laser Surgery. – 2004. – Vol.22(6). – P. 489–493.
21. Zhang C., Wang X., Kinoshita J.-I., et al. Effects of KTP laser irradiation, diode laser, and LED on tooth bleaching: a comparative study // Photomedicine and Laser Surgery. – 2007. – Vol. 25(2). – P. 91–95.
22. Frysh H. Chemistry of bleaching/in Complete Dental Bleaching, by Goldstein R.E. and Garber D.A. as eds.– Chicago, Ill, USA: Quintessence, 1995. – P. 25–33.
23. Kashima-Tanaka M., Tsujimoto Y., Kawamoto K., et al. Generation of free radicals and/or active oxygen by light or laser irradiation of hydrogen peroxide or sodium hypochlorite // Journal of Endodontics. – 2003. – Vol.29(2). – P. 141–143.
24. Takasaki A.A., Aoki A., Mizutani K., et al. Application of antimicrobial photodynamic therapy in periodontal and periimplant diseases // Periodontol. –2009. – Vol.51. – P. 109–140.
25. Gursoy H., Ozcakir-Tomruk C., Tanalp J., Yilmaz S. Photodynamic therapy in dentistry: a literature review // Clin Oral Investig. –2013. – Vol. 17(4). – P. 1113–25.doi: 10.1007/s00784–012–0845–7
26. Макаров В.И., Ахлюстина Е.В., Фаррахова Д.С., Поминова Д.В., Рябова А.В., Лощенов В.Б. Методы фотоники для оценки качества приживления кожных трансплантатов (обзор) // Biomedical Photonics. – 2016. – Т. 5, № 3. – С. 30–40.
27. Costa L.M., Matos F. de S., Correia A.M., et al. Tooth color change caused by photosensitizers after photodynamic therapy: An in vitro study // J Photochem Photobiol B. –2016. –Vol. 160. – P. 225–228. doi: 10.1016/j.jphotobiol.2016.04.019
28. Bennett Z.Y., Walsh L.J. Efficacy of LED versus KTP laser activation of photodynamic bleaching of tetracycline-stained dentine // Lasers in Medical Science. –2014.– Vol. 30(7). – P. 1823–8. doi: 10.1007/s10103–014–1675–4.

29. Tsubura S. Clinical evaluation of three months' nightguard vital bleaching on tetracycline-stained teeth using Polanight 10% carbamide gel: 2-year follow-up study, *Odontology*, 2010, vol. 98(2), pp. 134–138. doi:10.1007/s10266–010–0130–7
30. Juzeniene A. Chlorin e6-based photosensitizers for photodynamic therapy and photodiagnosis, *Photodiagnosis Photodyn Ther*, 2009, vol. 6(2), pp. 94–6.
31. Zorina O.A., Krechina E.K., Abaev Z.M., Korshunova A.V., Ponomaryov G.V., Ryabova A.V., Makarov V.I. Analysis of photosensitizer gel penetration through the teeth structure, *Stomatologiia*, 2018, vol. 97, no. 6, pp. 22–27. (in Russian)
32. Flors C., Fryer M.J., Waring J., Reeder B., Bechtold U., Mullineaux P.M., Nonell S., Wilson M.T., Baker N.R. Imaging the production of singlet oxygen in vivo using a new fluorescent sensor, Singlet Oxygen Sensor Green, *J. Experimental Botany, Oxygen Metabolism, ROS and Redox Signalling in Plants*, 2006, vol. 57(8), pp. 1725–1734.
33. John D. Hunter. Matplotlib: A 2D Graphics Environment, *Computing in Science & Engineering*, 2007, vol. 9, pp. 90–95. doi:10.1109/MCSE.2007.55
34. Waskom M., Botvinnik O., O'Kane D., Hobson P., et al. *mwaskom/seaborn: v0.9.0.* 2018. Available at: http://doi.org/10.5281/zenodo.1313201
35. Buchalla W., Attin T., Hilgers R.-D., Hellwig E. The effect of water storage and light exposure on the color and translucency of a hybrid and a microfilled composite, *The J. Prosthetic Dentistry,* 2002, vol. 87(3), pp. 264–270. doi.org/10.1067/mpr.2002.121743
36. Shahabi S., Assadian H., Mahmoudi Nahavandi A., Nokhbatolfoghahaei H. Comparison of Tooth Color Change After Bleaching With Conventional and Different Light-Activated Methods, *J. Lasers Med Sci*, 2018, vol. 9(1), pp. 27–31. doi:10.15171/jlms.2018.07

29. Tsubura S. Clinical evaluation of three months' nightguard vital bleaching on tetracycline-stained teeth using Polanight 10% carbamide gel: 2-year follow-up study // Odontology. –2010. – Vol. 98(2). – P. 134–138. doi:10.1007/s10266–010–0130–7
30. Juzeniene A. Chlorin e6-based photosensitizers for photodynamic therapy and photodiagnosis // Photodiagnosis Photodyn Ther. – 2009. – Vol. 6(2). – P. 94–6.
31. Зорина А.О., Кречина Е.К., Абаев З.М. и др. Анализ глубины проникновения геля фотосенсибилизатора в структуру тканей зубов / Стоматология. – 2018. – Т. 97, № 6. – С. 22–27.
32. Flors C., Fryer M.J., Waring J., et al. Imaging the production of singlet oxygen in vivo using a new fluorescent sensor, Singlet Oxygen Sensor Green // J. Experimental Botany, Oxygen Metabolism, ROS and Redox Signalling in Plants, Special Issue. – 2006. – Vol. 57(8). – P. 1725–1734.
33. John D. Hunter. Matplotlib: A 2D Graphics Environment // Computing in Science& Engineering. – 2007. – Vol. 9. – P. 90–95. doi:10.1109/MCSE.2007.55
34. Waskom M., Botvinnik O., O'Kane D., Hobson P., et al. mwaskom/seaborn: v0.9.0. – 2018. Available at: http://doi.org/10.5281/zenodo.1313201
35. Buchalla W., Attin T., Hilgers R.-D., Hellwig E. The effect of water storage and light exposure on the color and translucency of a hybrid and a microfilled composite // The J. Prosthetic Dentistry. – 2002. – Vol. 87(3). – P. 264–270. https://doi.org/10.1067/mpr.2002.121743
36. Shahabi S., Assadian H., Mahmoudi Nahavandi A., Nokhbatolfoghahaei H. Comparison of Tooth Color Change After Bleaching With Conventional and Different Light-Activated Methods // J. Lasers Med Sci.– 2018. – Vol. 9(1). – P. 27–31. doi:10.15171/jlms.2018.07

POTENTIAL FOR THE APPLICATION OF DYNAMIC SKIN THERMOGRAPHY AFTER LOCAL HYPOTHERMIA

Novikov I.A., Petrov S.Yu., Rein E.S., Borisenko T.E., Sdobnikova S.V., Lucevitch E.E., Avetisov S.E.
Research Institute of Eye Diseases, Moscow, Russia

Abstract

Infrared thermography is one of the widely used non-invasive diagnostic methods. While the procedure is mainly used for early malignant tumor diagnostics, a potential application for thermography was proposed in cardiovascular, skin, autoimmune diseases, arthritis, Reynaud's syndrome, burns, surgery and therapeutic treatment monitoring. The method of thermographic evaluation has not changed significantly since the end of 20th century. In this study we attempted to characterize the influence of skin capillary blood flow on surface temperature recuperation following local hypothermia. To improve sensitivity and standardize the procedure we developed a study protocol that involves minimizing or excluding the influence of external factors on study results. An original applicator was used to apply dosed hypothermia. Massive porcine tissue block was chosen as a passive model without active heat and mass transfer but with heat capacity, structure and heat dissipation characteristics similar to human tissues. 51 healthy volunteers were assigned to control group, while 16 patients with diabetes mellitus constituted the main study group. Cumulative temperature difference was calculated in all cases. It was 121,8±70,8 °C×s in the control group, 95,6±54,4 °C×s in the main study group and 307,2±43,4 °C×s in the passive model. Based on the study results, we made the following conclusions: absence of heat and mass transfer in the passive model complicates heat balance recuperation due to layered structure of the skin; heat balance recuperation curve is an individual parameter and is not influenced by age or gender.

Keywords: thermography, contactless dynamic thermography, thermal imaging device, cold test applicator, isothermic chamber, diabetes mellitus, skin capillary blood flow.

For citations: Novikov I.A., Petrov S.Yu., Rein E.S., Borisenko T.E., Sdobnikova S.V., Lucevitch E.E., Avetisov S.E. Potential for the application of dynamic skin thermography after local hypothermia // Biomedical Photonics. – 2019. – T. 8, № 3. – P. 29–35. doi: 10.24931/2413–9432–2019–8–3–29–35

Contacts: Rein E.S., e-mail: elenarein01@gmail.com

ПОТЕНЦИАЛ ПРИМЕНЕНИЯ ДИНАМИЧЕСКОЙ ТЕРМОГРАФИИ КОЖИ ПОСЛЕ ЛОКАЛЬНОЙ ГИПОТЕРМИИ

И.А. Новиков, С.Ю. Петров, Е.С. Рейн, Т.Е. Борисенко, С.В. Сдобникова, Е.Э. Луцевич, С.Э. Аветисов
Научно-исследовательский институт глазных болезней, Москва, Россия

Резюме

Метод дистанционной инфракрасной термографии – один из неинвазивных диагностических методов, широко применяемых в медицине. Помимо применения для ранней диагностики злокачественных новообразований было предложено его использование при сосудистых заболеваниях, кожных болезнях, ревматических заболеваниях, артритах, синдроме Рейно, ожогах, хирургии, мониторинге эффективности терапевтического лечения и др. Необходимо отметить, что с конца прошлого столетия технический уровень выполнения тестов существенно не менялся. В своей работе мы попытались охарактеризовать вклад капилляров системы кровоснабжения кожи в динамику восстановления температуры поверхности после локальной гипотермии. Для повышения чувствительности и стандартизации метода мы разработали протокол исследования, предполагающий максимальную стандартизацию условий внешней среды или исключение их влияния. Для дозированной локальной холодовой нагрузки использовали оригинальный аппликатор. В качестве пассивной тепловой модели с отсутствием активного тепломассопереноса, но с близкими к человеческим тканям свойствами теплоемкости, структурой и характером кондуктивного перераспределения тепла, была выбрана модель на основе массивного блока тканей свиньи. Группу контроля составили условно здоровые добровольцы. В группу контроля вошли 51 человека, в группу больных диабетом II типа –16 человек. Нами получены показатели интегральной разницы температур. Показатель интегральной разницы температур здорового человека составил 121,8±70,8 °C×c, пассивной модели – 307,2±43,4 °C×c, больного сахарным диабетом – 95,6±54,4 °C×c. Были сделаны следующие выводы: отсутствие тепломассопереноса в пассивной модели усложняет восстановление теплового баланса в виду многослойного строения кожи; кривая восстановления теплового баланса индивидуальна и не зависит от пола и возраста.

Ключевые слова: термография, бесконтактная динамическая термография, тепловизор, аппликатор для проведения холодовой пробы, изотермическая камера, сахарный диабет II типа, капиллярное кровообращение кожи.

Для цитирования: Novikov I.A., Petrov S.Yu., Rein E.S., Borisenko T.E., Sdobnikova S.V., Lucevitch E.E., Avetisov S.E. Potential for the application of dynamic skin thermography after local hypothermia, *Biomedical Photonics*, 2019, vol. 8, no. 3, pp. .29–35. doi: 10.24931/2413–9432–2019–8–3–29–35.

Контакты: Rein E.S., e-mail: elenarein01@gmail.com

Introduction

Noninvasive infrared thermography is one of the widely used diagnostic methods. The first practical application of diagnostic thermography was proposed in 1957 by R. Lawson, who discovered that skin temperature in the area of a breast tumor is higher than the temperature of the normal tissue [1]. In addition to its application for the early diagnosis of malignant tumors, its use was also suggested for vascular diseases (diabetes mellitus, thrombosis), skin diseases, rheumatic diseases, arthritis, Raynaud syndrome, burns, surgery, monitoring of the therapeutic treatment efficacy, etc [2–5]. It should be noted that since the end of the last century the technical level of tests has not changed significantly.

Currently almost all known varieties of thermographic diagnostics evaluate condition of tissues and organs that project their heat-generating properties onto the skin and mucosa surface directly above them. The use of thermography in diabetes mellitus, where the measurements of heat generation are aimed at identifying significant systemic disorders of innervation and blood circulation seems to be an exception [6, 7].

Diagnostic thermography in diabetes mellitus is an example of a potential application of local thermographic measurements for monitoring the development of various system level changes. Changes in the regulation of skin capillaries or their systemic degradation will evidently be reflected in the temperature fluctuations of any arbitrary local surface area of the body.

We assumed that creation of a new method of dynamic thermal evaluation, limited in depth to evaluate heat exchange in the skin no deeper than the layer of subcutaneous tissue, would significantly increase the sensitivity of thermography to changes of cutaneous microcirculation. An increase in sensitivity along with a strict standardization of test conditions may be sufficient to assess subtle changes in systemic capillary status.

Aim: to assess the contribution of the capillaries of the skin blood supply system to the dynamics of surface temperature recovery after local hypothermia.

Materials and methods

Room for thermographic research

When conducting dynamic thermography, in contrast to static measurements, external short-period temperature fluctuations introduce significant interference. To reduce the effect of external temperature fluctuations associated with convection turbulence, thermography was carried out in a room with a laminar air exchange system (fig. 1). The air inflow was provided through laminar nozzles by the air supply unit with the "Breezart 1000 lux" electric heater (Brizart LLC, Russia), and the outflow was executed from a low point using a BP-86–77–2.5 exhaust system (Zavod Musson LLC, Russia). The thermosetter of the air handling unit provided a constant temperature of 24 ± 0.25 °C. The measurements were carried out at an atmospheric pressure of 746 ± 10 mm Hg.

Isothermal chamber

The isothermal chamber was constructed to eliminate thermal range reflections from the surrounding objects on the surface of the skin. The size of the chamber was 50×50×190 cm. It was covered on the inside with a carbon dyed heat-absorbing material.

Applicator for dosed local hypothermia

The local cold test was performed using an original applicator, which is a polymer cylindrical hollow body, one of the ends of which is hermetically sealed with a 12.5 mm aluminum plate (fig. 2). Deionized water (endothermic phase transition at 0 °C) in a volume of 2 ml served as the working medium ensuring the constancy of the applicator surface temperature. Efficient heat transfer from the aluminum plate (working surface of the applicator) to the working medium was provided by the aluminum core. Prior to the test the applicator was cooled to a temperature of -18 °C, and then under the thermographic control it was heated until the surface

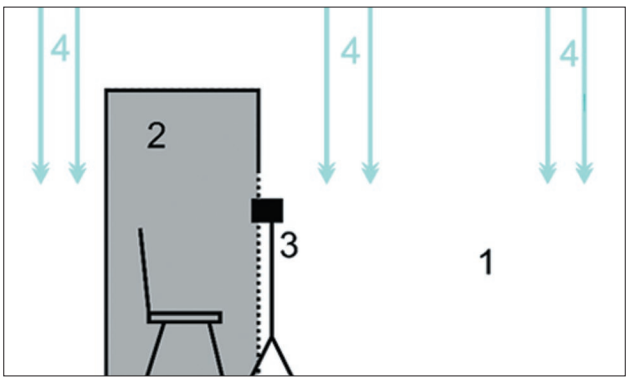

Fig. 1. Diagram of an isothermal chamber and a room for research (1 – room for thermographic research; 2 – isothermal chamber; 3 – infrared camera on tripod; 4 – air flow direction)
Рис. 1. Схематическое изображение изотермальной камеры и опытной комнаты (1 – комната для тепловых исследований; 2 – изотермальная камера; 3 – инфракрасная камера на штативе; 4 – направление воздушных потоков)

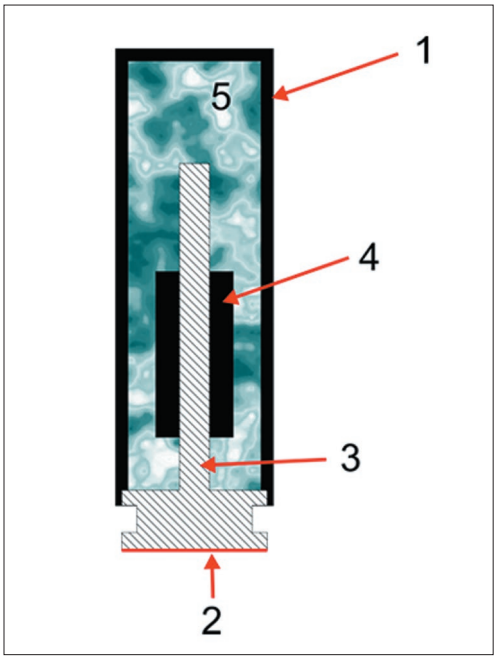

Fig. 2. Cold test applicator design (1 – polymer cylindric body; 2 – working surface of the applicator (12.5 mm aluminum plate); 3 – aluminum core; 4 – silver coupling mounted on the aluminum core; 5 – working medium (2 ml deionized water))
Рис. 2. Схема устройства аппликатора «холодного» теста (1 – полимерная оболочка в форме цилиндра; 2 – рабочая поверхность аппликатора (12,5 мм алюминиевая пробка); 3 – алюминиевая сердцевина; 4 – серебряная муфта, установленная на алюминиевую сердцевину); 5 – рабочая среда (2 мл деионизированной воды))

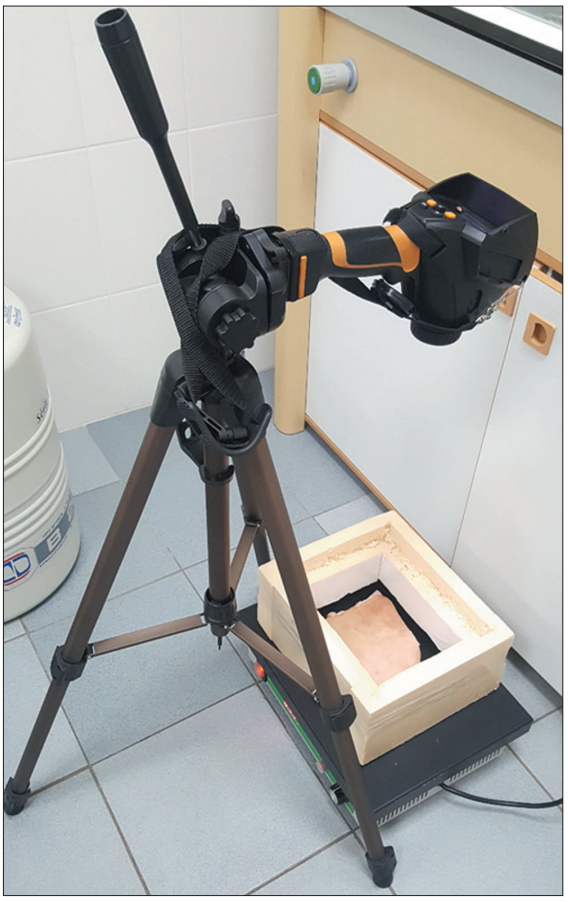

Fig. 3. Thermographic evaluation of the passive model
Рис. 3. Процесс тепловой оценки пассивной модели

temperature reached 0 °C. The temperature "jerk" at the moment of application, associated with the limited rate of heat transfer in water, was largely compensated for by silver coupling (Ag 99.9%) tightly mounted on the core.

Infrared camera

Testo 875 (Testo SE &Co. KGaA, Germany) infrared camera was used in the current study.

Image Quality: 160x120 pixel matrix, with thermographic image resolution of 320 × 240 and the spectral range of 8–14 μm. The study was conducted using a dynamic temperature scale with automatic recognition of a hot/cold point. Temperature resolution was 0.1°C.

Passive model of skin heat dynamics

A single porcine tissue block was chosen to be a passive model in our study with no active heat and mass transfer, but with heat capacity properties, structure and nature of conductive heat redistribution close to human tissues. A block of tissues measuring 20 × 25 × 6.5 cm included the epidermis, dermis, subcutaneous fat and muscle tissue. Bone and cartilaginous tissues were absent.

In the experiment the block was placed on the Ecros ES-HF3040 laboratory heating surface (Ekros-Analytika LLC, Russia), with a given surface temperature of 41 °C. To reduce heat loss in the lateral directions, the block was placed in a frame of foamed polyurethane (fig. 3). Dynamic thermographic measurements of the passive model were carried out after thermal balance between the passive model surface and the environment was reached.

A group of healthy volunteers

51 healthy volunteers (16 male and 35 female) aged between 21 to 89 took part in the study. Information about related diagnoses was registered according to medical records. Exclusion criteria were diseases of the cardiovascular system: hypertension, coronary heart disease, atherosclerosis, rheumatic heart diseases, and also diabetes mellitus type I and II.

A group of diabetes mellitus patients

16 patients with type 2 diabetes mellitus (10 male and 6 female) aged between 37 to 84 years were enlisted in the study. The presence of diabetes complications, such as renal failure, heart failure and ocular manifestations of diabetes, as well as duration of the disease and surgical interventions (microinvasive vitrectomy, panretinal laser coagulation) were noted based on medical records.

Pre-study adaptation

All subjects didn't receive any vasoactive drugs at least for 24 hours before the study. On the day the subjects were banned from drinking coffee, tea and smoking. The movement of a person into a room equipped for thermography was carried out in such a mode that the subject avoided noticeable loads on the cardiovascular system in accordance with his age and somatic condition. Given the insignificant temperature difference between the conditions of a thermostatically controlled room for thermographic research and other rooms of the institute, a rational pre-study adaptation time was 15 minutes. The timing of adaptation was selected on the basis of temperature stabilization of the passive model after 10–12 minute adaptation after transportation from an arbitrary room to a room for thermographic studies.

Data acquisition protocol

In the study of human skin temperature, the thermal imager was mounted horizontally on a tripod at a height of 110 cm from the floor directly at the entrance to the isothermal chamber. After initial thermographic evaluation the cold test applicator was put to the inferior zygomatic bone margin area for 20 seconds. The study area was chosen due to ease of access, high blood vessel density and a sufficiently long distance from organs that may interfere with the results of infrared imaging (e.g. air flow during respiration). Thermographic images were acquired each 20 seconds for 5 minutes following applicator removal. Immediately after this, similar manipulations were performed on the inferior zygomatic bone margin area on the other side.

During porcine tissue block evaluation, the infrared camera was installed vertically above the study surface. The applicator was put to the skin in the central part of the block surface. Image capturing mode, application time and thermogram recording intervals were the same.

Data processing

Thermographic images were processed and analyzed using specialized IR Soft program (version 3.1sp3). The lowest temperature in local hypothermia zone was acquired using the program (fig. 4).

After image processing empiric temperature recovery diagrams were drawn based on minimal recorded temperature in cold application zone.

According to the basic idea of trying to evaluate the active and passive components that determine heating of a skin surface area after local cooling, it became necessary to choose a smooth temperature recovery function. In further calculations, we took into account temperature fluctuations with respect to the smooth recovery curve, which is set parametrically, not absolute temperature values. As a similar basic curve, the logarithmic function of temperature recovery was reconstructed using the least square method for each test. The choice of the logarithmic law as the basis of the approximating function was motivated by its highest affinity for the obtained recovery temperatures when studying a passive model of pig tissue. Initially, when choosing the "basic" law, we compared all the options of nonlinear functions offered by SPSS Statistics (quadratic, cubic, power, logarithmic, exponential, etc.). When describing the temperature recovery curve of the passive model, the logarithmic function showed maximum determination coefficient R2 (the dispersion fraction of the dependent variable Y, specified by the predictor X).

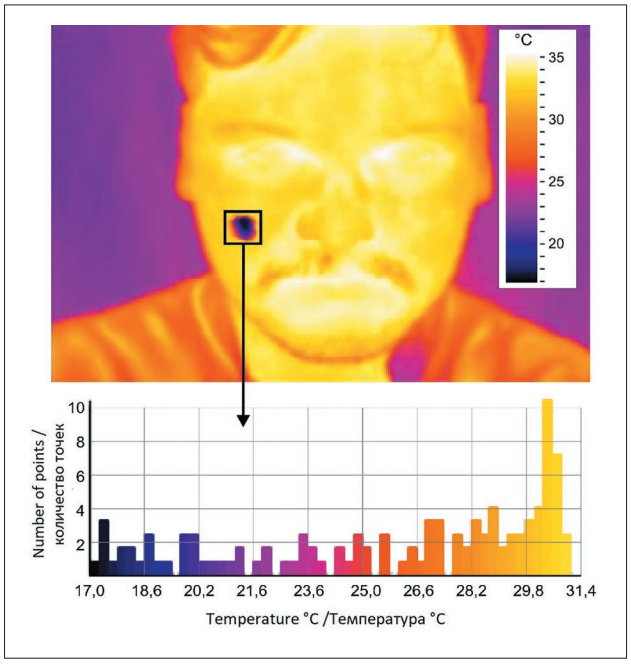

Fig. 4. Minimal temperature detection in cold application zone. A thermal image acquired using Testo 875 software and color reference for interpretation are shown above. Cooled zone is visible on the patient's right cheek after cold application. This area is cooler (marked with blue color) compared to surrounding tissues. Temperature distribution for the highlighted area is presented in the lower part of the picture. Minimal detected temperature in this area is used for all following calculations

Рис. 4. Измерение минимальной температуры в пределах предварительно охлажденного участка кожи. Сверху – полученная с помощью программного обеспечения Testo 875 термограмма поверхности лица и цветовая легенда для ее интерпретации. На правой щеке пациента видна локальная охлажденная зона, образовавшаяся после контакта с аппликатором. Относительно окружающих тканей, зона охлаждена (маркируется синим цветом). Для области выделенной прямоугольником на термограмме, в нижней части рисунка показано распределение температур. Для дальнейших вычислений была использована минимальная температура, обнаруженная в этой зоне

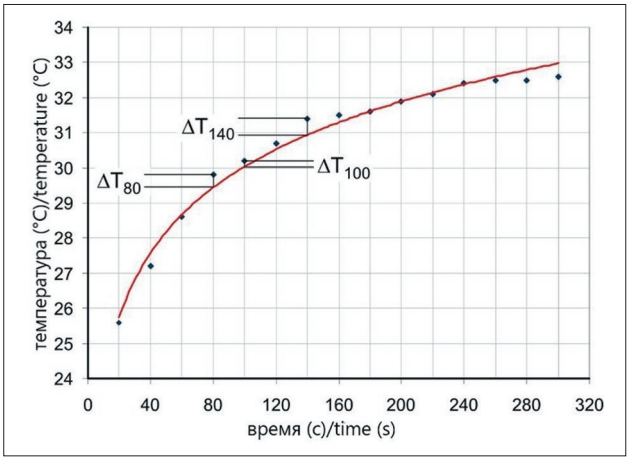

Fig. 5. Example of instantaneous deviations of the actual surface temperature recovery from the logarithmic trend
Рис. 5. Пример мгновенных отклонений реальной кривой восстановления температуры от логарифмического тренда

Thus, a logarithmic regression was individually calculated for each patient and passive model test, according to which the remainder modulus was calculated (fig. 5) for each point of the time axis with an interval of 20 seconds. Then the total parameter ∑ΔT characterizing these residues was calculated. The real temperature and its dynamics, approximated by the logarithmic law, made it possible to calculate the temperature deviation from the "ideal" restoration of the thermal balance of the surface (fig. 5). To exclude the dependence of the temperature beat volume on the fractionality of observations, the sum of these deviations was multiplied by the time between measurements: $\int\Delta T = \sum\Delta T \times t$ (°C × s). The presented indicator was conditionally called by us "cumulative temperature difference".

Statistical analysis was conducted using IBM SPSS Statistics 21 software package.

We used the nonparametric Mann-Whitney test to compare independent samples, given that the ∫ΔT distribution is different from the normal distribution for comparing groups by this indicator.

Results

Mean ∫ΔT value for thermographic evaluation of porcine tissue block passive model was 307.2 ±43.4 °C×s.

∫ΔT was significantly lower in the healthy volunteer study group (121.8±70.8 °C×s). High individual convergence of measurements was revealed for each person. At the same time, it was found out that the individual contralateral discrepancy ∫ΔT did not exceed 18%, and the discrepancy in a series of repetitions in a day time or more did not exceed 19%. There were no statistically gender or age-dependent significant differences in ∫ΔT. Similarly, no correlation was revealed between ∫ΔT and cardiovascular system disorders (hypertension, coronary heart disease, atherosclerosis, rheumatic heart diseases).

Table
Cumulative temperature difference (∫ΔT) in healthy individuals, in the passive model and in people with diabetes
Таблица
Интегральная разница температур (∫ΔT) у здоровых лиц, в пассивной модели и у лиц больных диабетом

Group Группа	Number of patients/cases Число пациентов/случаев	∫ΔT, °C×s ∫ΔT, °C×c
Healthy volunteers Здоровые добровольцы	51	121,8±70,8*
Passive model Пассивная модель	5	307,2±43,4
Diabetes mellitus Больные диабетом II типа	16	95,6±54,4*

Data expressed as mean (M) ± standard deviation (SD)
* difference in groups p=0,021
∫ΔT – cumulative temperature difference
Результаты представлены в виде среднего значения (M) ± стандартное отклонение (SD)
* разница в группах p=0.021
∫ΔT – интегральная разница температуры

The group of patients with verified diabetes showed statistically lower values of 95.6 ± 54.4 °C×s compared with the group of conditionally healthy people in contrast to the passive model, which demonstrated overestimated ∫ΔT index.

Discussion

In the current study we attempted to characterize individual systemic features of a human capillary network by means of a thermographic evaluation using dynamic thermography.

It is obvious that active heat and mass transfer facilitated by the capillary network in the epithelial tissues will influence the heat production of each surface area. This generally contributes to a static thermal balance value, which is a constant surface temperature in the given conditions.

Human tissues in direct contact with the environment play virtually no part in heat generation. They receive excess heat from internal organs, functioning as a kind of radiator, since it is the cover tissues that are most involved in heat removal process [8, 9]. Under conditions of room temperature (21–23°C) and relative humidity of 40–60%, the greatest amount of heat is removed from the body through radiation, i.e. in the form of infrared ray generation from the body surface [10]. There are many attempts to use static temperature indicators to assess the condition of both the underlying internal organs and the network of blood vessels actively transferring heat from them to the surface [1–5].

Dynamic measurements aimed at evaluating local vessel conditions are also known. In these measurements

vessel reactions were assessed mainly using cold test. I. Mizeva et al. [11] studied the relationship between blood flow and skin surface temperature during cold test using simultaneous thermometry and laser Doppler flowmetry (LDF). The authors sugggested 2 mechanisms for vascular reaction change based on LDF results the first mechanism is the rapid change in skin thermal conductivity associated with a decrease in "recruited" capillaries, and the second mechanism is a decrease in the force of temperature effects caused by constriction of arterioles and redirection of blood into arteriovenous anastomoses. However, no correlation between skin surface temperature deviation and LDF data was observed during cold test.

M. Davey et al. [12] questioned the hypothesis about the effect of skin blood flow on cold test results. The authors attempted to assess the influence of skin blood flow on the change in skin surface temperature in subjects not suffering from cold injury by comparing the change in blood flow during a cold test on a perfused and non-perfused foot. These results were compared with those of patients diagnosed with non-freezing cold injury. Based on the thermographic and LDF data they acquired the authors made a conclusion that any difference in skin surface temperature between the study groups was determined exclusively by the effect of blood flow.

All of the mentioned studies confirm the connection between the local and regional metabolism and the surface thermal dynamics. But at the same time, the question remains: does the nature of temperature recovery after local surface hypothermia bear information about subtle changes in the status of capillaries at the system level? We assumed that the weak thermal response of the local skin capillaries can be assessed by a detailed observation of the dynamics of temperature recovery after dosed cooling of the local surface area.

At the beginning of our work on the method development, we inaccurately assumed that hypothermia applied to a local area of the skin could trigger a sequence of regulatory reactions that intensify heat and mass transfer in the skin. These reactions will cause the temperature recovery curve to become more complicated. Properties of the temperature recovery curve became the main subject of our study.

To assess the dynamics of temperature recovery, an original applicator was developed, which not only can absorb a strictly dosed amount of heat, but also allows limiting the contact zone. A small area of the working surface of the applicator allows limiting the spread of the thermal front in the lateral direction and in depth for a short application time.

Using the example of a passive model of a block of porcine tissue, we attempted to give a thermographic characteristic of a tissue similar to the human tissue, but lacking active heat and mass transfer. As can be seen from the average values given in Table 1, the passive model is distinguished by a large deviation of the temperature curve from a smooth logarithmic function. At first glance the result may seem paradoxical – a more complex temperature recovery curve in the complete absence of the ability to control heat generation by the body – but it is explained by the layered structure of the epithelial tissues. Indeed, each of the layers of the skin and subcutaneous fatty tissue have sufficiently contrasting properties to create a complex passive thermal response to local hypothermia.

In these tissues both the heat capacity and the kinetic indices of conductive heat transfer are different, which gives the effect of the heat front lagging from different layers during restoration of temperature balance. In such a situation, the presence and activity of capillaries will smooth out the temperature response of the multipart structure, "mixing" the thermal response of the layers under observation and also allowing them to simultaneously cool down at the moment of cold application to the surface.

Normally, human skin also has a pronounced layered structure: the epidermis, dermis, and subcutaneous fatty tissue. Each of these layers has its own heat capacity and conductive properties. For this reason, skin structures that lack the ability to "mix" the temperature will produce a complex signal of the surface temperature recovery after contact with the cooled applicator has ceased.

To reduce the effect of thermal noise, standardization of physical conditions and an original infrared thermography protocol were proposed, which allowed to evaluate the effect of capillaries on the temperature recovery dynamics in a group of patients with well-studied pathology.

It is known that in patients with diabetes mellitus the capillaries of the skin are dilated. Such capillaries have a thick fibrotic basement membrane [13, 14]. This should affect the heat transfer within the skin layers, smoothing the effect of its layered structure, during temperature recovery after local hypothermia. The single measurements we carried out confirm this effect (see Table 1).

We believe that the proposed approach to dynamic thermography in combination with dosed local cold test, which allows to limit the thermal response of tissues to the depth of subcutaneous fatty tissue, gives much more information about capillary status than any other "global" tests.

Probably, in the future it will be necessary to move from the summation of the temperature difference between the real recovery curve and its mathematical model, which we have provided as examples for individual key points in time, to an integral description of a continuous process. But it will be rational after careful selection of the optimal approximation function of real data.

Conclusion

As a result of research (experiment), standardization of physical conditions and the original protocol of infra-

red thermography were proposed. An applicator for local dynamic thermography was created. The following conclusions were also made: the lack of heat and mass transfer in the passive model complicates the restoration of heat balance due to the multi-layered structure of the skin; the heat balance recovery curve is individual and does not depend on gender and age. We obtained the ∫ΔT indices of the integral temperature difference. The ∫ΔT indicator of a healthy person was 121.8±70.8°C×s; in the passive model it was 307.2 ±43.4°C×s; in diabetes it makes 95.6 ± 54.4°C×s. All the above results give the potential to use the method in medicine.

REFERENCES

1. Lawson R. Thermography; a new tool in the investigation of breast lesions, *Can. Serv. Med. J.*, 1957, vol. 8, no. 8, pp. 517–24.
2. Matteoli S., Coppini D., Corvi A. A novel image processing procedure for thermographic image analysis, *Med. Biol. Eng. Comput.*, 2018, vol. 56, no. 10, pp. 1747–1756.
3. Herrick A.L., Murray A. The role of capillaroscopy and thermography in the assessment and management of Raynaud's phenomenon, *Autoimmun. Rev.*, 2018, vol. 17, no. 5, pp. 465–472.
4. Lim M.J., Kwon S.R., Jung K.H., Joo K., Park S.G., Park W. Digital thermography of the fingers and toes in Raynaud's phenomenon, *J. Korean Med. Sci.*, 2014, vol. 29, no. 4, pp. 502–506.
5. Jones B.F. A reappraisal of the use of infrared thermal image analysis in medicine, *IEEE Trans. Med. Imaging.*, 1998, vol. 17, no. 6, pp. 1019–1027.
6. Staffa E. et al. Using noncontact infrared thermography for long-term monitoring of foot temperatures in a patient with diabetes mellitus, *Ostomy Wound Manage*, vol. 62, no. 4, pp. 54–61.
7. Silva N.C.M. et al. Reliability of infrared thermography images in the analysis of the plantar surface temperature in diabetes mellitus, *J. Chiropr. Med.*, 2018, vol. 17, no. 1, P. 30–35.
8. Van Marken Lichtenbelt W.D., Daanen H.A. Cold-induced metabolism, *Curr. Opin. Clin. Nutr. Metab. Care.*, 2003, vol. 6, no. 4, pp. 469–475.
9. Wilmore J.H. and Costill D.L. *Physiology of sport and exercise*, 2nd ed. Champaign, Illinois, Human Kinetics, 1999.
10. Katschinski D.M. On heat and cells and proteins, *News Physiol. Sci.*, 2004, vol. 19, pp. 11–15.
11. Mizeva I., Frik P., Podtaev S. Skin blood flow and temperature oscillations during cold pressor test, *Conf. Proc. IEEE Eng. Med. Biol. Soc.*, 2015, pp. 7382–7385.
12. Davey M., Eglin C., House J., Tipton M. The contribution of blood flow to the skin temperature responses during a cold sensitivity test, *Eur. J. Appl. Physiol.*, 2013, vol. 113, pp. 2411–2417.
13. Kovacic J.C. et al. The relationships between cardiovascular disease and diabetes, *Endocrinol. Metab. Clin. North Am*, 2014, vol. 43, no. 1, pp. 41–57.
14. Muris D.M., Houben A.J., Schram M.T., Stehouwer C.D. Microvascular dysfunction is associated with a higher incidence of type 2 diabetes mellitus: a systematic review and meta-analysis, *Arterioscler. Thromb. Vasc. Biol.*, 2012, vol. 32, no. 12, pp. 3082–3094.

ЛИТЕРАТУРА

1. Lawson R. Thermography; a new tool in the investigation of breast lesions // Can. Serv. Med. J. – 1957. – Vol. 8, No. 8. – P. 517–24.
2. Matteoli S., Coppini D., Corvi A. A novel image processing procedure for thermographic image analysis // Med. Biol. Eng. Comput. – 2018. – Vol. 56, No. 10. – P. 1747–1756.
3. Herrick A.L., Murray A. The role of capillaroscopy and thermography in the assessment and management of Raynaud's phenomenon // Autoimmun. Rev. – 2018. – Vol. 17, No. 5 – P. 465–472.
4. Lim M.J., Kwon S.R., Jung K.H., Joo K., Park S.G., Park W. Digital thermography of the fingers and toes in Raynaud's phenomenon // J. Korean Med. Sci. – 2014. – Vol. 29, No. 4. – P. 502–506.
5. Jones B.F. A reappraisal of the use of infrared thermal image analysis in medicine // IEEE Trans. Med. Imaging. – 1998. – Vol. 17, No. 6. – P. 1019–1027.
6. Staffa E. et al. Using noncontact infrared thermography for long-term monitoring of foot temperatures in a patient with diabetes mellitus // Ostomy Wound Manage. – Vol. 62, No. 4. – P. 54–61.
7. Silva N.C.M. et al. Reliability of infrared thermography images in the analysis of the plantar surface temperature in diabetes mellitus // J. Chiropr. Med. – 2018. – Vol. 17, No. 1. – P. 30–35.
8. Van Marken Lichtenbelt W.D., Daanen H.A. Cold-induced metabolism // Curr. Opin. Clin. Nutr. Metab. Care. – 2003. – Vol. 6, No. 4. – P. 469–475.
9. Wilmore J.H. and Costill D.L. Physiology of sport and exercise // 2nd ed. – Champaign, Illinois: Human Kinetics, 1999.
10. Katschinski D.M. On heat and cells and proteins // News Physiol. Sci. – 2004. – Vol. 19. – P. 11–15.
11. Mizeva I., Frik P., Podtaev S. Skin blood flow and temperature oscillations during cold pressor test // Conf. Proc. IEEE Eng. Med. Biol. Soc. – 2015. – P. 7382–7385.
12. Davey M., Eglin C., House J., Tipton M. The contribution of blood flow to the skin temperature responses during a cold sensitivity test // Eur. J. Appl. Physiol. – 2013. – Vol. 113. – P. 2411–2417.
13. Kovacic J.C. et al. The relationships between cardiovascular disease and diabetes // Endocrinol. Metab. Clin. North Am. – 2014. – Vol. 43, No. 1. – P. 41–57.
14. Muris D.M., Houben A.J., Schram M.T., Stehouwer C.D. Microvascular dysfunction is associated with a higher incidence of type 2 diabetes mellitus: a systematic review and meta-analysis // Arterioscler. Thromb. Vasc. Biol. – 2012. – Vol. 32, No. 12. – P. 3082–3094.

PHOTODYNAMIC THERAPY OF INTRADERMAL METASTATIC BREAST CANCER (LITERATURE REVIEW)

Rakhimzhanova R.I.[1], **Shanazarov N.A.**[1, 2], **Turzhanova D.E.**[1]
[1]Astana Medical University, Nur-Sultan, Republic of Kazakhstan
[2]Hospital of Medical Center of the Department of Presidential Affairs of the Republic of Kazakhstan, Nur-Sultan, Republic of Kazakhstan

Abstract

In recent years, an increase in the incidence of breast cancer has been observed throughout the world, and in 20% of cases, with the development of intradermal metastases. The possibilities of surgical and radiation treatment of intradermal breast metastases are quite limited, and the effectiveness of polychemotherapy using standard regimens does not exceed 22–27%, while the period of remission, in general, is only 2–3 months. Photodynamic therapy (PDT) is a promising treatment for intradermal metastases of breast cancer. The experience of using PDT in this nosology is quite limited, but the results show its high efficiency and safety. Thus, several Russian studies are devoted to assessing the effectiveness of PDT of intradermal breast metastases with Photolon, a chlorin series photosensitizer. According to the authors, the therapeutic effect was achieved in 85–97% of patients (the percentage of patients with full and partial effect was 73–85%). Studies on the effectiveness of PDT in patients with the same nosology using the Photosens photosensitizer show a slightly lower effectiveness – the therapeutic effect was achieved in 81.8% of cases, while the proportion of patients with full and partial effect was only about 50%. Several studies have been carried out abroad on models of metastatic breast cancer using new photosensitizers (e.g. sodium sinoporphyrin) and new combined PDT regimens (e.g. adjuvant PDT with fluorouracil or Capecitabine). The obtained results demonstrate the promise of new approaches: PDT with sodium sinoporphyrin inhibited the growth of both the tumor itself and its metastases; the use of adjuvant regimens led to an increase in the tumor cells differentiation in the animal model, the cessation of tumor and metastatic foci growth.

Keywords: breast cancer, skin metastases, photodynamic therapy, photosensitizer, photochemical reaction.

For citations: Rakhimzhanova R.I., Shanazarov N.A., Turzhanova D.E. Photodynamic therapy of intradermal metastatic breast cancer (literature review), *Biomedical Photonics*, 2019, vol. 8, no. 3, pp. 36–42 (in Russian). doi: 10.24931/2413–9432–2019–8–3–36–42.

Contacts: Turzhanova D.E., e-mail: dinara.turzhanov@mail.ru

ФОТОДИНАМИЧЕСКАЯ ТЕРАПИЯ ВНУТРИКОЖНЫХ МЕТАСТАЗОВ РАКА МОЛОЧНОЙ ЖЕЛЕЗЫ (ОБЗОР ЛИТЕРАТУРЫ)

Р.И. Рахимжанова[1], **Н.А. Шаназаров**[1, 2], **Д.Е. Туржанова**[1]
[1]Медицинский университет Астана, Нур-Султан, Республика Казахстан
[2]Больница Медицинского центра Управления делами Президента Республики Казахстан, Нур-Султан, Республика Казахстан

Резюме

В последние годы во всем мире наблюдается рост заболеваемости раком молочной железы (РМЖ), причем в 20% случаев при РМЖ происходит развитие внутрикожных метастазов. Возможности хирургического и лучевого лечения внутрикожных метастазов РМЖ достаточно ограничены, а эффективность полихимиотерапии с применением стандартных схем не превышает 22–27%, при этом срок ремиссии, как правило, составляет лишь 2–3 мес. Фотодинамическая терапия (ФДТ) является перспективным методом лечения внутрикожных метастазов РМЖ. Опыт применения ФДТ при данной нозологии достаточно ограничен, но полученные результаты демонстрируют его высокую эффективность и безопасность. Так, несколько российских исследований посвящены оценке эффективности ФДТ внутрикожных метастазов РМЖ с фотосенсибилизатором хлоринового ряда фотолон. По данным авторов, лечебный эффект был достигнут у 85–97% пациенток (доля пациенток с полным и частичным эффектом составляла 73–85%). Исследования эффективности ФДТ у пациенток с такой же нозологией с использованием фотосенсибилизатора фотосенс демонстрируют несколько меньшую эффективность – лечебный эффект был достигнут в 81,8% наблюдений, при этом доля пациенток с полным и частичным эффектом составляла только около 50%. За рубежом проведен ряд исследований на моделях метастазирующего РМЖ с использованием новых фотосенсибилизаторов (например, синопорфирина натрия) и новых комбинированных схем ФДТ (например, адъювантная ФДТ с 5-фторурацилом или капецитабином). Полученные результаты демонстрируют перспективность новых подходов: ФДТ с синопорфирином натрия ингибировала рост как самой опухоли, так и ее метастазов; применение адъювантных схем привело к повышению дифференцировки опухолевых клеток у животной модели, прекращению роста опухоли, а также метастатических очагов.

Ключевые слова: рак молочной железы, кожные метастазы, фотодинамическая терапия, фотосенсибилизатор, фотохимическая реакция.

Для цитирования: Рахимжанова Р.И., Шаназаров Н.А., Туржанова Д.Е. Фотодинамическая терапия внутрикожных метастазов рака молочной железы // Biomedical Photonics. – 2019. – Т. 8, № 3. – С. 36–42. doi: 10.24931/2413–9432–2019–8–3–36–42.

Контакты: Туржанова Д.Е., e-mail: dinara.turzhanov@mail.ru

Breast cancer, which affects about 1.2 million women in the world every year, over 52,000 in the Russian Federation and more than 4,000 in Kazakhstan, attracts focused attention of specialists because of its increasing prevalence and high mortality rate of the patients. Thus, according to official statistics, the incidence rate of malignant tumors of this localization in the Russian Federation in the period from 2008 to 2017 increased from 67.95 to 89.60 per 100,000 people, i.e., a 33.8% increase had place [1]. In the Republic of Kazakhstan, only from 2012 to 2017, the incidence of breast cancer increased from 21.3 to 24.5 per 100,000 population. Moreover, according to the forecasts of specialists of the International Agency for Research on Cancer, over the next two decades, the number of patients diagnosed with breast cancer will almost double [2].

Surgery still remains the main treatment against breast cancer: in accordance with the modern concept of surgery development, the scope of operations on the mammary gland is increasingly reduced to organ-preserving treatment, including limited removal of clinically negative axillary lymph nodes. In addition, an increase in survival and a decrease in mortality from malignant neoplasms of the mammary gland is associated with the appropriate use of systemic therapies [3].

However, the proportion of patients with stage III–IV of breast cancer is still high, reaching 45%, according to some reports [4]. In this context, in 20% of observed cases, the development of intradermal metastases is noted, mainly after surgical treatment. As a rule, the treatment of metastatic breast cancer includes systemic therapy (chemotherapy, hormone therapy) used in combination with radiation therapy and excision of the metastatic focus. However, it should be noted that surgical treatment in such cases is not always possible due to the multiple nature of the pathologic process and its high extent. In addition, the somatic state of patients after combined treatment often does not make it possible to perform an optimal volume of surgery. In turn, the possibilities of radiation treatment of breast metastases are often limited by the multiple nature of the metastasis process. The effectiveness of polychemotherapy with breast metastases in the skin, in case of standard regimens, does not exceed 22–27%, while the period of remission, as a rule, is only 2–3 months [5]. To achieve longer remission periods, it is necessary to administer multi-course polychemotherapy. It must be noted that radiation therapy and chemotherapy have an immunosuppressive effect, which is exacerbated in case of repeated courses. Other methods of treating skin metastases of breast cancer include electrochemotherapy, local chemotherapy (MILTEX), laser destruction, brachytherapy, hyperthermia, cryotherapy, etc.; however, the data on their effectiveness remains highly controversial [6]. Thus, the dissatisfaction with the results of treatment of breast cancer patients with skin metastases stimulates the search for new methods of therapy.

One of the current trends in modern oncology is the treatment of patients with intradermal metastases of breast cancer with the use of photodynamic therapy (PDT), which is now considered to be one of the most effective methods for malignancies treatment [7]. PDT is a non-systemic therapeutic procedure that begins to function in the presence of a combination of three separate components: a photoactivated photosensitizer, a specific light source and molecular oxygen [8–11]. This method is based on the fact that tumor cells are able to selectively accumulate certain photosensitizers in larger quantities than healthy tissues do [12, 13]. Subsequently, when irradiated with light the spectrum of which corresponds to the spectral composition of the absorption of the photosensitizer, a photochemical reaction takes place in the tumor cells. As a result, substances with cytotoxic activity are formed, and their action leads to tumor necrosis [14, 15].

The PDT method can be used independently or in combination with surgical and radiation treatment, as well as for palliative purposes [16]. The advantages of PDT are the high selectivity of tumor cell damage, the absence of serious side effects, the possibility of repeated courses of treatment, and the combination of diagnostic and treatment options in the same procedure. An additional advantage of PDT is its relative painlessness and the possibility of repeated courses.

However, the PDT method also has some drawbacks, including the following:

- a limited depth of penetration of light exposure into the tumor (from 2 to 15 mm, depending on the applied wavelength according to some data, and from 4 to 8 mm according to other data). The penetration depth is determined by the choice of the photosensitizer for the therapy [17];
- the dependence of treatment effect on the degree of oxygenation and blood supply to the tumor;

- the absence of morphological control after the treatment;
- the high cost of some photosensitizers [18].

General indications for PDT for exposure in accordance with the radical program are tumors that can selectively accumulate a photosensitizer and are accessible for laser radiation exposure, with an indolent exophytic and/or infiltrative component that does not exceed the depth of radiation penetration into the tissue. In cases where the tumor does not meet the above criteria, palliative PDT or the use of PDT in combination with other methods of exposure is possible [19].

Absolute contraindications for the procedure include respiratory and cardiovascular failure, decompensated diseases of the liver and kidneys, cachexia, intolerance to the drug. Among relative contraindications, allergic diseases can be mentioned [20].

A PDT procedure consists of introducing a photosensitizer (PS) in a way that is optimal for its accumulation in the tumor, and its activation under the influence of laser radiation at a certain wavelength. Therefore, the choice of PS has a significant impact on the efficiency of PDT of malignant tumors of various localization and on the radiation parameters, since the depth of the therapeutic effect on the neoplasm is determined by the spectral range of the PS. Thus, the maximum exposure depth is provided by sensitizers with a wavelength of spectral maximum exceeding 770 nm. Accordingly, the fluorescent properties of the sensitizer play an important role in the development of treatment tactics, evaluation of the drug biodistribution, and monitoring of the results [21].

An analysis of the literature data allows us to conclude that the use of PS of different classes significantly affects the effectiveness of PDT of neoplasms. Thus, the best results with respect to intradermal metastases of breast cancer were obtained with the use of tetramethahydroxyphenyl chlorin (Foscan, $\lambda = 652$ nm), sulfonated aluminum phthalocyanine (Photosens, $\lambda = 670$ nm), chlorine e_6 trisodium salt (Photolon, $\lambda = 661 \pm 5$ nm) [5, 22, 23].

According to some authors, the indications for the use of PDT in breast cancer are the following:

- Paget's desease T1–2N0M0;
- breast cancer relapse on the chest wall after surgical treatment;
- intradermal metastases after surgical, combined and complex treatment;
- primary breast cancer T1–2N0M0 (nodular form) with the patient's emphatic refusal from surgical treatment and the presence of severe concomitant diseases [24].

As for the effectiveness of PDT in patients with breast cancer, E.V. Goranskaya and M.A. Kaplan in his study demonstrated that PDT of skin metastases in breast cancer with a chlorine-type photosensitizer (Photolon) allows achieving a therapeutic effect in 85% of cases. In this context, complete regression was noted in 46%, and partial, in 39% of cases. Based on these data, the authors came to the conclusion that photodynamic therapy can be seen as a method that can achieve a good result with the least number of side effects, which makes it possible to recommend PDT for use in medical institutions [5]. In another study concerning the treatment of intradermal metastases of breast cancer, PDT demonstrated higher clinical efficacy: therapeutic effect was achieved in 97% of cases. At the same time, the authors note the high selectivity of the method in relation to the tumor tissue destruction, as well as the absence of severe local and systemic complications and the possibility of repeating the treatment. In addition, researchers mention the use of PDT for palliative purposes, as it will lead to tumor volume reduction and improve the quality of life of patients with breast cancer and its intradermal metastases [25].

The work by M.A. Kaplan et al. evaluated the effectiveness of PDT for intradermal metastases of breast cancer with the use of photolon. According to the results of treatment of 46 patients, 54.3% of which were found to have only intradermal metastases, and the rest also had organ metastases (in lymph nodes, bones, liver, lung tissue, and the second mammary gland), complete regression was noted in 33.6% of cases, partial regression in 39.4%, stabilization in 22.6% and progression only in 4.4%. An objective response was obtained in 73.0% of cases, and therapeutic response in 95.6% of cases [26].

Completely different results were obtained in the study by S.V. Evstifeev et al. for the evaluation of the effectiveness of PDT against intradermal metastases of breast cancer: full effect was achieved only in 22.7% of patients, partial in 27.3%, stabilization of the process was recorded in 31.8% of cases, and the rate of disease progression characterized by the appearance of new metastatic foci reached 18.2% [27]. It should be noted that in this study we used Photosens, a domestically produced synthetic porphyrin photosensitizer of the second generation. It is possible that the use of photosens as a photosensitizer in this study adversely affected the effectiveness of PDT compared to the study mentioned earlier.

Foreign researchers are constantly searching for new photosensitizers that ensure both high efficacy and safety in the treatment breast cancer and its metastases. In this regard, the results obtained by X. Wang et al. are of interest. The researchers evaluated the effect of PDT with sodium synoporphyrin on the proliferation and metastasis of tumor cells in the highly metastatic 4T1 cell line on a mouse xenograft model. As a result, it was found that the selected treatment tactic significantly increased the life expectancy of mice with breast cancer, and also inhibited the growth of both the tumor and its metastases, which is consistent with the results of *in vitro* experiments. In addition, the authors noted that PDT with this pharmaceutical product was more effective than therapy with

Photofrin, the PS which had already been registered. Preliminary toxicological results suggest that sodium synoporphyrin is a relatively safe medication. These data can be regarded as evidence of the promising prospects related to the use of this photosensitizer, which, however, requires further study [28].

In turn, S. Anand et al. suggested, in order to increase the effectiveness of PDT in breast cancer, that a neoadjuvant (5-fluorouracil) be used before PDT with aminolevulinic acid ester. This approach did increase the efficacy of PDT; however, a serious toxic effect of 5-fluorouracil was noted. In order to reduce it, the researchers proposed the use of the non-toxic precursor of 5-fluorouracil capecitabine in combination PDT mode. As a result, a significant increase in the differentiation of tumor cells in the animal model was demonstrated, as well as their death, which exceeded the level in the control group by 5 times. As a result, the authors noted that tumor growth stopped, as well as metastatic foci growth [29].

Foreign researchers devoted a lot of works to the assessment of the clinical efficacy of PDT in patients with skin metastases of breast cancer. For instance, P. Wyss et al. provide the results of the use of two different PDT protocols in the treatment of skin metastases. The first protocol included the administration of PS meta-tetra (hydroxyphenyl) chlorin at a dose of 0.10 mg/kg followed by irradiation at a dose of 5 J/cm^2, while in the second protocol the dose of PS was 0.15 mg/kg and the exposure was 10 J/cm^2. As a result, a complete clinical effect was observed in all patients, regardless of the PS dose or irradiation dose. The authors note that the healing rate mainly depended on the irradiated area of the site [30].

The authors of an extensive literature review on the use of PDT for the treatment of breast cancer provide numerous evidence of its clinical efficacy; the PS administered in the cases under consideration were various, and combined approaches were also used (a combination of PDT and immune therapy). However, it is emphasized that further research is necessary since the experience accumulated to date is still insufficient [31].

A number of authors provide data on the use of a matrix emitter on semiconductor diodes with a variable geometry of the radiating surface. Its advantages are the following:

- the possibility of simultaneous exposure of large metastatic lesions areas in the skin of the chest wall;
- shorter treatment sessions, more comfortable for the patient;
- the reduction of the incidence of severe necrotic phototoxic reactions of irradiated tissues due to the low power density of the light energy;
- the opportunity for prompt administration of a repeated PDT session in the presence of clinical indications, on an outpatient basis;
- accurate dosimetry;
- insignificant divergence of radiation over bright diodes, since the radiating surface of the device is congruently adjacent to the irradiated surface of the chest wall;
- optimal formation of irradiation fields by the use of the photosensitizer fluorescence method;
- the opportunity to control the local process without systemic treatment, which significantly improves the quality of life of patients [32].

In the study by M. L. Gelfond et al., a case study of 8 patients with regional breast cancer at stage III and more advanced, it was found that in three cases PDT with the use of a matrix emitter led to a complete regression of metastatic formations in the skin. Partial regression was achieved in 4 patients, which had required repeated sessions, and in 1 woman, vast necrosis areas developed in place of the affected areas of the chest wall tissue, after which the patient was excluded from the observation. The relapse-free survival median was 14 months. According to the authors, this experience testifies to the advantages of this technique over irradiation of each metastasis in the skin using a fiber with a focusing nozzle. This technology makes it possible to simultaneously irradiate relatively large areas of affected tissue and deliver the planned dose of light energy per unit time at a power density sufficient to excite the photochemical reaction. On the one hand, this can significantly reduce the total exposure time, and on the other, it creates more comfortable conditions for patients without reducing the effectiveness of the method [33].

Nevertheless, insufficient satisfaction with the effectiveness of the existing PDT protocols for skin metastases in patients with breast cancer leads to the search for new approaches to the procedure. Also, further development of the method will be associated with the synthesis of new photosensitizers characterized by more selective accumulation in the tumor, greater activity for the induction of singlet oxygen, and excitation at a longer wavelength. Of great importance is the development and implementation of methods for early monitoring of the procedure effectiveness and the identification of predictors of response to photodynamic therapy in order to individualize the exposure parameters [34].

A promising feature is the increased selectivity of PS accumulation in tumor tissue cells, which helps to minimize the effect on healthy tissues. In addition, this makes it possible to implement the principles of theranostics, when the same procedure includes both diagnostic and therapeutic options.

Currently, studies are underway on the use of antibody-directed delivery of PS to antigens of target cells. This method is essentially based on the use of viral particles incapable of reproduction which have PS in their composition, which ensures phototoxicity in PDT. The surface of these particles features specific antibodies

to antigens that are present on the plasma membrane of only cancer cells, which ensures targeted action [35]. However, it should be noted that at present, specific antigens have not been discovered for every specific form of cancer, and antigen verification attempts involve serious difficulties. Nevertheless, this method seems to be very promising, although it requires considerable efforts for its follow-up enhancement before being introduced into wide clinical practice.

Thus, breast cancer is one of the most pressing problems of modern oncology. This is largely due to the large number of patients with advanced stages of the tumor process and the difficulties involved in the treatment of metastases. Indeed, the currently used surgical, radiation and pharmaceutical methods are not always effective. In this regard, the method of photodynamic therapy, which has proven its effectiveness in the treatment of malignant tumors of various localizations, seems to be very promising. However, despite the active study of this method in the recent years, many issues remain unclear. Nevertheless, considerable experience has already been gained in its use for the treatment of skin metastases in patients with breast cancer. In this connection, the study of the possibilities of the photodynamic therapy method for the treatment of intradermal breast cancer metastases continues.

REFERENCES

1. *Zlokachestvennye novoobrazovaniya v Rossii v 2017 godu (zabolevaemost' i smertnost')* [Malignant neoplasms in Russia in 2017 (morbidity and mortality)], by Kaprin A.D., Starinskii V.V., Petrova G.V. as eds. Moscow, MNIOI im. P.A. Gertsena – filial FGBU «NMITS radiologii» Minzdrava Rossii, 2018. 250 p.
2. Rasulov S.R., Muradov A.M., Khamidov A.K., Khamidov Dzh.B. Endogenous intoxication syndrome in patients with breast cancer, *Vestnik IPO v SZ RT*, 2013, no. 1, pp. 14–16. (in Russian)
3. Semiglazov V.F. Strategic and practical approaches to solving the problem of breast cancer, *Voprosy onkologii*, 2012, vol. 58, no. 2, pp. 148–152. (in Russian)
4. Tverezovskii S.A., Cherenkov V.G., Petrov A.B., Strozhenkov M.M. Analysis of the status of diagnosis and treatment of breast cancer before and after the introduction of mammographic screening, *Onkologiya. Zhurnal. im. P.A. Gertsena*, 2015, no. 5, pp. 24–27. (in Russian)
5. Goranskaya E.V., Kaplan M.A. Photodynamic therapy of breast cancer metastases into skin, *Radiatsiya i risk (Byulleten' Natsional'nogo radiatsionno-epidemiologicheskogo registra)*, 2014, vol. 23, no. 3, pp. 34–42. (in Russian)
6. Tsyb A.F., Kaplan M.A, Romanko Yu.S. *Fotodinamicheskaya terapiya* [Photodynamic therapy]. Moscow, Meditsinskoe informatsionnoe agentstvo Publ., 2009. 192 p.
7. Li T., Yan L. Functional Polymer Nanocarriers for Photodynamic Therapy, *Pharmaceuticals (Basel)*, 2018, vol. 11(4), p. 133.
8. Mesquita M.Q., Dias C.J., Gamelas S., Fardilha M., Neves M.G.P.M.S., Faustino M.A.F. An insight on the role of photosensitizer nanocarriers for photodynamic therapy, *An. Acad. Bras. Cienc.*, 2018, vol. 90(1), pp. 1101–1130.
9. Ji C., Gao Q., Dong X., Yin W., Gu Z., Gan Z., Zhao Y., Yin M. A size-reducible nanodrug with an aggregation-enhanced photodynamic effect for deep chemo-photodynamic therapy, *Angew. Chem. Int. Ed. Engl.*, 2018, vol. 57(35), pp. 11384–11388.
10. Deng K., Li C., Huang S., Xing B., Jin D., Zeng Q., Hou Z., Lin J. Recent progress in near infrared light triggered photodynamic therapy, *Small*, 2017, vol. 13(44). doi: 10.1002/smll.201702299.
11. Hu J., Tang Y., Elmenoufy A.H., Xu H., Cheng Z., Yang X. Nanocomposite-based photodynamic therapy strategies for deep tumor treatment, *Small*, 2015, vol. 11(44), pp. 5860–5887.
12. Cheng Y., Cheng H., Jiang C., Qiu X., Wang K., Huan W., Yuan A., Wu J., Hu Y. Perfluorocarbon nanoparticles enhance reactive oxygen levels and tumour growth inhibition in photodynamic therapy, *Nat Commun*, 2015, vol. 6, pp. 8785.
13. Moret F., Reddi E. Strategies for optimizing the delivery to tumors of macrocyclic photosensitizers used in photodynamic therapy (pdt), *J. Porphyr. Phthalocyanines*, 2017, vol. 21, pp. 239–256.

ЛИТЕРАТУРА

1. Злокачественные новообразования в России в 2017 году (заболеваемость и смертность) / под ред. А.Д. Каприна, В.В. Старинского, Г.В. Петровой – М.: МНИОИ им. П.А. Герцена – филиал ФГБУ «НМИЦ радиологии» Минздрава России, 2018. –250 с.
2. Расулов С.Р., Мурадов А.М., Хамидов А.К., Хамидов Дж.Б. Синдром эндогенной интоксикации у больных раком молочной железы // Вестник ИПО в СЗ РТ. – 2013. – № 1. – С. 14–16.
3. Семиглазов В.Ф. Стратегические и практические подходы к решению проблемы рака молочной железы // Вопросы онкологии. – 2012. – Т. 58, № 2. – С. 148–152.
4. Тверезовский С.А., Черенков В.Г., Петров А.Б., Строженков М.М. Анализ состояния диагностики и лечения рака молочной железы до и после внедрения маммографического скрининга // Онкология. Журнал. им. П.А. Герцена. – 2015. – № 5. – С. 24–27.
5. Горанская Е.В., Каплан М.А. Фотодинамическая терапия метастазов рака молочной железы в кожу // Радиация и риск (Бюллетень Национального радиационно-эпидемиологического регистра). – 2014. – Т. 23, № 3. – С. 34–42.
6. Цыб А.Ф., Каплан М.А, Романко Ю.С. и др. Фотодинамическая терапия. – М.: Медицинское информационное агентство, 2009. – 192 с.
7. Li T., Yan L. Functional Polymer Nanocarriers for Photodynamic Therapy // Pharmaceuticals (Basel). – 2018. – Vol. 11(4). – P. 133.
8. Mesquita M.Q., Dias C.J., Gamelas S., et al. An insight on the role of photosensitizer nanocarriers for photodynamic therapy // An. Acad. Bras. Cienc. – 2018. – Vol. 90(1). – P. 1101–1130.
9. Ji C., Gao Q., Dong X., et al. A size-reducible nanodrug with an aggregation-enhanced photodynamic effect for deep chemo-photodynamic therapy // Angew. Chem. Int. Ed. Engl. – 2018. – Vol. 57(35). – P. 11384–11388.
10. Deng K., Li C., Huang S., et al. Recent progress in near infrared light triggered photodynamic therapy. // Small. – 2017. – Vol. 13(44). doi: 10.1002/smll.201702299.
11. Hu J., Tang Y., Elmenoufy A.H., et al. Nanocomposite-based photodynamic therapy strategies for deep tumor treatment // Small. – 2015. – Vol. 11(44). – P. 5860–5887.
12. Cheng Y., Cheng H., Jiang C., et al. Perfluorocarbon nanoparticles enhance reactive oxygen levels and tumour growth inhibition in photodynamic therapy // Nat Commun. – 2015. – Vol. 6. – P. 8785.
13. Moret F., Reddi E. Strategies for optimizing the delivery to tumors of macrocyclic photosensitizers used in photodynamic therapy (pdt) // J. Porphyr. Phthalocyanines. – 2017. – Vol. 21. – P. 239–256.
14. Шаназаров Н.А., Ахетов А.А., Сейдалин Н.К. Первый опыт применения фотодинамической терапии в Казахстане // Biomedical Photonics. – 2017. – Т. 6. – № 4s. – С. 37–38.

14. Shanazarov N.A., Akhetov A.A., Seidalin N.K. First experience of using photodynamic therapy in Kazakhstan, *Biomedical Photonics*, 2017, vol. 6, no. 4s, pp. 37–38. (in Russian)
15. Gyulov Kh.Ya., Shanazarov N.A. Experience of using photodynamic therapy in Chelyabinsk Regional Clinical Oncology Center, *Vestnik MTS UD PRK*, 2017, no. 3(68), pp. 10–12. (in Russian)
16. Gehl J., Matthiessen L.M., Humphreys A. Management of cutaneous metastases by electrochemotherapy, *J. Clin. Oncol.*, 2010, vol. 28, p. 15.
17. Sanarova E.V., Lantsova A.V., Dmitrieva M.V., Smirnova Z.S., Oborotova N.A. Photodynamic therapy – a way to increase the selectivity and effectiveness of tumor treatment, *Rossiiskii bioterapevticheskii zhurnal*, 2014, vol. 13, no. 3, pp. 109–118. (in Russian)
18. Istomin Yu.P., Artem'eva T.P., Tserkovskii D.A. . Clinical use of photodynamic therapy in oncology, *Zdravookhranenie (Minsk)*, 2016, no. 10, pp. 54–58. (in Russian)
19. Lamberti M.J., Vittar N.B.R., Rivarola V.A. Breast cancer as photodynamic therapy target: Enhanced therapeutic efficiency by overview of tumor complexity, *World J Clin Oncol*, 2014, vol. 5(5), pp. 901–907.
20. Gamayunov S.V., SHakhova N.M., Denisenko A.N., Korchagina K.S., Grebenkina E.V., Skrebtsova R.R., Karov V.A., Terekhov V.M., Terent'ev I.G. Photodynamic therapy – advantages of the new methodology and specifics of the service organization, *Tikhookeanskii meditsinskii zhurnal*, 2014, no. 2(56), pp. 101–104. (in Russian)
21. Ponyaev A.I., Glukhova Ya.S., Chernykh Ya.S. Photosensitizers for photodynamic therapy (review), *Izvestiya Sankt-Peterburgskogo gosudarstvennogo tekhnologicheskogo instituta (tekhnicheskogo universiteta)*, 2017, no. 41(67), pp. 71–78. (in Russian)
22. Banerjee S.M., MacRobert A.J., Mosse C.A., Periera B., Bown S.G., Keshtgar M.R.S. Photodynamic therapy: Inception to application in breast cancer, *The Breast*, 2017, vol. 31, pp. 105–113.
23. Pak D.D., Filonenko E.V., Saribekyan E.K. Intraoperative photodynamic therapy of patients with locally advanced stage IIIB and IIIC breast cancer, *Fotodinamicheskaya terapiya i fotodiagnostika*, 2013, vol. 2, no. 1, pp. 25–30. (in Russian)
24. George B.P., Abrahamse H. A Review on Novel Breast Cancer Therapies: Photodynamic Therapy and Plant Derived Agent Induced Cell Death Mechanisms, *Anticancer Agents Med Chem*, 2016, vol. 16(7), pp. 793–801.
25. Goranskaya E.V., Ragulin Yu.A., Kapinus V.N., Yaroslavtsaeva E.V., Shubina A.M., Spichenkova I.S., Skugareva O.A. Immediate results of photodynamic therapy of breast cancer intradermal metastases, *Onkokhirurgiya*, 2011, vol. 3, no. 2, pp. 21–22. (in Russian)
26. Kaplan M.A., Kapinus V.N., Popuchiev V.V., Romanko Yu.S., Yaroslavtseva-Isaeva E.V., Spichenkova I.S., Shubina A.M., Borgul' O.V., Goranskaya E.V. Photodynamic therapy: results and prospects, *Radiatsiya i risk (Byulleten' Natsional'nogo radiatsionno-epidemiologicheskogo registra)*, 2013, vol. 22, no. 3, pp. 115–123. (in Russian)
27. Evstifeev S.V., Kulaev M.T., Al'myashev A.Z., Skopin P.I., Begoulov I.V. Fluorescence diagnostics and photodynamic therapy of intradermal breast cancer metastases, *Zlokachestvennye opukholi*, 2017, vol. 7, no. 3-S1, pp. 75. (in Russian)
28. Wang X.,Hu J., Wang P., Zhang S., Liu Y., Xiong W., Liu Q. Analysis of the In Vivo and In Vitro Effects of Photodynamic Therapy on Breast Cancer by Using a Sensitizer, Sinoporphyrin Sodium, *Theranostics*, 2015, vol. 5(7), pp. 772–786.
29. Anand S., Denisyuk A., Bullock T., Govande M., Maytin E.V. A non-toxic approach for treatment of breast cancer and its metastases: capecitabine enhanced photodynamic therapy in a murine tumor mode, *J Cancer Metastasis Treat*, 2019, vol. 5, pp. 6.
30. Wyss P., Schwarz V., Dobler-Girdziunaite D., Hornung R., Walt H., Degen A., Fehr M. Photodynamic therapy of locoregional breast cancer recurrences using a chlorin-type photosensitizer, *Int J Cancer*, 2001, vol. 93(5), pp. 720–724
15. Гюлов Х.Я., Шаназаров Н.А. Опыт применения фотодинамической терапии в Челябинском областном клиническом центре онкологии и ядерной медицины // Вестник МЦ УД ПРК. – 2017. – № 3(68). – С. 10–12.
16. Gehl J., Matthiessen L.M., Humphreys A. Management of cutaneous metastases by electrochemotherapy // J. Clin. Oncol. – 2010. – Vol. 28. – P. 15.
17. Санарова Е.В., Ланцова А.В., Дмитриева М.В. и др. Фотодинамическая терапия – способ повышения селективности и эффективности лечения опухолей // Российский биотерапевтический журнал. – 2014. – Т. 13, № 3. – С. 109–118.
18. Истомин Ю.П., Артемьева Т.П., Церковский Д.А. Клиническое применение фотодинамической терапии в онкологии // Здравоохранение (Минск). – 2016. – № 10. – С. 54–58.
19. Lamberti M.J., Vittar N.B.R., Rivarola V.A. Breast cancer as photodynamic therapy target: Enhanced therapeutic efficiency by overview of tumor complexity // World J Clin Oncol. – 2014. – Vol. 5(5). – P. 901–907.
20. Гамаюнов С.В., Шахова Н.М., Денисенко А.Н. и др. Фотодинамическая терапия – преимущества новой методики и особенности организации службы // Тихоокеанский медицинский журнал. – 2014. – № 2 (56). – С. 101–104.
21. Поняев А.И., Глухова Я.С., Черных Я.С. Фотосенсибилизаторы для фотодинамической терапии (обзор) // Известия Санкт-Петербургского государственного технологического института (технического университета). – 2017. – № 41 (67). – С. 71–78.
22. Banerjee S.M., MacRobert A.J., Mosse C.A., et al. Photodynamic therapy: Inception to application in breast cancer // The Breast. – 2017. – Vol. 31. – P. 105–113.
23. Пак Д.Д., Филоненко Е.В., Сарибекян Э.К. Интраоперационная фотодинамическая терапия больных местнораспространенным раком молочной железы IIIB и IIIC стадий // Фотодинамическая терапия и фотодиагностика. – 2013. – Т. 2, №1. – С. 25–30
24. George B.P., Abrahamse H. A Review on Novel Breast Cancer Therapies: Photodynamic Therapy and Plant Derived Agent Induced Cell Death Mechanisms // Anticancer Agents Med Chem. – 2016. – Vol. 16(7). – P. 793–801.
25. Горанская Е.В., Рагулин Ю.А., Капинус В.Н. и др. Непосредственные результаты фотодинамической терапии внутрикожных метастазов рака молочной железы // Онкохирургия. – 2011. – Т. 3, № 2. – С. 21–22.
26. Каплан М.А., Капинус В.Н., Попучиев В.В. и др. Фотодинамическая терапия: результаты и перспективы // Радиация и риск (Бюллетень национального радиационно-эпидемиологического регистра). – 2013. –Т. 22, № 3. – С. 115–123.
27. Евстифеев С.В., Кулаев М.Т., Альмяшев А.З. и др. Флюоресцентная диагностика и фотодинамическая терапия внутрикожных метастазов рака молочной железы // Злокачественные опухоли. – 2017. – Т. 7, № 3-S1. – С. 75.
28. Wang X., Hu J., Wang P., et al. Analysis of the *In Vivo* and *In Vitro* Effects of Photodynamic Therapy on Breast Cancer by Using a Sensitizer, Sinoporphyrin Sodium // Theranostics. – 2015. – Vol. 5(7). – P. 772–786.
29. Anand S., Denisyuk A., Bullock T., et al. A non-toxic approach for treatment of breast cancer and its metastases: capecitabine enhanced photodynamic therapy in a murine tumor model // J Cancer Metastasis Treat. – 2019. – Vol. 5. – P. 6.
30. Wyss P., Schwarz V., Dobler-Girdziunaite D., et al. Photodynamic therapy of locoregional breast cancer recurrences using a chlorin-type photosensitizer // Int J Cancer. – 2001. – Vol. 93(5). – P. 720–724
31. Banerjee S.M., MacRobert A.J., Mosse C.A., et al.Photodynamic therapy: Inception to application in breast cancer // Breast. – 2017. – Vol. 31. – P. 105–113.
32. Гельфонд М.Л., Гафтон Г.И., Анисимов В.В. Неоадъювантная, интраоперационная и адъювантная фотодинамическая тера-

31. Banerjee S.M., MacRobert A.J., Mosse C.A., Periera B., Bown S.G., Keshtgar M.R.S. Photodynamic therapy: Inception to application in breast cancer, *Breast*, 2017, vol. 31, pp. 105–113.
32. Gel'fond M.L., Gafton G.I., Anisimov V.V. Neoadjuvant, intraoperative and adjuvant photodynamic therapy in combined treatment of certain nosological forms of malignant neoplasms in *Aktual'nye problemy lazernoi meditsiny: sbornik nauchnykh trudov* [Actual problems of laser medicine: collection of scientific papers] by Petrishchev N.N. as edt. Sankt-Peterburg, 2016, pp. 81–95.
33. Gel'fond M.L., Levchenko E.V., Mamontov O.Yu., Baldueva I.A., Nekhaeva T.L., Novik A.V., Anisimov V.V,, Semiletova Yu.V., Myasnyankin M.S. Neoadjuvant and intraoperative photodynamic therapy in the combined treatment of malignant neoplasms, *Fotodinamicheskaya terapiya i fotodiagnostika*, 2013, vol. 2, no. 3, pp. 54. (in Russian)
34. Wang Y., Xie Y., Li J., Peng Z.H., Sheinin Y., Zhou J., Oupický D. Tumor-penetrating nanoparticles for enhanced anticancer activity of combined photodynamic and hypoxia-activated therapy, *ACS Nano*, 2017, vol. 11, pp. 2227–2238.
35. Sobolev A.S. Modular nanotransporters – a multipurpose anticancer drug delivery platform, *Vestnik rossiiskoi akademii nauk*, 2013, vol. 83, no. 8. pp. 685–697. (in Russian)

пия в комбинированном лечении некоторых нозологических форм злокачественных новообразований // Актуальные проблемы лазерной медицины: сборник научных трудов. / под ред. Н. Н. Петрищева. – Спб., 2016. – С. 81–95.
33. Гельфонд М.Л., Левченко Е.В., Мамонтов О.Ю. и др. Неоадъювантная и интраоперационная фотодинамическая терапия в комбинированном лечении злокачественных новообразований // Фотодинамическая терапия и фотодиагностика. – 2013. – Т. 2, № 3. – С. 54.
34. Wang Y., Xie Y., Li J. et al. Tumor-penetrating nanoparticles for enhanced anticancer activity of combined photodynamic and hypoxia-activated therapy // ACS Nano. – 2017. – Vol. 11. – P. 2227–2238.
35. Соболев А.С. Модульные нанотранспортеры – многоцелевая платформа для доставки противораковых лекарств // Вестник российской академии наук. – 2013. – Т. 83, № 8. – С. 685–697.

EFFECTIVENESS OF PHOTODYNAMIC THERAPY OF A PATIENT WITH EARLY CENTRAL LUNG CANCER AND CYSTIC FIBROSIS

Borzenko E.S.[1], Reshetov I.V.[2], Fatyanova A.S.[2], Ogdanskaya K.V.[2], Gafarov M.M.[2], Romanko Yu.S.[2, 3]

[1]Amur State Medical Academy, Blagoveshchensk, Russia
[2]Sechenov First Moscow State Medical University, Moscow, Russia
[3]A. Tsyb Medical Radiological Research Centre – branch of the National Medical Research Radiological Centre of the Ministry of Health of the Russian Federation (A. Tsyb MRRC), Obninsk, Russia

Abstract

The authors describe a clinical observation with full clinical effect after multi-course photodynamic therapy of a patient with central lung cancer and cystic fibrosis using Photoditazine. Photoditazine was administered intravenously at a dose of 0.8 mg/kg 2 hours before the irradiation session. Irradiation parameters: power density – 150 mW/cm^2, energy density – 200 J/cm^2. In total, 3 courses of photodynamic therapy were performed. As a result of the treatment, a complete regression of the tumor was noted. The patient has been under dynamic observation for 2 years after treatment, no relapse was observed.

Keywords: photodynamic therapy, photoditazine, central lung cancer, cystic fibrosis.

For citations: Borzenko E.S., Ogdanskaya K.V., Reshetov I.V., Fatyanova A.S., Gafarov M.M., Romanko Yu.S. Effectiveness of photodynamic therapy of a patient with early central lung cancer and cystic fibrosis, *Biomedical Photonics*, 2019, vol. 8, no. 3, pp. 43–45 (in Russian). doi: 10.24931/2413–9432–2019–8–3–43–45.

Contacts: Ogdanskaya K.V., e-mail: ksenia28r@mail.ru

ЭФФЕКТИВНОСТЬ ФОТОДИНАМИЧЕСКОЙ ТЕРАПИИ БОЛЬНОЙ РАННИМ ЦЕНТРАЛЬНЫМ РАКОМ ЛЁГКОГО И МУКОВИСЦИДОЗОМ

Е.С. Борзенко[1], И.В. Решетов[2], А.С. Фатьянова[2], К.В. Огданская[2], М.М. Гафаров[2], Ю.С. Романко[2, 3]

[1]Амурская государственная медицинская академия, Благовещенск, Россия
[2]Первый МГМУ им. И.М. Сеченова (Сеченовский Университет), Москва, Россия
[3]МРНЦ им. А.Ф. Цыба – филиал ФГБУ «НМИЦ радиологии» Минздрава России, Обнинск, Россия

Резюме

Авторы описывают клиническое наблюдение с полным клиническим эффектом после многокурсовой фотодинамической терапии больной центральным раком легких и муковисцидозом с использованием фотодитазина. Фотодитазин вводили внутривенно в дозе 0,8 мг/кг за 2 ч до проведения сеанса облучения. Параметры облучения: плотность мощности – 150 мВт/см^2, плотность энергии – 200 Дж/см^2. Всего было проведено 3 курса фотодинамической терапии. В результате проведенного лечения отмечена полная регрессия опухоли. Пациентка находится под динамическим наблюдением в течение 2 лет после лечения, рецидива не выявлено.

Ключевые слова: фотодинамическая терапия, фотодитазин, центральный рак лёгкого, муковисцидоз.

Для цитирования: Борзенко Е.С., Решетов И.В., Фатьянова А.С., Огданская К.В., Гафаров М.М., Романко Ю.С. Эффективность фотодинамической терапии больной ранним центральным раком лёгкого и муковисцидозом // Biomedical Photonics. – 2019. – Т. 8, № 3. – С. 43–45. doi: 10.24931/2413–9432–2019–8–3–43–45.

Контакты: Огданская К.В., e-mail: ksenia28r@mail.ru

Introduction

According to world statistics, one of the leading places in the structure of the incidence of malignant diseases is occupied by tumors of the broncho-pulmonary systems. Only in 2017 in Russia malignant tumors of these localizations were diagnosed in more than 62 thousand patients [1].

Currently, one of the endoscopic treatments for carcinoma in situ of central lung cancer (CLC) is photodynamic therapy (PDT). PDT shows high efficiency with a minimum of complications, which is especially important in the treatment of patients with severe concomitant pathology [2–5], which, among other things, includes some genetic diseases.

One of these diseases is cystic fibrosis, a systemic hereditary disease caused by a mutation in the transmembrane regulator of cystic fibrosis gene and characterized by damage to the glands of external secretion, as well as severe disturbances in the functioning of the respiratory and gastrointestinal tract. The total number of adult patients with cystic fibrosis in Russia annually is about 3.5 thousand people with a total incidence of the disease of 1/100 thousand of the population [6]. It has been proven that mutations of the transmembrane conductivity regulator (CFTR) causing cystic fibrosis are associated with a high risk of various types of cancer, especially malignant lung tumors [7].

The following is a clinical example of the effectiveness of PDT in a patient with central lung cancer and cystic fibrosis.

Patient K., age 47 years old, has been observed since 2006 at the Scientific Medical Center «Family Doctor» of the Amur State Medical Academy (SMC) with the main diagnosis: cystic fibrosis, mixed form of the disease. Concomitant diseases: chronic broncho-obstructive bronchitis, moderate; respiratory failure of 2 severity; secondary pulmonary emphysema; chronic pulmonary heart, etc. The diagnosis was established on the basis of an in-depth examination of the patient and a number of studies (studying the clinical symptoms of the disease, parameters of bronchial obstruction, genetic examination, bronchoscopy, computed tomography, morphological studies). The patient received pathogenetic and symptomatic therapy for cystic fibrosis and concomitant pathology. Every year, the general condition of the patient worsened, despite the prescribed treatment.

In 2016, with a planned treatment and diagnostic bronchoscopy, the patient found carcinoma in situ spurs of the upper lobar bronchus on the right, a tumor measuring 0.6 cm × 0.2 cm (Fig. 1*a*). Conducted a morphological study of the biopsy. Preinvasive carcinoma was verified. To determine the further tactics of treatment for the patient by the medical commission of the SMC, a decision was made on the need for consultation with leading specialists of the First Moscow State Medical University named after I.M. Sechenov Ministry of Health of Russia and the MRRC them. A.F. Tsyba - a branch of the Federal State Budgetary Institution Scientific Research Center for Radiology of the Ministry of Health of Russia: a decision was made collectively to conduct PDT, due to

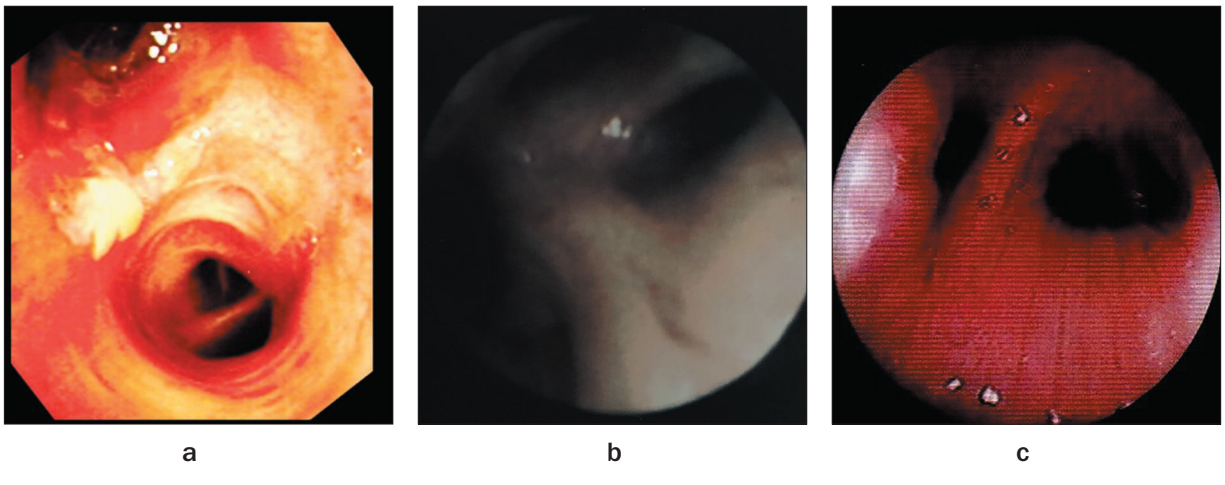

Рис. 1. Результаты бронхоскопии:
a – до ФДТ;
b – через 6 мес после ФДТ;
c – через 24 мес после ФДТ
Fig. 1. Bronchoscopy results:
a – before PDT;
b – 6 months after PDT;
c – 24 months after PDT

the fact that the generally accepted methods of treating CRL were contraindicated due to the severity of bronchial obstruction, hypoxemia, and the risk of unwanted adverse reactions to chemoradiotherapy .

A PDT session was performed 2 hours after intravenous, drip administration of photoditazine (VETA-GRAND LLC, Russia, registration certificate No. LS 001246 of 05/18/2012) at a dose of 0.8 mg / kg body weight. A quartz fiber with a cylindrical diffuser at a distance of 1 mm from the neoplasm was introduced through the instrument channel of the endoscope. 2 hours after the introduction of the photosensitizer, a PDT session was performed on a Crystal apparatus with a radiation wavelength of 662 nm (R&D Center Technika-PRO, Russia). The laser power density was 150 mW/cm^2, and the energy density was 200 J/cm^2. In total, the patient underwent 3 courses of PDT: the second one 1 week after the first, the third one 1 month later.

During the first week after PDT, the patient retained a slight pain syndrome in the irradiated area, which was stopped by taking analgesics. Eight days after PDT, during the follow-up sanitation bronchoscopy, necrosis of the neoplasm with fibrinous deposits, hyperemia and edema of the surrounding mucous membrane were revealed. There were no other complications during treatment.

When bronchoscopy performed after 6 months (Fig. 1*b*) and 2 years after the treatment, relapse was not detected.

Conclusion

The presented clinical observation shows the effectiveness of PDT in a patient with severe combined pathology - central lung cancer and cystic fibrosis. Thus, photodynamic therapy has great potential for use in patients with severe concomitant pathology as an effective and safe method for the treatment of central lung cancer.

REFERENCES

1. *Zlokachestvennye novoobrazovaniya v Rossii v 2017 godu (zabolevaemost' i smertnost')* [Malignant neoplasms in Russia in 2017 (morbidity and mortality)], by Kaprin A.D., Starinskii V.V., Petrova G.V. as eds. Moscow, MNIOI im. P.A. Gertsena – filial FGU «NMIRC» Minzdrava Rossii Publ., 2018. 250 p.
2. Sokolov V.V., Filonenko E.V. Photodynamic therapy for patients with early central lung cancer, *Fotodinamicheskaya terapiya i fotodiagnostika*. 2013, vol. 2, no. 4, pp. 3–6. (in Russian)
3. Kaplan M.A., Kapinus V.N., Popuchiev V.V., Romanko Yu.S., Yaroslavtseva-Isaeva E.V., Spichenkova I.S., Shubina A.I., Borgul O.V., Goranskaya E.V. Photodynamic therapy: results and prospects, *Radiatsiya i risk*, 2013, vol. 22, pp. 115–125.
4. Sokolov V.V.., Filonenko E.V., Telegina L.V., Boulgakova N.N., Smirnov V.V. Combination of fluorescence imaging and local spectrophotometry in fluorescence diagnostics of early cancer of larynx and bronchi, Quantum Electronics, 2002, vol. 32(11), pp. 963–969.
5. *Chislennost' naseleniya Rossiiskoi Federatsii po munitsipal'nym obrazovaniyam na 1 yanvarya 2017 goda. Federal'naya Sluzhba Gosudarstvennoi Statistiki (Rosstat)* [The population of the Russian Federation by municipalities as of January 1, 2017. Federal State Statistics Service (Rosstat)]. Moscow, 2017.
6. Zhang, J., Wang, Y., Jiang, X., Hsiao C. Cystic fibrosis transmembrane conductance regulator—emerging regulator of cancer, *Cell. Mol. Life Sci.*,2018, vol. 75(10), pp. 1737–1756.

ЛИТЕРАТУРА

1. Злокачественные новообразования в России в 2017 году (заболеваемость и смертность) / под ред. А.Д. Каприна, В.В. Старинского, Г.В. Петровой. – М.: МНИОИ и. П.А. Герцена – филиал ФГБУ «НМИЦ радиологии» Минздрава России, 2018. – 250 с.
2. Соколов В.В., Филоненко Е.В. Фотодинамическая терапия больных ранним центральным раком легкого // Фотодинамическая терапия и фотодиагностика. – 2013. – Т. 2, № 4. – С. 3–6.
3. Каплан М.А., Капинус В.Н., Попучиев В.В., Романко Ю.С., Ярославцева-Исаева Е.В., Спиченкова И.С., Шубина А.И., Борчуев О.В, Горанская Е.В. Фотодинамическая терапия: результаты и перспективы // Радиация и риск. – 2013. – Т. 22. – С. 115–125.
4. Sokolov V.V.., Filonenko E.V., Telegina L.V., Boulgakova N.N., Smirnov V.V. Combination of fluorescence imaging and local spectrophotometry in fluorescence diagnostics of early cancer of larynx and bronchi // Quantum Electronics. – 2002. – Vol. 32(11). – P. 963–969.
5. Численность населения Российской Федерации по муниципальным образованиям на 1 января 2017 года. Федеральная Служба Государственной Статистики (Росстат). – М. 2017.
6. Zhang, J., Wang, Y., Jiang, X., Hsiao C. Cystic fibrosis transmembrane conductance regulator—emerging regulator of cancer // Cell. Mol. Life Sci. – 2018. – Vol.75 (10). – P. 1737–1756.